REPUBLIC OF TURKEY YILDIZ TECHNICAL UNIVERSITY GRADUATE SCHOOL OF NATURAL AND APPLIED SCIENCES

MAXIMAL RATIO TRANSMISSION BASED MULTIPLE ANTENNA RELAYING SYSTEMS WITH INTERFERENCE

Awfa A. M. Ali ALADWANI

DOCTOR OF PHILOSOPHY THESIS

Department of Electronics and Communications Engineering

Communications Program

Advisor

Assoc. Prof. Dr. Tansal GÜÇLÜOĞLU

REPUBLIC OF TURKEY YILDIZ TECHNICAL UNIVERSITY GRADUATE SCHOOL OF NATURAL AND APPLIED SCIENCES

MAXIMAL RATIO TRANSMISSION BASED MULTIPLE ANTENNA RELAYING SYSTEMS WITH INTERFERENCE

A thesis submitted by Awfa A. M. Ali ALADWANI in partial fulfillment of the requirements for the degree of **DOCTOR OF PHILOSOPHY** is approved by the committee on 04.12.2020 in Department of Electronics and Communications Engineering, Communications Program.

Assoc. Prof. Dr. Tansal GÜÇLÜOĞLU Yildiz Technical University Advisor

Approved By the Examining Committee

Assoc. Prof. Dr. Tansal GÜÇLÜOĞLU, Advisor Yildiz Technical University Asst. Prof. Dr. Aktül KAVAS, Member Fatih Sultan Mehmet Foundation University Assoc. Prof. Dr. Eylem ERDOĞAN, Member Istanbul Medeniyet University Assoc. Prof. Dr. Hamid TORPİ, Member Yildiz Technical University Prof. Dr. Hasari ÇELEBİ, Member Gebze Technical University

I hereby declare that I have obtained the required legal permissions during data collection and exploitation procedures, that I have made the in-text citations and cited the references properly, that I haven't falsified and/or fabricated research data and results of the study and that I have abided by the principles of the scientific research and ethics during my Thesis Study under the title of Maximal Ratio Transmission Based Multiple Antenna Relaying Systems With Interference supervised by my supervisor, Assoc. Prof. Dr. Tansal GÜÇLÜOĞLU. In the case of a discovery of false statement, I am to acknowledge any legal consequence.

Awfa A. M. Ali ALADWANI

Signature

Dedicated to my father, Prof. Dr. Abdulwahhab Aladwani, my mother, my wife Zena, and my kids

ACKNOWLEDGEMENTS

In order to accomplishment this work, there has been a lovely group of individuals whose contributions and support have enabled me to reach this goal. I am forever indebted to so many people for their unwavering support throughout this journey. I will endeavor to acknowledge these special individuals, but for those I may miss, I sincerely apologize.

I would like to thank, first of all, my family and lovely friends for their constant support. Your unconditional love and encouragement have been my greatest motivation on this journey. To my family, thank you for your patience, endurance, and serenity as I took this journey.

I am indebted to my advisor, Assoc. Prof. Dr. Tansal GÜÇLÜOĞLU, for his guidance, enthusiasm that enhanced my experience throughout my graduate studies. I have great reverence for Assoc. Prof. Dr. Tansal GÜÇLÜOĞLU, both as a researcher and as a person. I aspire to imbibe his professional ethics, diligence, and discipline. He is the best advisor I could have hoped for and has been a great influence in my life.

I would like to thank my thesis monitor committee members, Asst. Prof. Dr. Aktül KAVAS, and Assoc. Prof. Dr. Eylem ERDOĞAN, for their encouragement, motivation, and constructive feedback on this dissertation.

I am greatly thankful to the Faculty of Electrical Engineering, in particular, the Department of Electronic and communications Engineering for the support during my graduate studies. I would like to specifically thank the department's staff for their guidance and support. Last, but not the least, I would like to thank my fellow Graduate students for their camaraderie and feedback on my work. I have benefited greatly by collaborating with all of you on various topics that led to this dissertation.

Awfa A. M. Ali ALADWANI

TABLE OF CONTENTS

LI	ST O	F SYME	BOLS	viii	
LI	ST O	F ABBR	REVIATIONS	ix	
LI	ST OI	F FIGU I	RES	xi	
Αŀ	3STR	ACT		xiii	
Ö	ZET			xv	
1 INTRODUCTION			CTION	1	
	1.1	Litera	ture Review	1	
	1.2	Object	tive of the Thesis	3	
	1.3	Hypot	hesis	5	
	1.4	Organ	iization	6	
	1.5	Notati	ions	7	
2	BACKGROUND				
	2.1	Wirele	ess Communication Systems	8	
	2.2	2.2 Wireless Channel Modeling		8	
		2.2.1	Rayleigh Fading Channel	9	
		2.2.2	Nakagami-m Fading Channel	9	
		2.2.3	Weibull Fading Channel	10	
	2.3	Interfe	erence Modeling	10	
	2.4	Space	Diversity Techniques	12	
		2.4.1	Cooperative Relaying	12	
		2.4.2	Transmit Diversity	15	
		2.4.3	Receive Diversity	16	
	2.5	Perfor	mance Evaluation Tools	16	
		2.5.1	Outage Probability	16	
		2.5.2	Average Error Probability	16	
		2.5.3	Ergodic Capacity (Average Channel Capacity)	17	
		254	Asymptotic Analysis, Diversity and Array Gain	17	

3	IMP	ACT O	F CO-CHANNEL INTERFERENCE ON TWO-WAY RELAYING	
	NET	WORK	S WITH MAXIMAL RATIO TRANSMISSION	18
	3.1 Introduction			18
3.2 System and Channel Models			n and Channel Models	21
	3.3	Perfor	mance Analysis	23
		3.3.1	System Outage Probability	27
		3.3.2	Sum Symbol Error Rate	27
		3.3.3	Asymptotic Analysis	29
		3.3.4	Ergodic Sum Rate	31
		3.3.5	Impact of Channel Estimation Errors	32
	3.4	Nume	rical Results and Discussion	34
	3.5	Chapte	er Summary	41
4 EXACT PERFORMANCE ANALYSIS OF MAXIMAL RATIO TRANSMISS			RFORMANCE ANALYSIS OF MAXIMAL RATIO TRANSMISSION	
	ON	DECOL	DE-AND-FORWARD RELAYING SYSTEM UNDER THE IMPACT	
	OF (CO-CHA	ANNEL INTERFERENCE	42
	4.1	Introd	uction	42
	4.2	Systen	n and Channel Models	45
	4.3	SINR S	Statistical Analysis	46
		4.3.1	The CDFs Derivation	47
		4.3.2	The PDFs derivation	49
	4.4	Perfor	mance analysis	49
		4.4.1	Outage Probability	49
		4.4.2	Average Bit Error Probability	50
		4.4.3	Ergodic Capacity	51
		4.4.4	Asymptotic Analysis	51
	4.5	Nume	rical Results and Discussion	54
	4.6	Chapte	er Summary	60
5	EXA	CT PER	RFORMANCE ANALYSIS OF MAXIMAL RATIO TRANSMISSION	
	WIT	H MUI	TI-HOP DECODE-AND-FORWARD INTERFERENCE-LIMITED	
	REL	AYING	SYSTEM OVER WEIBULL FADING CHANNEL	61
	5.1	Introd	uction	61
	5.2	Systen	n and Channel Models	63
	5.3	SIR St	atistical Analysis	65
		5.3.1	The CDFs Derivation	65
		5.3.2	The PDFs Derivation	72
5.4 Performance a		Perfor	mance analysis	74
		5.4.1	Outage Probability	74
		5 4 2	Average Bit Error Probability	75

		5.4.3 Asymptotic Analysis	76	
	5.5	5 Numerical Results and Discussion		
	5.6	Chapter Summary	82	
6	RESULTS AND DISCUSSION			
	6.1	Conclusions	83	
	6.2	Future Works	84	
RE	FERE	ENCES	86	
A	Deri	rivation of (3.20)		
В	Deri	rivation of (3.41)		
С	Deri	erivation of (4.11)		
D	Deri	Derivation of (4.13)		
E	Deri	Derivation of (4.16)		
F	Deri	vation of (4.19)	104	
PU	PUBLICATIONS FROM THE THESIS			

LIST OF SYMBOLS

Binomial coefficient equivalent to $a!/b!(a-b)!$
bold letter denote vector
CDF of the random variable X
expectation of a random variable X
Fox's H-function
Frobenius norm
Gamma function
Hermitian transpose (conjugate transpose)
italic letter specify scalar variable
lower incomplete Gamma function
Meijer's G-function
PDF of the random variable X
Pochhammer's symbol equivalent to $\Gamma(a+s)/\Gamma(a)$
standard Gaussian tail probability function
transpose
Tricomi confluent hypergeometric function
upper incomplete Gamma function

LIST OF ABBREVIATIONS

AF amplify-and-forward

G_a array gain (coding gain)

ABEP average bit error probability

AEP average error probability

CEE channel estimation error

CSI channel state information

CCI co-channel interference

CDF cumulative distribution function

DF decode-and-forward

 G_d diversity gain

EGC equal gain combining

ESR ergodic sum rate

EGBMGF extended generalized bivariate Meijer G-function

i.i.d independent and identically distributed

i.n.i.d independent and non-identically distributed

INR interference-to-noise ratio

LOS line of sight

MRT maximal ratio transmission

MRC maximum ratio combining

MMSE minimum mean square error

MGF moment generating function

MIMO multiple-input multiple-output

MISO multiple-input single-output

N-LOS non-line of sight

OWRNs one-way relay networks

OP outage probability

PDF probability density function

SC selection combining

SIR signal-to-interference ratio

SINR signal-to-interference-plus-noise ratio

SNR signal-to-noise ratio

SIMO single-input multiple-output

SISO single-input single-output

STBC space-time block code

STC space-time code (Alamouti's code)

SSER sum symbol error rate

SER symbol error rate

TAS transmit antenna selection

TWRNs two-way relay networks

LIST OF FIGURES

Figure 2.1	Emerging communication networks [36]	11
Figure 2.2	Cooperative Relaying Schemes	13
Figure 2.3	Relay categories	14
Figure 2.4	Maximal Ratio Transmission Vs Maximum Ratio Combining	15
Figure 3.1	Block diagram of TWRN with maximal ratio transmission and CCI	
	at the relay.	21
Figure 3.2	System outage probability considering different SIR values, $\gamma_{\rm th}=0$	
	dB and $N = 6$	35
Figure 3.3	System outage probability of AF-TWRN with CCI for different	
	number of antennas, $\gamma_{th} = 0$ dB	36
Figure 3.4	System outage probability of AF-TWRN with different numbers of	
	co-channel interference signals, $\gamma_{\rm th}=0$ dB and $L_1=L_2=2.$	36
Figure 3.5	System outage probability with different values for the constant	
	interference power, $\gamma_{\rm th}=0$ dB and $L_1=L_2=2.\dots\dots$	37
Figure 3.6	Sum SER performance of AF-TWRN with CCI for different number	
	of antennas	37
Figure 3.7	Sum SER performance of AF-TWRN with CCI for different number	
	of interference signals, $L_1 = L_2 = 2$	38
Figure 3.8	Achievable sum rate with different numbers of CCI Signals, power	
	and different number of antennas	39
Figure 3.9	System outage probability of AF-TWRN with CCI and different CEE	
	values, $\gamma_{th} = 0$ dB and $L_1 = L_2 = 2$	39
Figure 3.10	System outage probability vs SINR threshold for different number	
	of antennas, $P_I = 10$ dB and $\Omega_{e_1} = \Omega_{e_2} = 0.01$	40
Figure 3.11	Sum SER performance of AF-TWRN with different number of	
	antennas, different values of CEE, $P/P_I = 30$ dB and $N = 6$	41
Figure 4.1	Block diagram of dual-hop maximal ratio transmission with CCI at	
	the relay and destination	45
Figure 4.2	Outage probability as a function of average SNR for different	
	number of antennas with constant signal-to-interference ratio	55

Figure 4.3	Outage probability as a function of average SNR for different	
	Nakagami-m fading severity parameter with constant	
	signal-to-interference ratio	55
Figure 4.4	Average bit error probability as a function of average SNR for	
	different number of antennas with constant signal-to-interference	
	ratio	56
Figure 4.5	Average bit error probability as a function of average SNR for	
	different number of antennas with constant interference power	56
Figure 4.6	Average bit error probability as a function of average SNR with	
	different values of the constant interference power	57
Figure 4.7	Ergodic capacity as a function of average SNR for different number	
	of CCI signals with constant signal-to-interference ratio	58
Figure 4.8	Ergodic capacity as a function of average SNR for different number	
	of antennas with constant interference power	59
Figure 5.1	Block diagram of MRT based multi-antenna multi-hop	
	decode-and-forward (DF) relaying networks with co-channel	
	interference	64
Figure 5.2	Outage probability versus average per-hop signal power for the	
	direct and multi-hop cooperative links, $N = 1, 3. \dots$	78
Figure 5.3		
	multi-hop with different fading parameter values, $N = 3$	79
Figure 5.4	Outage probability versus per-hop average signal-to-interference	
	ratio for the multi-hop with different interference fading parameter	
	values, $N = 3$	79
Figure 5.5	Average bit error probability versus per-hop average	
	signal-to-interference ratio for the multi-hop with different	
_	number of antennas, $N = 3$	80
Figure 5.6	Average bit error probability versus average per-hop signal power	
	for the multi-hop with different interference power values, $N = 3$.	81

Maximal Ratio Transmission Based Multiple Antenna Relaying Systems With Interference

Awfa A. M. Ali ALADWANI

Department of Electronics and Communications Engineering
Doctor of Philosophy Thesis

Advisor: Assoc. Prof. Dr. Tansal GÜÇLÜOĞLU

The use of multi-antennas techniques has been well-known for increasing wireless communication reliability by providing more diversity gains. However, due to increased computational complexity at the receiver, only a few of many multi-input multi-output (MIMO) techniques are practically preferable. Maximal ratio transmission (MRT) approach is one of those simple and thus feasible MIMO techniques (e.g., Alamouti scheme). MRT can achieve full spatial diversity without increasing receiver complexity. Thus, it is highly suitable for transmissions from base stations to the size, delay, and power-constrained mobile units and relays in cooperative communication such as a two-way relaying network (TWRN) and one-way relaying network (OWRN). On the other hand, Co-channel interference (CCI) is one of the significant factors that degrade a wireless communication network's performance. For instance, In the next-generation cellular networks, CCI will increase further since the number of users in the same cluster increases, and there will be many sensors, IoT, and WiFi devices. Moreover, the size of the cells will decrease to increase energy efficiency and reduce latency. Thus, there will be more cells using the same frequency due to frequency reuse of limited bandwidth. Besides, the deployment of cognitive and non-orthogonal multiple access methods will make the CCI level climb further. Therefore, it is highly essential to investigate and reduce the impact of CCI on the performance of popular relaying schemes. Motivated by that, in the third chapter of the thesis, we analyzed the reliability of amplify-and-forward (AF) TWRNs system under Raleigh fading and co-channel interference impairment by using the MRT technique. Moreover, in the

fourth chapter and under Nakagami-m fading channel, the employing of MRT is investigated on decode-and-forward (DF) dual-hop relaying networks working in an interference environment. Besides, chapter five of the thesis explored the performance enhancement by applying MRT on the proposed multi-antenna multi-hop relaying network in interference-limited environment undergoing the critical Weibull fading channel. In all proposed systems, many analytical results are derived and validated by Monte-Carlo simulation via extensively numerical examples. The investigations infer that MRT can be a good option for next-generation wireless communication networks to suppress the performance losses and limitations of CCI in a low complexity way.

Keywords: Multiple-input multiple-output, relaying system, maximal ratio transmission, co-channel interference, Nakagami-m and Weibull fading channels.

YILDIZ TECHNICAL UNIVERSITY GRADUATE SCHOOL OF NATURAL AND APPLIED SCIENCES

Maksimum Oran İletim Tabanlı Girişimli Çoklu Anten Röleleme Sistemleri

Awfa A. M. Ali ALADWANI

Elektronik ve Haberleşme Mühendisliği Anabilim Dalı Doktora Tezi

Danışman: Doç. Dr. Tansal GÜÇLÜOĞLU

Çoklu anten tekniklerinin kullanımının daha fazla çeşitlilik kazanımı sağlayarak kablosuz iletişim güvenilirliğini arttırdığı iyi bilinmektedir. Bununla birlikte, alıcıdaki artan hesaplama karmasıklığı nedeniyle, çoklu-giris çoklu-çıkış (MIMO) tekniklerinin sadece birkaçı pratik olarak tercih edilmektedir. Örneğin, maksimum oran iletim (MRT) yaklaşımı, basit ve pratikte uygulanabilir MIMO tekniklerinden biridir. MRT, alıcı karmaşıklığını arttırmadan tam uzaysal çeşitlilik elde edebilir. Bu nedenle, baz istasyonlarından boyut, gecikme ve güç kısıtlamalı mobil üniteler ve rölelerle iletişimdeki iki yönlü röle ağı (TWRN) ve tek yönlü röle ağı (OWRN) gibi işbirlikli iletimde son derece uygundur. Diğer yandan, ortak-kanal girişimi (CCI), bir kablosuz iletişim ağının performansını düşüren önemli faktörlerden biridir. Örneğin, yeni nesil hücresel şebekelerde, aynı kümedeki kullanıcı sayısı, sensör, IoT ve WiFi cihazları artacağı için CCI daha da artacaktır. Dahası, enerji verimliliğini artırmak ve gecikmeyi azaltmak için hücrelerin boyutu küçülecektir. Böylece, sınırlı bant genişliğinin tekrar kullanımı nedeniyle aynı frekansı kullanan daha fazla hücre olacaktır. bilişsel-radyo ve dikey olmayan çoklu erişim yöntemlerinin uygulanması ile CCI seviyesi daha da yükselecektir. Bu nedenle, popüler röleleme yapılarının performansı üzerindeki CCI etkisini araştırmak ve azaltmak son derece önemlidir. Bu motivasyonla bu tezde, MRT tekniğini kullanarak Raleigh sönümlemesi ve ortak kanal girişim bozukluğu altında güçlendir ve ilet (AF) TWRN sistemlerinin güvenilirliği analiz edilmektedir. Ayrıca, Nakagami-m sönümleme kanalındaki MRT kullanımının bir girişim ortamında çalışan çöz ve ilet (DF) çift sekmeli aktarma ağları üzerindeki etkisi araştırılmaktadır. Ek olarak, Weibull sönümleme kanalındaki girişim sınırlı çok antenli, çok sekmeli aktarma ağınad MRT uygulandığındaki performans artışı sunulmaktadır. Önerilen tüm sistemlerde, çok sayıda analitik sonuç, kapsamlı sayısal örnekler için türetilip Monte-Carlo simülasyonu ile doğrulanmaktadır. Araştırmalar, MRT'nin yeni nesil kablosuz iletişim ağlarındaki CCI nedeniyle oluşan performans kayıplarını ve sınırlamalarını düşük karmaşıklıkla bastırması için iyi bir seçenek olabileceğini göstermektedir.

Anahtar Kelimeler: Çok girişli çoklu çıkış, röle sistemi, maksimum oran iletimi, ortak kanal girişimi, Nakagami-m ve Weibull sönümleme kanalları.

VII DIZ TEVNÍV ÜNÍVEDSÍTESÍ

1 INTRODUCTION

1.1 Literature Review

For the ever-increasing need for multimedia content, upcoming wireless technologies aspire to reach higher data speeds and more efficient quality of service (QoS). However, multi-path fading and co-channel interference (CCI) have been challenging limitations to achieve that, especially with the conventional single-input single-output (SISO) wireless networks [1, 2]. Furthermore, wireless channels can undergo severe fading and result in unreliable communication, so increasing the system's diversity order is highly desirable to reduce the probability of deep fading. As a result, several transmission and reception techniques have been developed and utilized to increase system diversity orders. For example, the maximal ratio transmission (MRT) scheme can be used when the transmitter has multiple antennas. It results in low receiver complexity while reaping the benefits of increased diversity, while the well-known maximum ratio combining (MRC) can be used when the receiver has multiple antennas. In general, the fundamental concept of these approaches is increasing the variety of spaces (antennas) by transmitting or receiving several replicas of the information signal [3, 4].

Similar to multiple antenna transmission, cooperative/relaying communications proposed in [5, 6], are favored to provide extremely high speed, power-efficient, reliable, and wide coverage wireless communication systems by exploiting a nearby mobile unit or fixed relays. Consequently, research on the well-known two-way relaying networks (TWRN) has been applied to the current communication scenarios [7–9]. For example, authors in [7] present the scheme of overlay cognitive radio with TWRN. Besides, the model of TWRN with non-orthogonal multiple access (NOMA) is proposed in [8]. Likewise, one-way relaying networks (OWRNs) has also been studied recently. Specifically, Cai et al. [10] explore device-to-device communications while physical layer security (PLS) of OWRN is investigated in [11]. Furthermore, Solanki et al. [12] deals with cognitive radio (CR), hardware impairment, and channel estimation error (CEE).

Maximal Ratio Transmission (MRT) has been proposed by [3] to achieve maximum signal to noise power ratio at the receiver by adjusting the scaling factors of transmit antennas. MRT can achieve full diversity order while not increasing the computational complexity of the receiver. It has become popular since complexity increases the size and power consumption of mobile units, which is a significant problem, especially in wireless sensor networks (WSN) and the internet of things (IoT). In [13], the authors investigated a scenario of TWRN over Nakagami-m fading channels. When two sources each have multiple antennas communicate via a single antenna relay using AF technique, they analyzed and compared the SSER of two schemes: MRT beamforming and antenna selection. Yadav et al. [14] evaluated the impact of adopting MRT on the AF TWRN system and investigate the optimization problem of the joint power allocation and relay location to minimize the system error probability. Similarly, [15] deals with the performance of an AF-TWRN-MRT with relay selection and derive OP and SER over Nakagami-m fading channels. Recently, Kefeng et al. [16] analyze the outage probability, throughput, and energy-efficiency of AF-TWRNs employing MRT/MRC at the relay node under the effect of hardware impairment. Likewise, MRT's performance with the one-way DF relaying has been investigated over Rayleigh fading [17] and Nakagami-m fading channels [18]. The error performance of the dual-hop AF relaying with MRT over Nakagami-m fading is presented in [19]. Similarly, Eylem et al. [20] derive an upper-bound outage, lower-bound error probabilities, and ergodic capacity for AF relaying system over Rayleigh fading channel. Furthermore, an error probability of multi-hop DF relay networks with MRT over cascaded Nakagami-m fading channel is studied in [21]. All of the above MRT related works considered noise-limited scenarios and neglected the effects of co-channel interference.

On the other hand, due to the drawback of wireless communication, co-channel interference is a serious problem, especially in cellular systems. Due to spectrum reuse, it will increase even more in next-generation networks containing a tremendous number of devices, i.e., when wireless standards adopt Cognitive Radio and NOMA techniques, allowing transmission with CCI to increase the user capacity. In practice, cooperative communications often suffer from co-channel interference. Attentive to this, the influence of co-channel interference has been examined in the scope of wireless relaying networks (e.g., [22–25] and references therein). More specifically, in [22] the performance of two-way AF relaying systems has been investigated over (i.n.i.d.) Rayleigh fading channel with the effect of a finite number of CCI, where all nodes have a single antenna, the authors obtained the outage probabilities, and SEP used the harmonic mean upper bound of the SINR random variable to derive their closed-form results. In [25], the outage probability, error rate, and

achievable rate are investigated for an AF TWRN when all the two noisy-nodes and the interference-limited relay having a single antenna. Besides, the two-way interference-limited AF relaying system's performance in terms of system outage probability and SEP is analyzed in [24] over (i.n.i.d.) Nakagami-m fading channels. The authors also solved practical optimization problems analytically to enhance system performance by minimizing the outage probability. Furthermore, the ergodic capacity of AF relaying systems in the presence of interference over Nakagami-m fading for dual-hop [26], and multi-hop [27] are provided when all terminals are equipped with a single antenna.

1.2 Objective of the Thesis

MRT based AF-TWRN with CCI is studied in chapter three. Obviously, TWRNs are popular in the literature since they allow the exchange of information within two time slots compared to the use of four time slot when dual hop transmission is employed between two sources. Therefore, TWRNs can be useful in increasing the range/coverage or decreasing the transmit power to have higher energy efficiency in a spectrally efficient way. Co-channel interference (CCI) is one of the major limitations for reliability and capacity especially in cellular networks which will contain more users and base stations in the future as small cells and IoT are becoming popular. Although CCI is unavoidable, there are few works considering CCI in communication scenarios since the mathematical analysis is quite complicated. The use of MIMO techniques have been well known for increasing reliability by providing more diversity gains. However, due to increased computational complexity of the receiver, only few of many MIMO techniques are practically preferable. MRT approach is one of those simple and thus feasible MIMO techniques (e.g. Alamouti scheme). MRT can achieve full spatial diversity without increasing receiver complexity and thus highly suitable for transmissions from base stations to the size, delay and power constrained mobile units and relays in cooperative communication such as TWRNs. In our system model, we assume Rayleigh fading which is common when there is no strong component due to line of sight. With the motivation of investigating the use of MRT based AF-TWRN in cellular, Wi-Fi or ad-hoc and sensor networks, we investigate the performance of two-way relaying systems with multiple co-channel interferers at the single antenna AF relay and two sources (e.g., base stations, access points, coordinators or routers) having multiple antennas. Our contributions start with obtaining the upper bound of the cumulative distribution function of SINR. Then, tight lower bound expressions of OP, SER and upper bound of system ergodic sum rate are derived and illustrated with extensive numerical examples. Besides, the effect of channel estimation errors, the array and diversity gains are investigated too. We believe our results are important since impact of CCI can be considerably eliminated by employing MRT.

Furthermore, in chapter four, the considered low complexity DF dual-hop MRT scheme which can be a preferable low-cost solution for high speed and reliable wireless networks, such as, next generation cellular networks with coordinated base stations having massive multiple antennas serving to internet of things (IoT) devices or utilizing low complexity relays to extend coverage for terminals with limited mobility. Moreover, DF OWRN MRT can also be good fit for coverage extension in road-side vehicular relaying systems and coordinator devices of wireless sensor and actuator systems. In addition, due to the mathematical difficulty of analyzing the general case (i.e., MRT with multi-antenna relaying networks impaired by finite number of CCI signal at the relay and destination nodes), most of the existing studies have only analyzed outage probability and/or considered single antenna nodes and/or some CCI-free nodes. The novelty of this work comes from the fact that there is no previous work which studied the improvement of reliability in one-way relay networks under co-channel interference by using the low complexity MRT technique. In this chapter, we have derived an exact expression for OP, ABEP, ergotic capacity performances of dual-hop DF undergo Nakagami-m fading channels with co-channel interference. We have compared performances with some numerical examples and illustrated how much can MRT suppress the adverse effects of CCI in the mentioned system. Finally, the theoretical results are validated with Monte-Carlo simulations.

Finally, in chapter five, we investigate the multi-hop communications based MRT and co-channel interference, which can be a practical model in wireless sensor networks, and one of the solutions to mitigate the path-loss in mmWave channels. In general, we need the sum of multiple random variables which is the essential key point to investigate the performance of MRT and MRC (similarly, the arbitrary number of CCI). Likewise, the ratio of two RVs is another challenge to evaluate CCI studies is wanted too. To the best of our knowledge, the sum and ratio of Weibull RVs do not present in literature. However, the majority of previous studies have only analyzed a noise-limited system with single antenna nodes or direct link with limited cases (i.e., integer Weibull parameter, i.i.d random variable, etc.). The remainders used the approximated PDF of the sum or ratio (approximated by Padé approximation method, or approximate the Weibull PDF to a simpler distribution and estimate the parameter by moment based estimation method, or assuming large number of Weibull RVs, then approximate the PDF of the sum as normal distribution PDF using Gaussian limit theorem). A comprehensive investigation for MRT (nor MRC) based multi-hop DF relaying with CCI has not been investigated yet. Thus, in this study, novel exact statistics expressions are provided for MRT-based multi-antenna multi-hop decode-and-forwards system under the impact of co-channel interference. Specifically,

the desired power distribution CDF, PDF and MGF are derived. Then, the CDF and PDF of the equivalent per-hop and end-to-end (e2e) system SIR are computed. Furthermore, exact average bit error and outage probabilities are obtained for the Weibull fading channel.

1.3 Hypothesis

This thesis deals with three different cooperative relaying networks, which all have attracted considerable interest recently due to their numerous advantages and practical usages. Specifically, to provide extremely high speed, power-efficient, reliable, and wide coverage wireless communication systems by exploiting a nearby mobile unit or fixed relays. In the MRT based AF-TWRN with CCI scenario, the Rayleigh fading channel is assumed. This channel is commonly used to model the multi-path fading when non-line of sight (N-LOS) between the transmitter and receiver is present. Besides, only the relay node is impaired by multiple CCI signals and noise. In practice, small size and low complexity user can behave as a relay to establish reliable links between two base stations in a cellular network, or two routers in a WiFi network, or between two coordinators in a wireless sensor network when larger range and better energy efficiency are needed. If the selected user is close to the edge of cells/clusters, then the CCI level can be considerable compared to negligible CCI at two source terminals, which can be at the center of neighboring cells. In the second scenario, i.e., the dual-hop decode-and-forward (DF) relaying network with an arbitrary number of co-channel interference signals with noise at the relay and destination nodes, the independent and non-identically distributed (i.n.i.d) Nakagami-m fading distribution which adequately describes the empirical and experimental data is used. Moreover, receivers are assumed to know the desired channel coefficients perfectly but know nothing about the interferer channels, which can be considered a "worst-case" scenario. In MRT based multi-hop decode-and-forward (DF) relaying Interference-limited networks, our third scenario in chapter five, all the channels between the nodes and the interference signals are subject to independent and non-identically distributed (i.n.i.d) Weibull fading channels. This channel characterizes the amplitude fading, particularly associated with mobile radio systems operating in the 800/900 MHz spectrum and modeling the current 5G millimeter wave (mmWave) applications such as cellular communication and the Internet of Things (IoT). Furthermore, each i-th receiver node (where i = $1, \dots, N$) in the network is impaired by a single dominant interferer from an external source. It is worth mentioning that the assumption of a single dominant interference signal in this scenario is practical and important. For example, in a well planned cellular network, the system will likely be subjected to a single dominant interferer.

1.4 Organization

The thesis is organized as follows:

- Chapter 2 gives brief description about wireless systems, wireless channels, interference modeling, space diversity techniques, cooperative networks and the important mathematical tools.
- In chapter 3, MRT technique is proposed as a solution for AF-TWRNs to suppress the performance loss caused by unavoidable CCI plus noise distortion at the single antenna relay receiver. The novelty of this investigation comes from the fact that there is no previous work which studied the improvement of reliability in two-way relay networks under co-channel interference by using the low complexity MRT technique. Our comprehensive analysis provides with the OP, SER, ESR performances, array and diversity gains as well as the effect of channel estimation errors. We have compared performances with some numerical examples and illustrated how much can MRT suppress the adverse effects of CCI in TWRNs. Note that the presence of CCI completely changes the SNR statistics and the performance, therefore it is not similar to other existing TWRN studies. Unlike many papers presenting only lengthy OP expressions, we have provided closed form SINR, OP, SER, ESR, array and diversity gain results which are quite useful for system designers.
- In chapter 4. exact expressions of performance indicators decode-and-forward dual-hop relaying with MRT are derived and verified by simulation results over Nakagami-m channels. The investigations of the proposed system are started with probability density, cumulative distribution functions of the signal-to-interference-plus-noise ratio (SINR) RV derivations. Then, average error probability, outage probability, and ergodic capacity are derived. Due to the co-channel interference effect on the relay and destination nodes, we show that the performance degradation can be overcome with the use of low complexity MRT approach.
- Chapter 5 proposes a novel mathematical techniques to derive the exact SIR statistics of multi-antenna multi-hop relaying system with MRT. under the well-known weibull fading channel, we obtaining the desired power distribution CDF, PDF and MGF. Then, the CDF and PDF of the equivalent per-hop and end-to-end (e2e) system SIR are provided. Furthermore, exact and asymptotic expressions of error and outage probabilities are derived and validated by Monte-Carlo simulation.

• Chapter 6 provides the conclusions of the thesis and some future works are also presented.

1.5 Notations

Bold letters denote vectors where italic symbols specify scalar variables. The following symbols $(\cdot)^T$, $(\cdot)^H$ and $\|\cdot\|$ are used for transpose, Hermitian transpose and Frobenius norm, respectively. $\Pr[\cdot]$, $\mathbb{E}[\cdot]$, $f_X(\cdot)$ and $F_X(\cdot)$ represent probability, expectation operation, probability density function (PDF) and cumulative distribution function (CDF) of a random variable (RV) X, respectively. Binomial coefficient shown as $\binom{a}{b}$ is equivalent to a!/b!(a-b)! while the standard Gaussian tail probability function Q(x) is defined as $(1/\sqrt{2\pi})\int_x^\infty e^{-t^2/2}dt$.

2 BACKGROUND

In this section, the basic ideas which can be useful to understand the presentation of the thesis better, is given. Specifically, Wireless Communication Systems, wireless channel models, interference modeling, system Performance evaluation tools, and space diversity techniques.

2.1 Wireless Communication Systems

Wireless communications can be described as the data transmission from one place to another through wireless medium by using electromagnetic waves [28]. The received signal (y) for a single-input single-output (SISO) system over fading channel h (denote the channel coefficient) can be mathematically expressed as

$$y = hx + n, (2.1)$$

where n is the additive white Gaussian noise (AWGN) and x denote the transmitted symbol. Generally, two phenomena named large-scale and small-scale effects badly on wireless channels [28]. Large-scale, includes path loss and shadowing. The path loss depends on the distance between transmitter and receiver and can reduce the received SNR. Shadowing on other hand, deteriorates the signal quality due to the transmitter-receiver obstacles. The small-scale effect known as multi-path fading is the attenuation deviation varies with time or frequency, resulting in multi-dimensional transmitted signal deviation.

2.2 Wireless Channel Modeling

In recent decades, wireless networking has grown dramatically to satisfy the increasing demand for high data levels [29]. Indoor and outdoor applications systems were developed where mobility is a very significant feature that limits the system

performance. One key element in designing these systems is understanding the wireless channel characteristics. When the amplitude of obtained signals fluctuates, it will follow various statistical distributions [30]. Thus, examples of major distributions of wireless channels (i.e., Rayleigh, Nakagami-m, and Weibull distributions) are provided below.

2.2.1 Rayleigh Fading Channel

The Rayleigh distribution is typically used to model the multi-path fading when non-line of sight (N-LOS) between the transmitter and receiver is presents. The PDF of the Rayleigh distribution is expressed as [31]

$$f_X(x) = \frac{2x}{\sigma^2} \exp\left(-\frac{x^2}{\sigma^2}\right),\tag{2.2}$$

where $(x \ge 0)$ and $(\sigma^2 = E[X^2])$ are the envelope (i.e., the channel fading amplitude) and average power of the envelope, respectively. Let X^2 be the squared envelop (i.e., the channel gain), using [32],

$$f_{X^2}(x) = \frac{f_X\left(\sqrt{x}\right)}{2\sqrt{x}},\tag{2.3}$$

by substitute (2.2) into (2.3), results

$$f_{X^2}(x) = \frac{1}{\bar{\gamma}} \exp\left(-\frac{x}{\bar{\gamma}}\right),\tag{2.4}$$

where $f_{X^2}(x)$ is the PDF of the instantaneous SNR, while $(\bar{\gamma} = PE[X^2]/N_o)$ denote the average SNR per received symbol.

2.2.2 Nakagami-m Fading Channel

The Nakagami fading distribution adequately describes the empirical and experimental data compared to the Rayleigh distribution [33]. The received signal envelope has a PDF expressed as

$$f_X(x) = \left(\frac{2m}{\sigma^2}\right)^m \frac{x^{2m-1}}{\Gamma(m)} \exp\left(-\frac{m}{\sigma^2}x^2\right),\tag{2.5}$$

where $(m \ge \frac{1}{2})$ is the Nakagami-m fading parameter. The severity of this channel

depend inversely on (m) value, i.e., small value correspond to severe fading conditions. In addition, Nakagami-m fading distribution can model many other fading channels readily by selecting a specific values of fading parameter m, such as, one-sided Gaussian (m=1/2), Rayleigh (m=1) and Rician with K factor $(m=(K+1)^2/(2K+1))$ distributions. by substitute (2.5) in (2.3), the distribution of received signal power (received SNR) can derived as

$$f_{X^2}(x) = \left(\frac{m}{\bar{\gamma}}\right)^m \frac{x^{m-1}}{\Gamma(m)} \exp\left(-\frac{m}{\bar{\gamma}}x\right). \tag{2.6}$$

2.2.3 Weibull Fading Channel

In a multi-path environment, the Weibull distribution characterizes the amplitude fading, particularly that associated with mobile radio systems operating in the 800/900 MHz spectrum [32, 34]. The Weibull probability density function can be written as

$$f_X(x) = \beta \left(\frac{\omega}{\sigma^2}\right)^{\frac{\beta}{2}} x^{\beta - 1} \exp\left(-\left(\frac{\omega}{\sigma^2}x^2\right)^{\frac{\beta}{2}}\right), \tag{2.7}$$

The parameters $\omega = \Gamma\left(1 + \frac{2}{\beta}\right)$, and $(\beta > 0)$ are Weibull fading parameter. As β increases, the severity of the fading decreases. In the special case when $\beta = 1$, Weibull distribution becomes an exponential distribution, and for $\beta = 2$ proposed channel becomes Rayleigh distribution [35]. by using (2.3), results

$$f_{X^2}(x) = \frac{\beta}{2} \left(\frac{\omega}{\bar{\gamma}} \right)^{\frac{\beta}{2}} x^{\frac{\beta}{2} - 1} \exp\left(-\left(\frac{\omega}{\bar{\gamma}} x \right)^{\frac{\beta}{2}} \right), \tag{2.8}$$

which is the PDF of the received SNR.

2.3 Interference Modeling

Co-channel interference (CCI) is one of the major factors that degrades the performance of a wireless communication network [37, 38]. Specifically, it can be a serious problem effects the coverage, reliability, and throughput. In cellular networks, CCI will increase further since the number of users in the same cluster increases. For example, there will be ultra-dense networks, device-to-device communication, IoT, vehicular ad-hoc networks, and intelligent transportation systems as shown

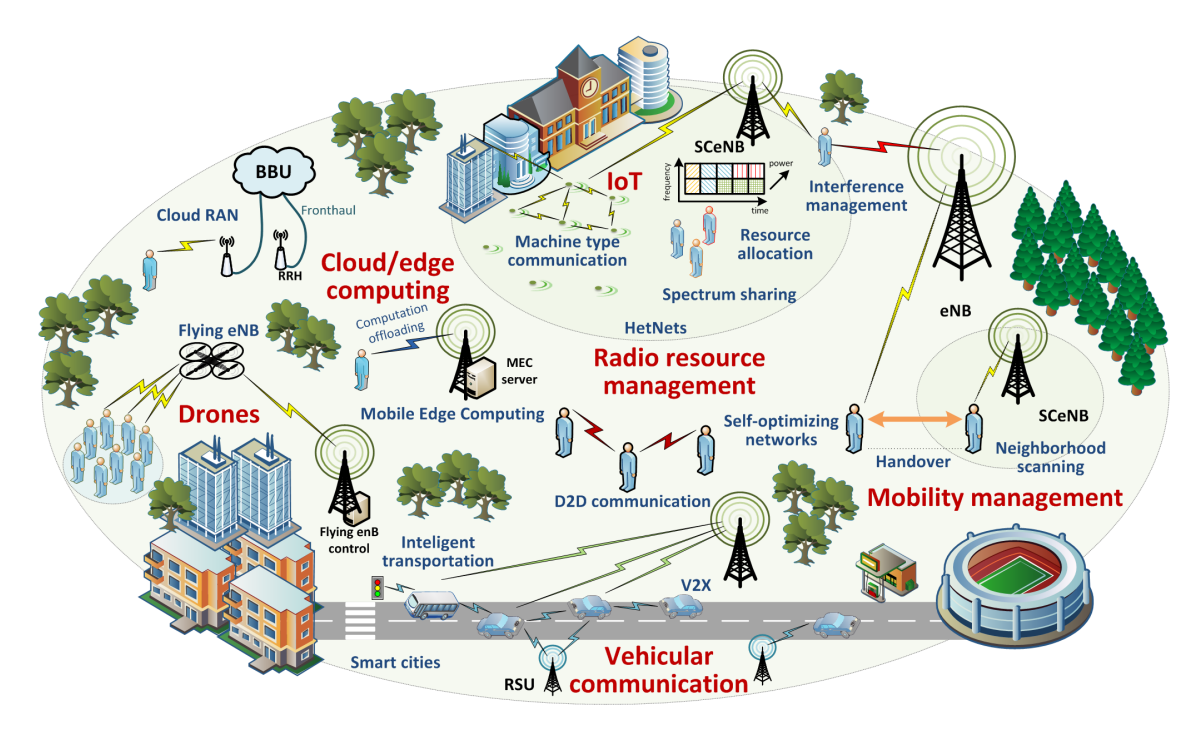


Figure 2.1 Emerging communication networks [36]

in Figure 2.1. Moreover the size of cells will decrease for energy efficiency and reduction of latency and thus there will be more cells using the same frequency due to frequency reuse of limited bandwidth [39–41]. Besides, deployment of cognitive and non-orthogonal multiple access method will make CCI level climb further [42, 43]. Co-channel interference is caused by the signals of other users and applications using the same frequency band [44]. There are two general models for interference. Let us start with the conventional model named (Interference plus noise scenario). When the received signal (y) for a single-input single-output (SISO) system under the fading channel (h) (denote the channel coefficient) can be mathematically expressed as

$$y = h x + \sum_{i}^{N} h_{Ii} x_{Ii} + n, (2.9)$$

where h_{Ii} and x_{Ii} denote the channel coefficient and transmitted symbol of the i-th interference signal, and N is the number of CCI signal. The signal-to-interference-plus-noise ratio (SINR) in this scenario can be written as

$$SINR = \frac{P_S |h|^2}{P_I \sum_{i}^{N} |h_{Ii}|^2 + N_o} = \frac{\gamma}{\gamma_I + 1},$$
 (2.10)

denote $\gamma = P_S |h|^2/N_0$ and $\gamma_I = P_I \sum_i^N |h_{Ii}|^2/N_0$ as instantaneous SNR and instantaneous interference-to-noise ratio (INR) of the desired and interference signals

at the receiver, respectively. Besides, P_S , P_I , h_{Ii} , and N_o are the desired signal transmitted power, interference power, channel coefficient of i-th CCI signal, and noise variance, respectively.

The second interference model named (Interference limited scenario) can be modeled if the CCI power (P_I) is high compared with the noise power (N_o) such that the impact of noise is negligible. Thus, the expression in (2.10) can be reduced to the signal-to-interference ratio (SIR) as

$$SIR = \frac{\frac{P_S|h|^2}{N_o}}{\frac{P_I \sum_{i}^{N} |h_{Ii}|^2}{N}} = \frac{\gamma}{\gamma_I},$$
 (2.11)

Note that, the influence of interference depends on the amount and location of the interferers [45, 46]. However, the number and location of the interfering sources may be determined based on the type of wireless network, i.e., whether the network is either planned, unplanned, or hybrid [47, 48]. In this thesis, We analyze only the planned networks. Nevertheless, the study presented can readily be generalized to support other networks.

2.4 Space Diversity Techniques

2.4.1 Cooperative Relaying

Cooperative diversity suggested in [5, 6], is accomplished using relays receiving the source signal and transmitting them to the destination. Typically, these systems operate over two phases. The signal transmitted from the source is received by single or multiple relays in the first phase. In the second one, orthogonal (non-interfering) channels could be used by relay to transmit the destination signal after certain processing. Destination combines the relay transmitted signals and the direct signal from the first phase to improve the SNR. This process creates several fading channels between the source and the destination. Since the relays are usually in various physical locations, spatial separation of the relays leads to independent fading, eventually generating a diversity gain.

2.4.1.1 Two-way and One-way Relaying

One-way (dual-hop) half-duplex relay networks which shown in Figure 2.2 (b), lose half of the throughput compared to the direct communication due to the fact that the relay cannot transmit and receive simultaneously. To overcome this drawback, a

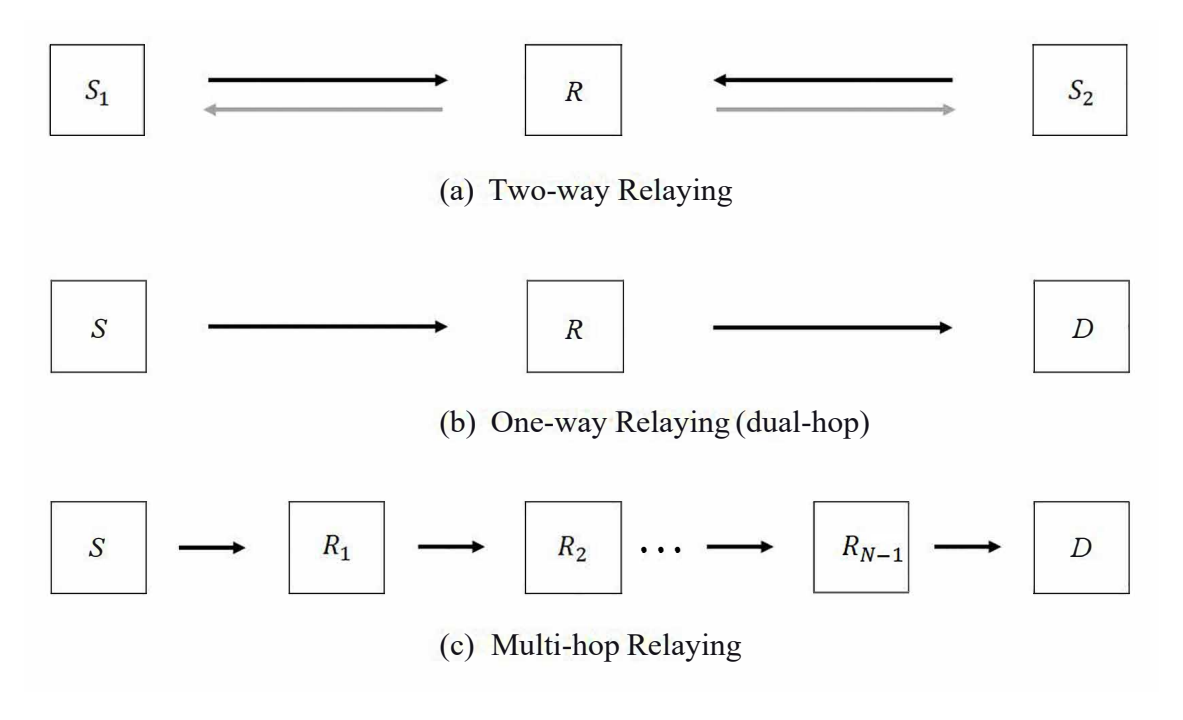


Figure 2.2 Cooperative Relaying Schemes.

two-way (or bi-directional) relay network is proposed as in Figure 2.2 (a), where two nodes, namely S_1 and S_2 , transmit simultaneously to the relay R in the first phase, and in the second phase the relay R forwards its received signals to both terminals S_1 and S_2 . With this strategy, this loss of throughput can be remarkably compensated.

2.4.1.2 Multi-hop Relaying

In multi-hop relaying, a transmission between a source node *S* and destination node *D* is composed of multiple hops as illustrated in Figure 2.2 (c). Multi-hop transmission can significantly reduce the transmit power compared to direct communications. In addition, because of transmit power constraints, multi-hop transmission also leads to remarkable coverage extensions by dividing a total end-to-end transmission into a group of shorter paths.

2.4.1.3 Relay Categories

Relays can be user nodes or fixed terminals known as infrastructure relays. According to their processing functionality, can be divided in to two major categories, Amplify-and-Forward (AF), Decode-and-Forward (DF) as shown in Figure 2.3. Although AF and DF have the same diversity order for the same system. Amplify forward (AF) relaying is computationally less complex than decode and forward (DF) approach. However, the AF performs worse than DF because it transmits the noisy signal with the interference as well. The system enhancement becomes

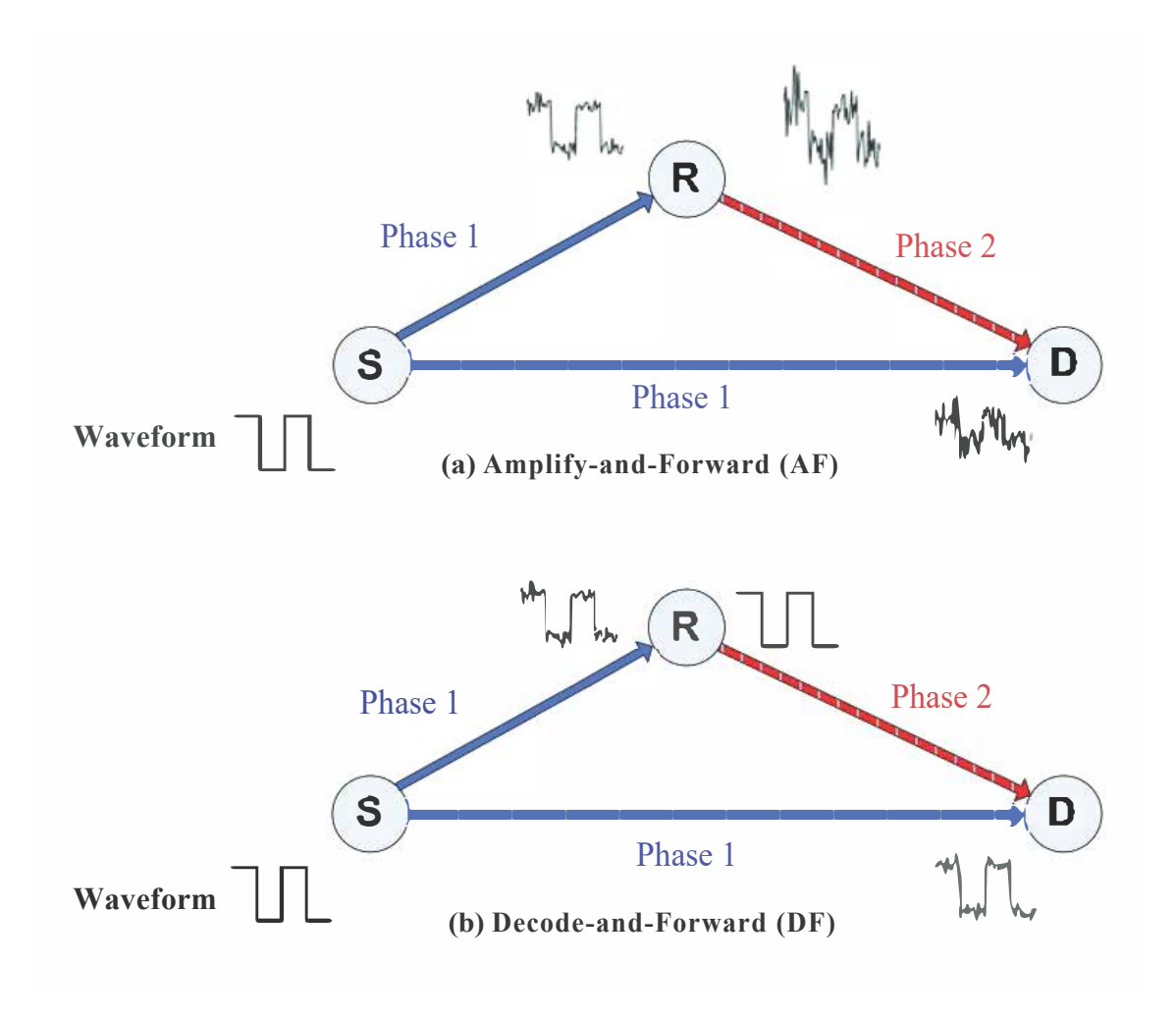


Figure 2.3 Relay categories.

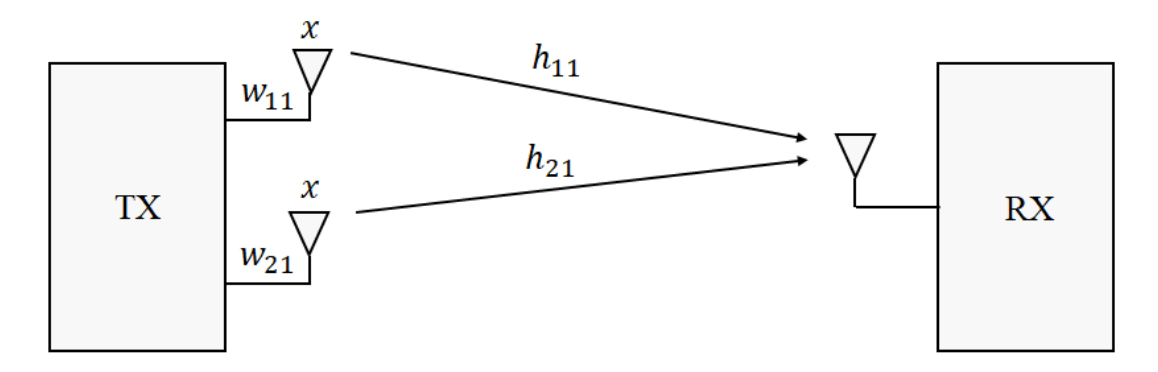
critical especially when noise and/or interference has a high power. DF can be more preferable considering the increased interference in the next generation wireless systems exploiting cognitive radio and non-orthogonal multiple access (NOMA) approaches. The performance gap between AF and DF can also be seen in [49, 50], this comparisons in one-way relaying systems are also valid for two-way relaying systems. The functional works for AF and DF are summarized as follows

2.4.1.4 Amplify-and-Forward

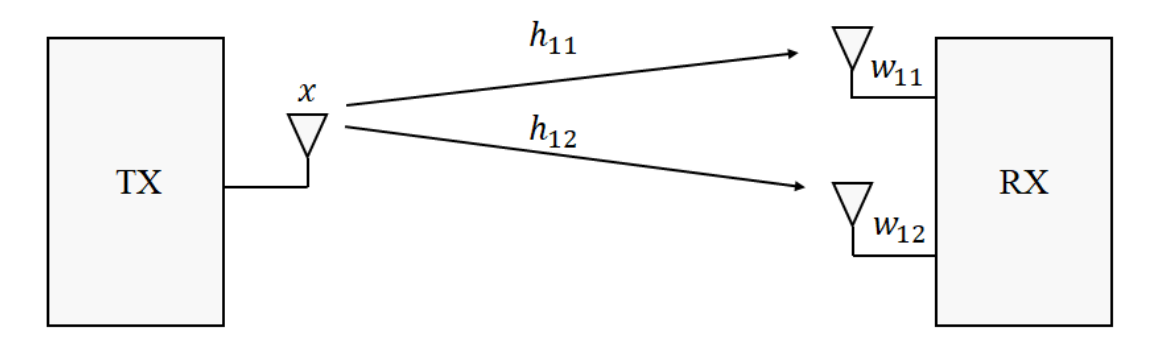
Amplify-and-Forward relay is the simplest form of the relays as shown in Figure 2.3 (a). As the name suggests, it amplifies the received signal and re-transmits. Hence, there will be an amplification of the noise and interference as well.

2.4.1.5 Decode-and-Forward

Decode-and-Forward relays will sample, demodulate and decode the received signal. The decoded and regenerated signal is then transmitted to the destination as shown



(a) Maximal ratio transmission (MRT)



(b) Maximum ratio combining (MRC)

Figure 2.4 Maximal Ratio Transmission Vs Maximum Ratio Combining.

in Figure 2.3 (b). These relays do not have the drawback of noise and interference amplification.

2.4.2 Transmit Diversity

Transmit diversity techniques are applied to MIMO transmitters or multiple-input single-output (MISO) systems to achieve high diversity and array gain. By sending the signal over multiple transmit antennas, MIMO systems can provides high diversity order proportional to the number of antennas.

2.4.2.1 Maximal Ratio Transmission

Maximal ratio transmission (MRT) [3] which shwon in Figure 2.4 (a), is a diversity transmission scheme example. The same signals are sent through all the transmitting antennas. However, to increase the received SNR, the transmitting signal for each antenna is multiplied by a specific weight factor, which depends on the available channel state information (CSI). It is worth mentioning that employing MRT in relaying systems, can be preferable as it can employ a simple relay.

2.4.3 Receive Diversity

Receive diversity methods are used at the receivers of MIMO or single-input multiple-output (SIMO) antenna systems to combine the received signals from all receive antennas to achieve diversity gain. The conventional well-known combining diversity techniques are equal gain combining (EGC), MRC, and SC. In EGC, all the received signals at the receive antennas are multiplied with the same weight [4]. Besides, the SC technique, only the maximum received signal, is selected while all the other weaker signals are neglected [51]. A comparison of these techniques is studied in [4]. The authors have shown that, by assuming the same number of receive antennas, EGC, MRC, and SC all perform the same diversity order but obtain different array gain for MIMO systems.

2.4.3.1 Maximum Ratio Combining

Maximum ratio combining (MRC) which illustrated in Figure 2.4 (b), each individual received signals multiplied with a weight based on the fading available channel state information (CSI) to maximize the SNR at the receiver [52, 53]. MRC obtains the highest array gain, among others (i.e., EGC and SC); however, it requires perfect CSI at the receiver.

2.5 Performance Evaluation Tools

2.5.1 Outage Probability

Outage Probability (OP) is an important performance indicator for wireless communications and can be introduced as the SNR or SINR cumulative probability function falls below a specific threshold γ_{th} . Mathematically speech, it can be written as

$$P_{\text{out}} = \int_0^{\gamma_{\text{th}}} f_{\gamma}(\gamma) \, d\gamma = F_{\gamma}(\gamma_{\text{th}}). \tag{2.12}$$

2.5.2 Average Error Probability

Average error probability (AEP) is one of the most studied and the most revealing performance metric about the overall fidelity and system behavior over a AWGN channel. For most of modulations in a fading environment, the average error Probability is defined as

$$\bar{P}_e = \int_0^\infty P_e(e|\gamma) f_\gamma(\gamma) \, d\gamma, \qquad (2.13)$$

where, $P_e(e|\gamma)$ is the AWGN conditional error probability for the given SNR or SINR [54].

2.5.3 Ergodic Capacity (Average Channel Capacity)

Ergodic capacity can be introduced as the average mutual information rate between transmitter and receiver.

$$C_{e2e} = \mathbb{E}[\log_2(1+\gamma)],\tag{2.14}$$

where γ can be the SNR or SINR at the receiver.

2.5.4 Asymptotic Analysis, Diversity and Array Gain

Since the exact forms of error probability and OP often do not provide any details on diversity order and array gain. It is necessary to provide simple forms of these performance indicators by assuming the average SNR going to infinity ($\bar{\gamma} \to \infty$) and keep the dominant terms. Consequently, diversity and array gains can be computed as [55]

$$G_d = -\lim_{\bar{\gamma} \to \infty} \frac{\log(P_X(\bar{\gamma}))}{\log(\bar{\gamma})},\tag{2.15}$$

$$G_a = -\lim_{\bar{\gamma} \to \infty} \left(\bar{\gamma}^{G_d} P_X \right)^{-1/G_d}, \tag{2.16}$$

where P_X can be the error or outage probability.

IMPACT OF CO-CHANNEL INTERFERENCE ON TWO-WAY RELAYING NETWORKS WITH MAXIMAL RATIO TRANSMISSION

Amplify-and-forward (AF) two-way relay networks (TWRNs) have become popular to provide spectrally efficient communication when range extension or energy efficiency is needed by utilizing a simple relay. However, their performance can be significantly degraded in practice due to co-channel interference (CCI) which is increasing due to growing number of wireless devices and recent cognitive and non-orthogonal multiple access techniques. With the motivation of improving the performance of AF-TWRNs, the use of maximal ratio transmission (MRT) is investigated to achieve high reliability while requiring low receiver complexity for the relay. First, the signal-to-interference-plus-noise ratio (SINR) expression is formulated and upper bounded. Then, tight lower bound expressions of outage probability (OP), sum symbol error rate (SSER), and upper bound ergodic sum rate (ESR) for each source and for the overall system are obtained. Besides, array and diversity gains are provided after deriving the asymptotic expressions of OP and SSER at high signal-to-noise ratio (SNR). Furthermore, the impact of channel estimation errors on the performance is also included. Finally, Monte Carlo simulation results which corroborate our theoretical findings are illustrated.

3.1 Introduction

Two-way relaying is a promising transmission technique to be used in next generation wireless networks where the relay can receive the sum of two source signals and then broadcast [56–58]. TWRNs allow the exchange of information within two time slots compared to four slots in dual hop relaying between two sources. Therefore, TWRNs can be useful in increasing the coverage or decreasing the transmit power in a spectrally efficient way. In order to have a low complexity relay for practical TWRNs, the amplify-and-forward (AF) approach is more preferable compared to other

methods such as decode-and-forward (DF) which requires more processing [59]. Recently, TWRN technique has been applied to new communication scenarios. For example, Bastami et al. [7] considers the multiple-input multiple-output (MIMO) TWRN scheme with overlay cognitive radio (CR) while TWRN with non-orthogonal multiple access (NOMA) is proposed in [8]. In addition, Refs. [60, 61] study the energy harvesting technique on TWRN under the effect of practical hardware impairments. Finally, physical layer security of AF-TWRN considering imperfect channel state information (CSI) is explored in [62].

Co-channel interference (CCI) is caused by the signals of other users and applications using the same frequency band [44], and it can be a serious problem limiting the coverage, reliability and throughput especially in WiFi, cellular, and ad-hoc networks. Besides, next generation wireless networks will contain even more number of users and with internet of things (IoT) devices which will further intensify the undesired effects of interference. Furthermore, new wireless techniques such as NOMA [42], and CR [43] will also increase CCI. In the literature, Liang et al. [63, 64], investigate the outage probability performance of amplify-and-forward (AF) and decode-and-forward (DF) two-way relaying system respectively, considering multiple CCI signals at sources. In [65], the symbol error probability performance is presented for DF-TWRN with CCI, while the impact of CCI on AF-TWRN has been studied by Ikki et al. [22] for Rayleigh fading and by Costa et al. [23] for Nakagami-m fading where outage and symbol error probabilities (SEP) are obtained when all nodes have only single antenna. In [25], the outage probability (OP), error performance, and achievable rate are investigated for an AF-TWRN with CCI and channel estimation errors (CEE). Optimization of relay position and power allocation for maximum performance of AF-TWRN with CCI are explored in [24]. Recently, Shukla et al. [66] has studied the performance of single antenna users in cellular TWRN with CCI and CEE.

Utilizing multiple antennas can be highly useful in performance improvement. For example, maximal ratio transmission has been proposed in [3] to achieve maximum signal to noise power ratio at the receiver by adjusting the scaling weights of transmitted signals. Without increasing the computational complexity of the receiver, MRT can achieve full spatial diversity, thus it has become preferable especially for transmissions from base stations to the size, delay and power constrained mobile units and relays. In [13], Yang et al. investigate the sum symbol error rate (SSER) of TWRN with single antenna relay, beamforming and antenna selection. Yadav et al. [14] investigates the optimization of performance for TWRN with MRT and derive closed form error probability and ergodic sum rate (ESR). Similarly, [15] deals with the performance of an AF-TWRN-MRT with relay selection and derive OP and SER over Nakagami-m fading channels. Recently, Kefeng et al. [16] analyze the outage

probability, throughput and energy-efficiency of AF-TWRNs employing MRT/MRC at the relay node under the effect of hardware impairment.

Its worth mentioning that relays can have multiple antennas, however, using only one antenna at the relay will be satisfactory enough and more feasible since extra channel estimation, synchronization, etc. will complicate the system and increase the cost and delay. Clearly the analysis for the AF TWRN MRT system with CCI will also be much more complicated and thus the theoretical study for outage, SER, diversity/array gains may be intractable. Furthermore, in the literature, most of the existing studies considering CCI in TWRNs with amplify-and-forward and even with decode-and-forward [22–25, 63–66] relaying, deal with single antenna sources and do not include any multiple antenna techniques and also ignore the additional effect of noise for simplicity of the mathematical analysis. On the other hand, MRT studies in [3, 13–16] consider interference-free scenarios since taking CCI into account changes the statistics of the system SNR extremely thus complicating the analysis tremendously. Besides, two-way relay networks have attracted considerable interest recently due to their numerous advantages and practical usages. Even though there are several TWRN papers in the literature, there is no previous work which studied the improvement of reliability in two-way relay networks under co-channel interference with the help of popular low complexity MRT technique. Therefore, with the motivation of having a reliable communication via a low complexity relay, this paper provides a comprehensive investigation of the use of MRT at the sources of AF-TWRN system where the relay is under the effect of multiple co-channel interference signals plus noise. The contributions of the paper can be listed as follows:

- Lower bound of outage probabilities for each source and the overall system are derived for an arbitrary number of antennas and interferers.
- Lower bound of symbol error rates for each source and for the overall system are analyzed.
- Asymptotic sum symbol error rate and outage probability expressions, diversity and array gains are obtained.
- A tight upper bound of the ergodic sum rate is investigated for the proposed structure.
- To get insight regarding the performance in practice, the effect of channel estimation errors is studied.
- Numerical examples are illustrated to verify our theoretical results and compare several cases.

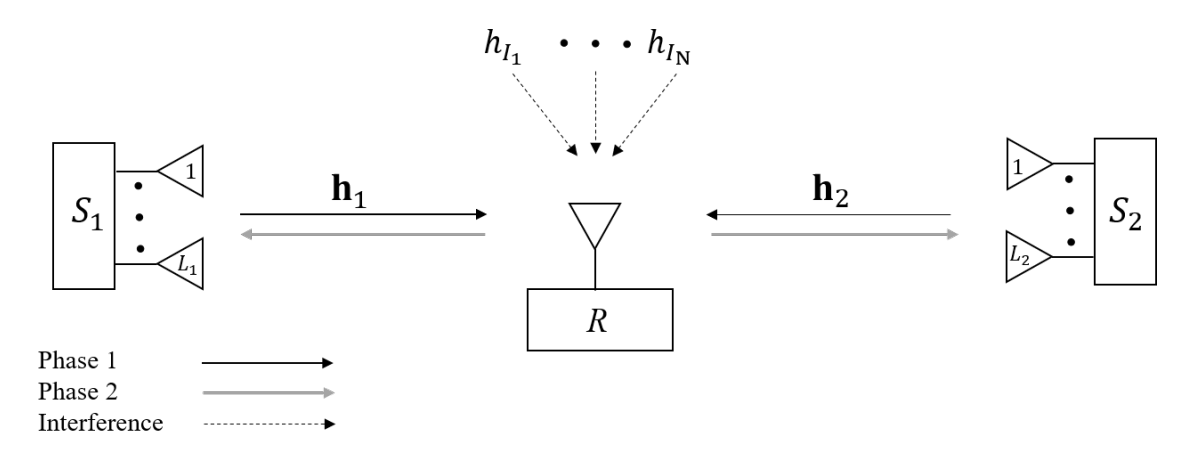


Figure 3.1 Block diagram of TWRN with maximal ratio transmission and CCI at the relay.

The remainder of the chapter is organized as follows. System and channel models are described in Section 3.2. In Section 3.3, the cumulative distribution function (CDF) of SINR for each source and end-to-end (e2e) system are obtained with and without CEE. Moreover, OP, SSER, ESR, diversity and array gain expressions are derived. Section 3.4 presents the numerical examples obtained by Monte Carlo simulations. Finally, conclusions are summarized in Section 3.5.

3.2 System and Channel Models

An AF-TWRN system with two source terminals S_1 and S_2 having L_1 and L_2 antennas respectively, is considered where sources communicate via a single antenna relay 1 R which is exposed to N co-channel interference signals from other users in the network 2 as depicted in Figure 3.1. \mathbf{h}_1 and \mathbf{h}_2 are $L_1 \times 1$ and $L_2 \times 1$ channel vectors between $S_1 \to R$ and $S_2 \to R$ respectively. h_{Ii} is the flat fading coefficient of i-th interference channel. The direct link between two source terminals is assumed to be unavailable due to large path loss and/or deep shadowing. Channel coefficients at each hop are modeled as independent and identically distributed (i.i.d) Rayleigh flat fading. For the performance analysis in the next section, the CSI is assumed to be available at both sources and at the relay, then, the effect of imperfect CSI is also explored later. The communication between two source terminals is divided into two phases. In the first

¹Using only one antenna of the relay will be satisfactory enough and more feasible compared to use of multiple antennas at user or relay since extra channel estimation, synchronization, etc. will complicate the system and increase the cost and delay.

²In practice, a small size and low complexity user can behave as a relay to establish reliable links between two base stations in a cellular network (e.g., [56, 66]), or between two routers in a WiFi network, or between two coordinators in a wireless sensor network when larger range and better energy efficiency are needed. If the selected user is close to the edge of cells/clusters, then the CCI level can be considerable compared to negligible CCI at two source terminals which can be at the center of neighboring cells [23].

phase, S_1 and S_2 transmit their unit energy signals x_1 and x_2 respectively by using MRT technique. Without loss of generality, all nodes are assumed to have equal transmit powers, $P_{S_1} = P_{S_2} = P_R = P$ and denote the power of interference signals as P_I . Then, the received signal at the relay R can be written as follows

$$y_R = \sqrt{Pd_1^{-\alpha}} \mathbf{h}_1 \mathbf{w}_1 \ x_1 + \sqrt{Pd_2^{-\alpha}} \mathbf{h}_2 \mathbf{w}_2 \ x_2 + \sqrt{PI} \sum_{i=1}^N h_{Ii} \ x_{Ii} + n_R, \tag{3.1}$$

where exponential-decay path loss model is assumed with α denoting the path loss exponent. Distances between $S_1 \to R$ and $S_2 \to R$ are shown as d_1 and d_2 , respectively. x_{Ii} is the i-th unit energy interfering signal affecting R. In the second phase, the relay amplifies the sum of the received signals with a scaling factor G and then broadcasts to S_1 and S_2 . By using maximum ratio combining (MRC), the received signals at both sources can be expressed as

$$y_{S_1} = \mathbf{w}_1^T \left(\sqrt{P d_1^{-\alpha}} G \mathbf{h}_1^T y_R + \mathbf{n}_1 \right),$$

$$y_{S_2} = \mathbf{w}_2^T \left(\sqrt{P d_2^{-\alpha}} G \mathbf{h}_2^T y_R + \mathbf{n}_2 \right).$$
(3.2)

MRT weight vectors \mathbf{w}_1 and \mathbf{w}_2 are specified as $\mathbf{w}_1 = (\mathbf{h}_1^H / || \mathbf{h}_1 ||)$ and $\mathbf{w}_2 = (\mathbf{h}_2^H / || \mathbf{h}_2 ||)$. Noise samples n_R and elements of \mathbf{n}_1 , \mathbf{n}_2 vectors are modeled as complex additive white Gaussian noise with zero mean and variance N_0 . The relay scaling factor [23, 67, 68] is given as

$$G^{-1} = \sqrt{Pd_1^{-\alpha} \|\mathbf{h}_1\|^2 + Pd_2^{-\alpha} \|\mathbf{h}_2\|^2}.$$
 (3.3)

Using channel reciprocity in TWRN, the two sources can cancel their self interference term (i.e. the effect of their transmitted signals). Substituting (3.1) in (3.2) and after some algebraic manipulations, the SINRs can be obtained as

$$\gamma_{S_{1}} = \frac{\gamma_{1}\gamma_{2}}{\gamma_{1}\gamma_{I} + 2\gamma_{1} + \gamma_{2}} = \frac{\gamma_{1}(\frac{\gamma_{2}}{\gamma_{I}+2})}{\gamma_{1} + (\frac{\gamma_{2}}{\gamma_{I}+2})},$$

$$\gamma_{S_{2}} = \frac{\gamma_{1}\gamma_{2}}{\gamma_{2}\gamma_{I} + 2\gamma_{2} + \gamma_{1}} = \frac{\gamma_{2}(\frac{\gamma_{1}}{\gamma_{I}+2})}{\gamma_{2} + (\frac{\gamma_{1}}{\gamma_{I}+2})},$$
(3.4)

where $\gamma_1 \triangleq \frac{P}{N_0} d_1^{-\alpha} ||\mathbf{h}_1||^2$ and $\gamma_2 \triangleq \frac{P}{N_0} d_2^{-\alpha} ||\mathbf{h}_2||^2$ are the instantaneous SNRs at $S_1 \to R$

and $S_2 \to R$ hops and $\gamma_I \triangleq \frac{P_I}{N_0} \sum_{i=1}^N |h_{Ii}|^2$ is the instantaneous interference-to-noise power ratio (INR) at the relay.

3.3 Performance Analysis

In this section, first, upper bounds of CDFs of the SINRs for the sources and e2e system are obtained. Secondly, lower bounds of OP and SER expressions are derived. Then asymptotic OP and SER analyses are carried out, thus diversity and array gains are provided. Finally, the upper bound of ergodic sum rate and the effect of CEE are presented.

Since that exact results would be more preferable compared to bounds. However, closed form exact results have been derived for only some scenarios where the mathematical analysis is tractable. To the best of our knowledge, there is no closed-form exact result for AF-TWRN with CCI even for single antenna sources. This is because γ_{S_1} and γ_{S_2} are highly correlated when they contain three common random variables, γ_1 , γ_2 , and γ_I and resulting in highly complicated three integrals. Because of this, all of the previous TWRN-CCI studies resort to finding a bound even for interference-only environment (where the noise term is neglected). Accordingly, it is mathematically intractable to obtain the exact performance results for TWRNs with CCI and similar to previous studies [22–25, 66], upper bounds on γ_{S_1} and γ_{S_2} in (3.4) can be written as

$$\gamma_{S_1}^{\text{up}} = \min\left(\gamma_1, \frac{\gamma_2}{(\gamma_I + 2)}\right),
\gamma_{S_2}^{\text{up}} = \min\left(\gamma_2, \frac{\gamma_1}{(\gamma_I + 2)}\right).$$
(3.5)

Then, CDFs of the random variables $\tilde{\gamma}_1 = \gamma_2/(\gamma_I + 2)$ and $\tilde{\gamma}_2 = \gamma_1/(\gamma_I + 2)$ can be expressed as

$$F_{\tilde{\gamma}_{1}}(\gamma) = \mathbb{E}_{\gamma_{I}} \Big[\Pr[\gamma_{2} \leq (\gamma_{I} + 2)\gamma] \Big]$$

$$= \int_{0}^{\infty} F_{\gamma_{2}}((z+2)\gamma) f_{\gamma_{I}}(z) dz.$$
(3.6)

Note that the instantaneous SNRs, γ_1 and γ_2 are central Chi-square distributed random

variables with $2L_1$ and $2L_2$ degrees of freedom, respectively. Then their PDF and CDF are given as [3]

$$f_{\gamma_1}(x) = \frac{x^{L_1 - 1} e^{-x/\Omega_1}}{\Omega_1^{L_1} \Gamma(L_1)},$$
(3.7)

$$f_{\gamma_2}(y) = \frac{y^{L_2 - 1} e^{-y/\Omega_2}}{\Omega_2^{L_2} \Gamma(L_2)},$$
(3.8)

$$F_{\gamma_1}(x) = 1 - \sum_{m=0}^{L_1 - 1} \frac{e^{-x/\Omega_1}}{m!} \left(\frac{x}{\Omega_1}\right)^m,$$
(3.9)

$$F_{\gamma_2}(y) = 1 - \sum_{w=0}^{L_2 - 1} \frac{e^{-y/\Omega_2}}{w!} \left(\frac{y}{\Omega_2}\right)^w, \tag{3.10}$$

where $\Gamma(\cdot)$ is the Gamma function ([69] [eqn 8.339.1]). Average SNRs are denoted as $\Omega_1 = d_1^{-\alpha}\bar{\gamma}$ and $\Omega_2 = d_2^{-\alpha}\bar{\gamma}$ using $\bar{\gamma} = P/N_0$. Similarly, γ_I is distributed as central Chi-square random variable with 2N degrees of freedom where its PDF is [22]

$$f_{\gamma_I}(z) = \frac{z^{N-1} e^{-z/\Omega_I}}{\Omega_I^N \Gamma(N)},\tag{3.11}$$

where average INR is shown as $\Omega_I = P_I/N_0$. By substituting (3.10) and (3.11) into (3.6) and after several algebraic manipulations to solve the integral, (3.6) is equivalently expressed as

$$F_{\tilde{\gamma}_{1}}(\gamma) = \int_{0}^{\infty} \left(1 - \sum_{w=0}^{L_{2}-1} \frac{e^{-(z+2)\gamma/\Omega_{2}}}{w!} \Lambda_{1}^{w} \right) \frac{z^{N-1} e^{-z/\Omega_{I}}}{\Omega_{I}^{N} \Gamma(N)} dz$$

$$= 1 - \sum_{w=0}^{L_{2}-1} \frac{e^{-\frac{2\gamma}{\Omega_{2}}}}{w!} \left(\frac{2\gamma}{\Omega_{2}} \right)^{w} \left(\frac{2}{\Omega_{I}} \right)^{N} U\left(N, N + w + 1, \frac{2\gamma}{\Omega_{2}} + \frac{2}{\Omega_{I}} \right),$$
(3.12)

where $\Lambda_1 = (z+2)\gamma/\Omega_2$ and U(a,b,z) is the Tricomi confluent hypergeometric function ³, defined by the integral $U(a,b,z) = \frac{1}{\Gamma(a)} \int_{0}^{\infty} t^{a-1}(t+1)^{-a+b-1} e^{-zt} dt$ ([69]

³The Tricomi confluent hypergeometric function and the Meijer's G-function can easily evaluated numerically by using well-known software programs such as MAPLE or MATHEMATICA.

[eqn 9.211.4]). To this end, the CDF of $\gamma_{S_1}^{\mathrm{up}}$ can be derived as

$$\begin{split} F_{\gamma_{S_{1}}^{\text{up}}}(\gamma) &= \Pr\Big[\min\left(\gamma_{1}, \tilde{\gamma}_{1}\right) \leqslant \gamma\Big] \\ &= 1 - \Pr\left[\gamma_{1} > \gamma\right] \Pr\left[\tilde{\gamma}_{1} > \gamma\right] \\ &\stackrel{(a)}{=} 1 - (1 - F_{\gamma_{1}}(\gamma))(1 - F_{\tilde{\gamma}_{1}}(\gamma)) \\ &\stackrel{(b)}{=} F_{\gamma_{1}}(\gamma) + F_{\tilde{\gamma}_{1}}(\gamma) - F_{\gamma_{1}}(\gamma)F_{\tilde{\gamma}_{1}}(\gamma). \end{split} \tag{3.13}$$

Now, substituting (3.9) and (3.12) into step (a) of (3.13) yields

$$F_{\gamma_{S_1}^{\text{up}}}(\gamma) = 1 - \sum_{m=0}^{L_1 - 1} \sum_{w=0}^{L_2 - 1} \frac{e^{-\frac{\gamma}{\Omega_1}} e^{-\frac{2\gamma}{\Omega_2}}}{m! w!} \left(\frac{\gamma}{\Omega_1}\right)^m \left(\frac{2\gamma}{\Omega_2}\right)^w \left(\frac{2}{\Omega_I}\right)^N U\left(N, N + w + 1, \frac{2\gamma}{\Omega_2} + \frac{2}{\Omega_I}\right), \tag{3.14}$$

and similarly, the CDF of $\gamma_{S_2}^{\rm up}$ can be derived as

$$F_{\gamma_{S_2}^{\text{up}}}(\gamma) = 1 - \sum_{w=0}^{L_2 - 1} \sum_{m=0}^{L_1 - 1} \frac{e^{-\frac{\gamma}{\Omega_2}} e^{-\frac{2\gamma}{\Omega_1}}}{w! m!} \left(\frac{\gamma}{\Omega_2}\right)^w \left(\frac{2\gamma}{\Omega_1}\right)^m \left(\frac{2}{\Omega_I}\right)^N U\left(N, N + m + 1, \frac{2\gamma}{\Omega_1} + \frac{2}{\Omega_I}\right).$$
(3.15)

Finally, the end-to-end SINR of the system can be expressed as [24]

$$\gamma_{e2e} = \min\left(\gamma_{S_1}, \gamma_{S_2}\right) \le \min\left(\gamma_{S_1}^{\text{up}}, \gamma_{S_2}^{\text{up}}\right) \triangleq \gamma_{e2e}^{\text{up}}.$$
 (3.16)

In the literature, some papers (e.g., [22]) have derived performance expressions based on γ_{S_1} , however, it is not the correct e2e SINR of two-way relaying systems. The upper bound CDF of e2e SINR can be derived by using (3.16) as follows

$$F_{\gamma_{\text{e2e}}^{\text{up}}}(\gamma) = \Pr\left[\min\left(\gamma_{S_1}^{\text{up}}, \gamma_{S_2}^{\text{up}}\right) \leq \gamma\right]$$

$$= \Pr\left[\min\left(\min(\gamma_1, \tilde{\gamma}_1), \min(\gamma_2, \tilde{\gamma}_2)\right) \leq \gamma\right]. \tag{3.17}$$

The computation of this CDF is highly complicated since $\gamma_{S_1}^{up}$ and $\gamma_{S_2}^{up}$ are correlated as they contain common random variables γ_1 , γ_2 and γ_I . To this end, similar to [67], the following Lemma is introduced.

Lemma 3.1. SINRs for S_1 and S_2 can be further upper bounded by dividing (3.4) to $\gamma_1 = \frac{P}{N_0} d_1^{-\alpha} ||\mathbf{h}_1||^2$ and $\gamma_2 = \frac{P}{N_0} d_2^{-\alpha} ||\mathbf{h}_2||^2$ as follows

$$\begin{split} \gamma_{S_1} &= \frac{\gamma_2}{\gamma_I + 2 + \frac{\gamma_2}{\gamma_1}} \leqslant \tilde{\gamma}_1, \\ \gamma_{S_2} &= \frac{\gamma_1}{\gamma_I + 2 + \frac{\gamma_1}{\gamma_2}} \leqslant \tilde{\gamma}_2, \end{split} \tag{3.18}$$

due to the fact that both γ_1 *and* $\gamma_2 > 0$.

The Lemma we introduced above allowed us to obtain a quite tight bound demonstrated by our numerical examples even for the worst case when CCI power is increasing with the transmission power, i.e., P/P_I is assumed constant, (please see Fig. 3.2 and 3.3). On the other hand, our analytical bounds are almost exact (see Fig. 3.5 and 3.10) when interferer powers are assumed constant as in many papers. With the help of this new bound, (3.17) can be simplified to its conditioned version depending only on γ_I

$$\begin{split} F_{\gamma_{\text{e2e}}^{\text{up}}}(\gamma) &= \mathbb{E}_{\gamma_{I}} \Big[\Pr \Big[\min \left(\tilde{\gamma}_{1}, \tilde{\gamma}_{2} \right) \leq \gamma \Big] \Big] \\ &= \mathbb{E}_{\gamma_{I}} \Big[1 - \Pr \left[\tilde{\gamma}_{1} > \gamma \right] \Pr \left[\tilde{\gamma}_{2} > \gamma \right] \Big] \\ &\stackrel{(a)}{=} \mathbb{E}_{\gamma_{I}} \Big[1 - (1 - F_{\tilde{\gamma}_{1}}(\gamma))(1 - F_{\tilde{\gamma}_{2}}(\gamma)) \Big] \\ &\stackrel{(b)}{=} \mathbb{E}_{\gamma_{I}} \Big[F_{\tilde{\gamma}_{1}}(\gamma) + F_{\tilde{\gamma}_{2}}(\gamma) - F_{\tilde{\gamma}_{1}}(\gamma) F_{\tilde{\gamma}_{2}}(\gamma) \Big], \end{split} \tag{3.19}$$

Then, the unconditional CDF of $\gamma_{\rm e2e}^{\rm up}$ can be derived as

$$F_{\gamma_{\text{e2e}}^{\text{up}}}(\gamma) = 1 - \sum_{m=0}^{L_1 - 1} \sum_{w=0}^{L_2 - 1} \frac{e^{-\frac{2\gamma}{\Omega_1}} e^{-\frac{2\gamma}{\Omega_2}}}{m! w!} \left(\frac{2\gamma}{\Omega_1}\right)^m \left(\frac{2\gamma}{\Omega_2}\right)^w \left(\frac{2}{\Omega_I}\right)^N \times U\left(N, N + m + w + 1, \frac{2\gamma}{\Omega_1} + \frac{2\gamma}{\Omega_2} + \frac{2}{\Omega_I}\right).$$
(3.20)

Proof. The detailed derivation is shown in Appendix A.

This closed form upper bound on CDF of e2e SINR is in a simple form with the help of **Lemma** 3.1. In addition, for the case of no interference, i.e., N = 0, the CDF can be reduced to

$$F_{\gamma_{\text{e2e}}^{\text{up}}}(\gamma) = 1 - \sum_{m=0}^{L_1 - 1} \sum_{w=0}^{L_2 - 1} \frac{e^{-\frac{2\gamma}{\Omega_1}} e^{-\frac{2\gamma}{\Omega_2}}}{m!w!} \left(\frac{2\gamma}{\Omega_1}\right)^m \left(\frac{2\gamma}{\Omega_2}\right)^w.$$
(3.21)

Note that even exact results may not provide useful insights due to use of complicated functions. For example, for an "interference-free" (i.e. no CCI) system where single antennas transceivers are used, the closed-form expression for the system SINR CDF, $F_{\gamma_{e2e}}(\gamma)$ can be derived by using the technique in [70, 71]. However, the results are still approximate as the integral region is made larger and the final expression is in term of special functions (Bessel, hypergeometric, etc.). Moreover, the final expression includes an integral which can only be solved numerically to provide some insights. Thus, it is too complicated and would not be useful in finding other performance metrics such as the symbol error rate and the ergodic sum rate.

3.3.1 System Outage Probability

The outage probability for S_i is defined as the probability that SINR for the link $S_i \to R \to S_j$ falls below a threshold $\gamma_{\rm th}$, where $i,j \in \{1,2\}$ and $i \neq j$. System outage on the other hand can be defined as at least one of the source nodes being in outage. As a result, the lower bound on system OP is actually the CDF of $\gamma_{\rm e2e}^{\rm up}$ random variable evaluated at $\gamma_{\rm th}$ and can be written as

$$P_{out} \ge \Pr[\gamma_{\text{e2e}}^{\text{up}} \le \gamma_{\text{th}}] = F_{\gamma_{\text{e3e}}^{\text{up}}}(\gamma_{\text{th}}). \tag{3.22}$$

3.3.2 Sum Symbol Error Rate

SSER can be defined as the summation of SER at S_1 and S_2 nodes, and it is another important performance criterion in TWRNs. Mathematically, it can be expressed as [72]

$$P_{sys}(e) = P_{s_1}(e) + P_{s_2}(e). (3.23)$$

For several signal constellations employed in practical systems, the SER can be written as $a\mathbb{E}[Q(\sqrt{2b\gamma})]$, where Q(x) is the standard Gaussian tail probability function define

as $(1/\sqrt{2\pi})\int_x^\infty e^{-t^2/2}dt$, a and b are modulation coefficients, i.e., $\{a=1,b=0.5\}$ for BFSK modulation, $\{a=1,b=1\}$ for BPSK and $\{a=2(M-1)/M,b=3/(M^2-1)\}$ for M-ary PAM. Then SER can be evaluated by using the CDF-based approach [25] as

$$P_{s_i}(e) \ge \frac{a\sqrt{b}}{2\sqrt{\pi}} \int_0^\infty \gamma^{-1/2} e^{-b\gamma} F_{\gamma_{s_i}^{\text{up}}}(\gamma) d\gamma, \ i = 1, 2.$$
 (3.24)

To simplify the derivation of (3.24), CDFs of $\gamma_{S_1}^{\rm up}$ and $\gamma_{S_2}^{\rm up}$ can be expressed in a more tractable form. The mathematical identity $U(a,a+n+1,z)=z^{-a}\sum_{s=0}^n \binom{n}{s}(a)_s z^{-s}$ ([73][eqn 13.2.8]) where $(a)_s=\Gamma(a+s)/\Gamma(a)$ is Pochhammer's symbol, can help expanding the Tricomi confluent hypergeometric function to a finite sum series. After substitution the simplified versions of (3.14) and (3.15) in (3.24) with some mathematical manipulations and by utilizing ([69] [eqn 9.211.14]), the lower bound of SER for S_1 and S_2 can be expressed as ⁴

$$P_{s_{i}}(e) \geq \frac{a}{2} - \frac{a}{2} \sqrt{\frac{b}{\pi}} \sum_{m=0}^{L_{i}-1} \sum_{w=0}^{L_{j}-1} \sum_{n=0}^{w} {w \choose n} \frac{2^{w-n}}{m!w!} \frac{\Gamma(N+n)}{\Gamma(N)} \left(\frac{1}{\Omega_{i}}\right)^{m} \left(\frac{1}{\Omega_{j}}\right)^{w} \Gamma\left(m+w+\frac{1}{2}\right) \Omega_{I}^{n} \times \left(\frac{\Omega_{j}}{\Omega_{I}}\right)^{m+w+\frac{1}{2}} U\left(m+w+\frac{1}{2}, m+w-N-n+\frac{3}{2}, \frac{b\Omega_{j}}{\Omega_{I}} + \frac{\Omega_{j}}{\Omega_{I}\Omega_{i}} + \frac{2}{\Omega_{I}}\right),$$
(3.25)

furthermore, it is worth mentioning that for no interference case, the SER in (3.25) can be simplified as

$$P_{s_{i}}(e) \ge \frac{a}{2} - \frac{a}{2} \sqrt{\frac{b}{\pi}} \sum_{m=0}^{L_{i}-1} \sum_{w=0}^{L_{j}-1} \frac{\left(m+w-\frac{1}{2}\right)!}{m!w!} \left(\frac{1}{\Omega_{i}}\right)^{m} \left(\frac{2}{\Omega_{j}}\right)^{w} \left(\frac{1}{\Omega_{i}} + \frac{2}{\Omega_{j}} + b\right)^{-m-w-\frac{1}{2}}.$$
(3.26)

By substituting the SER of S_1 and S_2 into (3.23), the lower bound of SSER can be easily obtained in closed-form.

⁴In the sequel, OP, SER and ESR for any source can be obtained by replacing the subscript i and j with $i, j \in \{1, 2\}$ such that $i \neq j$.

3.3.3 Asymptotic Analysis

In this subsection, in order to extract the diversity and array gains, P_{out} and $P_{sys}(e)$ are simplified by assuming high SNR values (i.e., $\bar{\gamma} \to \infty$). Using the Maclaurin series expansion of the exponential function [74]. The PDF of γ_1 and γ_2 in (3.7) and (3.8) can be approximated respectively as

$$f_{\gamma_1}(x) \approx \frac{x^{L_1 - 1}}{\Omega_1^{L_1} \Gamma(L_1)},$$
 (3.27)

$$f_{\gamma_2}(y) \approx \frac{y^{L_2 - 1}}{\Omega_2^{L_2} \Gamma(L_2)}.$$
 (3.28)

Then, by integrating these PDFs with respect to x and y, CDFs can be written as follows

$$F_{\gamma_1}(x) \approx \frac{1}{L_1!} \left(\frac{x}{\Omega_1}\right)^{L_1},$$
 (3.29)

$$F_{\gamma_2}(y) \approx \frac{1}{L_2!} \left(\frac{y}{\Omega_2}\right)^{L_2}.$$
 (3.30)

Recall that step (*b*) in both (3.13) and (3.19) can be simplified by ignoring the last multiplication term; $F_{\gamma_{S_1}^{up}}(\gamma) \approx F_{\gamma_1}(\gamma) + F_{\tilde{\gamma}_1}(\gamma)$ and $F_{\gamma_{e2e}^{up}}(\gamma) \approx \mathbb{E}_{\gamma_I}[F_{\tilde{\gamma}_1}(\gamma) + F_{\tilde{\gamma}_2}(\gamma)]$. To this end, by using these approximations, following the same procedure and after some mathematical manipulations, asymptotic CDFs for γ_{S_1} , γ_{S_2} and γ_{e2e} can be given as

$$F_{\gamma_{S_i}}^{\infty}(\gamma) \approx \frac{1}{L_i!} \left(\frac{\gamma}{\Omega_i}\right)^{L_i} + \frac{2^N}{\Omega_I^N L_j!} \left(\frac{2\gamma}{\Omega_j}\right)^{L_j} U\left(N, N + L_j + 1, \frac{2}{\Omega_I}\right), \tag{3.31}$$

$$\begin{split} F_{\gamma_{\text{e2e}}}^{\infty}(\gamma) &\approx \\ \frac{2^{N}}{\Omega_{I}^{N} L_{1}!} \left(\frac{2\gamma}{\Omega_{1}}\right)^{L_{1}} U\left(N, N + L_{1} + 1, \frac{2}{\Omega_{I}}\right) + \frac{2^{N}}{\Omega_{I}^{N} L_{2}!} \left(\frac{2\gamma}{\Omega_{2}}\right)^{L_{2}} U\left(N, N + L_{2} + 1, \frac{2}{\Omega_{I}}\right). \end{split} \tag{3.32}$$

For the interference-free system, (3.32) becomes

$$F_{\gamma_{e2e}}^{\infty}(\gamma) \approx \left(\frac{2\gamma}{\Omega_1}\right)^{L_1} \frac{1}{L_1!} + \left(\frac{2\gamma}{\Omega_2}\right)^{L_2} \frac{1}{L_2!}.$$
 (3.33)

Furthermore, by substituting the asymptotic CDFs of γ_{S_1} and γ_{S_2} in (3.24) with the help of ([73][eqn 13.2.8]) and some mathematical simplifications, asymptotic expressions of SER for S_1 and S_2 can be derived as

$$P_{s_{i}}^{\infty}(e) = \frac{a}{2\sqrt{\pi}} \frac{(L_{i} - 0.5)!}{L_{i}!} \left(\frac{1}{b\Omega_{i}}\right)^{L_{i}} + \frac{a}{2\sqrt{\pi}} \frac{(L_{j} - 0.5)!}{L_{j}!\Gamma(N)} \left(\frac{2}{b\Omega_{j}}\right)^{L_{j}} \sum_{w=0}^{L_{j}} {L_{j} \choose w} \left(\frac{\Omega_{I}}{2}\right)^{w} \times \Gamma(N + w).$$
(3.34)

Having this result, the asymptotic SSER can be directly obtained from (3.23). As a special case, asymptotic SERs for S_1 and S_2 in interference-free system are provided as

$$P_{s_i}^{\infty}(e) = \frac{a}{2\sqrt{\pi}} \frac{(L_i - 0.5)!}{L_i!} \left(\frac{1}{b\Omega_i}\right)^{L_i} + \frac{a}{2\sqrt{\pi}} \frac{(L_j - 0.5)!}{L_j!} \left(\frac{2}{b\Omega_j}\right)^{L_j}.$$
 (3.35)

In order to find the asymptotic system OP expression, both ([55] [Prop. 5]) and (3.32) are used where γ is replaced with γ_{th} and a large value of $\bar{\gamma}$ is assumed. Then, P_{out}^{∞} can be obtained as

$$P_{out}^{\infty} = \mathscr{G}\left(\frac{\gamma_{\text{th}}}{\bar{\gamma}}\right)^{\min(L_1, L_2)} + \text{H.O.T.}, \tag{3.36}$$

where H.O.T denotes high order terms and the scaling factor \mathscr{G} is given as

$$\mathscr{G} =$$

$$\begin{cases}
\frac{2^{N}}{\Omega_{I}^{N}L_{1}!} \left(\frac{2}{d_{1}^{-\alpha}}\right)^{L_{1}} U\left(N, N + L_{1} + 1, \frac{2}{\Omega_{I}}\right), & L_{1} < L_{2} \\
\frac{2^{N}}{\Omega_{I}^{N}L_{1}!} \left(\frac{2}{d_{1}^{-\alpha}}\right)^{L_{1}} U\left(N, N + L_{1} + 1, \frac{2}{\Omega_{I}}\right) + \frac{2^{N}}{\Omega_{I}^{N}L_{2}!} \left(\frac{2}{d_{2}^{-\alpha}}\right)^{L_{2}} U\left(N, N + L_{2} + 1, \frac{2}{\Omega_{I}}\right), & L_{1} = L_{2} \\
\frac{2^{N}}{\Omega_{I}^{N}L_{2}!} \left(\frac{2}{d_{2}^{-\alpha}}\right)^{L_{2}} U\left(N, N + L_{2} + 1, \frac{2}{\Omega_{I}}\right), & L_{1} > L_{2}, \\
\frac{2^{N}}{\Omega_{I}^{N}L_{2}!} \left(\frac{2}{d_{2}^{-\alpha}}\right)^{L_{2}} U\left(N, N + L_{2} + 1, \frac{2}{\Omega_{I}}\right), & (3.37)
\end{cases}$$

Furthermore, by using $P_{out}^{\infty} \approx (G_a \bar{\gamma})^{-G_d}$ as described in [55], the diversity gain G_d and the array gain G_a can be written as

$$G_d = \min(L_1, L_2),$$

$$G_a = \frac{1}{\gamma_{th}} (\mathcal{G})^{-1/G_d}.$$
(3.38)

Note that, even though CCI degrades the array gain considerably, it does not decrease the diversity gain.

3.3.4 Ergodic Sum Rate

The ergodic sum rate which is measured by bits/s/Hz, is an important performance indicator as it can provide insight about the maximum transmission rate. For TWRNs, it is expressed as the summation of the ergodic rates of S_1 and S_2 , and thus for our system model, it can be written as [14, 23]

$$ESR = \frac{1}{2} \left(\mathbb{E}[\log_2(1 + \gamma_{S_1})] + \mathbb{E}[\log_2(1 + \gamma_{S_2})] \right), \tag{3.39}$$

where the factor 1/2 appears since data exchange needs two time slots. To the best of our knowledge, the closed form solution of the above expression can not be obtained. However, an approximate expression for the ergodic sum rate can be derived using the Jensen's inequality ⁵. Specifically, an upper bound on the ergodic sum rate in (3.39)

⁵Jensen's inequality: Suppose that X is a random variable with expectation μ , and function g is convex and finite. Then $\mathbb{E}[g(X)] \leq g(\mathbb{E}[X])$ ([75] [eqn 5.5]).

is obtained as

$$ESR \le \frac{1}{2} \left[\log_2(1 + \mathbb{E}[\gamma_{S_1}^{\text{up}}]) + \log_2(1 + \mathbb{E}[\gamma_{S_2}^{\text{up}}]) \right]. \tag{3.40}$$

where $\mathbb{E}[\gamma_{S_1}^{\mathrm{up}}]$ and $\mathbb{E}[\gamma_{S_2}^{\mathrm{up}}]$ can be obtained as

$$\mathbb{E}[\gamma_{S_{i}}^{\text{up}}] = \frac{1}{\Gamma(N)} \sum_{m=0}^{L_{i}-1} \sum_{w=0}^{L_{j}-1} \sum_{n=0}^{w} {w \choose n} \left(\frac{1}{\Omega_{i}}\right)^{m} \left(\frac{1}{\Omega_{j}}\right)^{w} \frac{\Omega_{I}^{n} 2^{w-n}}{m! w!} \left(\frac{\Omega_{I}}{\Omega_{j}}\right)^{-m-w-1} \times G_{1,2}^{2,1} \left(\frac{\frac{1}{\Omega_{i}} + \frac{2}{\Omega_{j}}}{\frac{\Omega_{I}}{\Omega_{j}}}\right| \begin{array}{c} -m - w \\ 0, -m - w + N + n - 1 \end{array}\right).$$
(3.41)

Proof. The detailed derivation is shown in Appendix B.

Where $G_{1,2}^{2,1}(\cdot|\cdot)$ is the Meijer's G-function ([69] [eqn 9.301]). By substituting $\mathbb{E}[\gamma_{S_1}^{\text{up}}]$ and $\mathbb{E}[\gamma_{S_2}^{\text{up}}]$ into (3.40), the closed-form upper bound of ergodic sum rate is obtained.

3.3.5 Impact of Channel Estimation Errors

In practice, channel coefficients are estimated at the receiver and thereby, can not be known perfectly. Channel estimation errors depend on the type of the estimator and the number of pilot symbols. In general, by using linear minimum mean square error (MMSE), the channel coefficients can be modeled as [25]

$$\mathbf{h}_1 = \hat{\mathbf{h}}_1 + \mathbf{e}_1,$$

 $\mathbf{h}_2 = \hat{\mathbf{h}}_2 + \mathbf{e}_2,$ (3.42)

where the estimation error \mathbf{e}_1 , \mathbf{e}_2 and channel estimates $\hat{\mathbf{h}}_1$ and $\hat{\mathbf{h}}_2$ are assumed to be mutually independent and follow complex Gaussian distribution with zero mean and variances Ω_{e_1} , Ω_{e_2} , $\hat{\Omega}_1 = \Omega_1 - \Omega_{e_1}$ and $\hat{\Omega}_2 = \Omega_2 - \Omega_{e_2}$, respectively. Note that MRT based weight vectors become $\hat{\mathbf{w}}_1 = (\hat{\mathbf{h}}_1^H / || \hat{\mathbf{h}}_1 ||)$ and $\hat{\mathbf{w}}_2 = (\hat{\mathbf{h}}_2^H / || \hat{\mathbf{h}}_2 ||)$. Substituting (3.42) into (3.1), (3.2) and (3.3), and after removing the self-interference term with some further

simplifications, the instantaneous SINRs can be written as

$$\gamma_{S_{1}} = \frac{\gamma_{1}\gamma_{2}}{(\gamma_{1} + \chi_{1})\gamma_{I} + \psi_{1}\gamma_{1} + \beta_{1}\gamma_{2} + \lambda_{1}},
\gamma_{S_{2}} = \frac{\gamma_{1}\gamma_{2}}{(\gamma_{2} + \chi_{2})\gamma_{I} + \psi_{2}\gamma_{2} + \beta_{2}\gamma_{1} + \lambda_{2}},$$
(3.43)

where, $\chi_1=(Pd_1^{-\alpha}/N_0)\Omega_{e_1},\ \psi_1=2+(Pd_2^{-\alpha}/N_0)\Omega_{e_2},\ \beta_1=1+(Pd_1^{-\alpha}/N_0)\Omega_{e_1},\ \lambda_1=(2Pd_1^{-\alpha}/N_0)\Omega_{e_1}+(Pd_2^{-\alpha}/N_0)\Omega_{e_2}+(Pd_1^{-\alpha}/N_0)(Pd_2^{-\alpha}/N_0)\Omega_{e_1}\Omega_{e_2},\ \chi_2=(Pd_2^{-\alpha}/N_0)\Omega_{e_2},\ \psi_1=2+(Pd_1^{-\alpha}/N_0)\Omega_{e_1},\ \beta_2=1+(Pd_2^{-\alpha}/N_0)\Omega_{e_2}\ \text{and}\ \lambda_2=(2Pd_2^{-\alpha}/N_0)\Omega_{e_2}+(Pd_1^{-\alpha}/N_0)\Omega_{e_1}+(Pd_2^{-\alpha}/N_0)(Pd_1^{-\alpha}/N_0)\Omega_{e_2}\Omega_{e_1}.$ It is worth mentioning that Ω_{e_1} and Ω_{e_2} reflect the amount of estimation error. When $\Omega_{e_1}=\Omega_{e_2}=0$, perfect CSI is used and (3.43) becomes equal to (3.4). Channel estimation errors are usually small in practical operations, thus $\chi_1,\ \chi_2,\ \lambda_1$ and λ_2 can be neglected (as in [76, 77]), since their values are much smaller compared to the SNR values γ_1 and γ_2 in the denominator. Then, (3.43) can be written as

$$\gamma_{S_1} \approx \frac{\gamma_1 \gamma_2}{\gamma_1 \gamma_I + \psi_1 \gamma_1 + \beta_1 \gamma_2} = \frac{\frac{\gamma_1}{\beta_1} (\frac{\gamma_2}{\gamma_I + \psi_1})}{\frac{\gamma_1}{\beta_1} + (\frac{\gamma_2}{\gamma_I + \psi_1})},$$

$$\gamma_{S_2} \approx \frac{\gamma_1 \gamma_2}{\gamma_2 \gamma_I + \psi_2 \gamma_2 + \beta_2 \gamma_1} = \frac{\frac{\gamma_2}{\beta_2} (\frac{\gamma_1}{\gamma_I + \psi_2})}{\frac{\gamma_2}{\beta_2} + (\frac{\gamma_1}{\gamma_I + \psi_2})}.$$
(3.44)

Although not shown here, by using Monte Carlo simulations the mean square error between (3.43) and (3.44) is observed to be close to zero for a wide SNR ranges when $\Omega_{e_1} = \Omega_{e_2} \leq 0.01$. Therefore, this SINR approximation can be safely used. Accordingly, the upper bound given in (3.5) becomes

$$\gamma_{S_1}^{\text{up}} = \min\left(\frac{\gamma_1}{\beta_1}, \frac{\gamma_2}{(\gamma_I + \psi_1)}\right),
\gamma_{S_1}^{\text{up}} = \min\left(\frac{\gamma_2}{\beta_2}, \frac{\gamma_1}{(\gamma_I + \psi_2)}\right).$$
(3.45)

Using this result and following the same derivation steps, CDFs of source SINRs ${}_{,}F_{\gamma_{S_1}^{\text{up}}}(\gamma)$

and $F_{\gamma_{S_2}^{\text{up}}}(\gamma)$ can be obtained as

$$F_{\gamma_{S_i}^{\text{up}}}(\gamma) = 1 - \sum_{m=0}^{L_i - 1} \sum_{w=0}^{L_j - 1} \frac{e^{-\frac{\beta_i \gamma}{\Omega_i}} e^{-\frac{\psi_i \gamma}{\Omega_j}}}{m! w!} \left(\frac{\beta_i \gamma}{\Omega_i}\right)^m \left(\frac{\psi_i \gamma}{\Omega_j}\right)^w \left(\frac{\psi_i}{\Omega_I}\right)^N U\left(N, N + w + 1, \frac{\psi_i \gamma}{\Omega_j} + \frac{\psi_i}{\Omega_I}\right). \tag{3.46}$$

Furthermore, by applying **Lemma** 3.1 with some mathematical manipulations with the help of ([69] [eqn 1.111 and 3.351.3]), the CDF of e2e SINR can be derived as

$$F_{\gamma_{\text{e2e}}^{\text{up}}}(\gamma) = 1 - \sum_{m=0}^{L_{1}-1} \sum_{w=0}^{L_{2}-1} \sum_{j=0}^{m} \sum_{v=0}^{w} {m \choose j} {w \choose v} \frac{e^{-\frac{\psi_{2}\gamma}{\Omega_{1}}} e^{-\frac{\psi_{1}\gamma}{\Omega_{2}}}}{m!w!\Omega_{I}^{N}\Gamma(N)} \left(\frac{\psi_{2}\gamma}{\Omega_{1}}\right)^{m} \left(\frac{\psi_{1}\gamma}{\Omega_{2}}\right)^{w} \times \frac{(N+j+v-1)!}{\psi_{2}^{j}\psi_{1}^{\nu}(\frac{\gamma}{\Omega_{1}} + \frac{\gamma}{\Omega_{2}} + \frac{1}{\Omega_{I}})^{N+j+v}}.$$
(3.47)

By utilizing the CDF expressions in (3.46) and (3.47), OP, SER and ESR can be easily derived in the presence of channel estimation errors similar to perfect CSI case. Although the lengthy derivations are not presented here to avoid repetition, the effect of channel estimation errors is illustrated and discussed in the next section.

3.4 Numerical Results and Discussion

In this section, our analytical results are compared with Monte Carlo simulations. The OP curves are plotted by using (3.20) and (3.36), and the curves for the SSER are plotted based on (3.23). Plots of upper bound of ESR correspond to the expression in (3.40). For illustration purposes, the distances between each source and the relay are assumed to be identical and normalized to unity

Figure 3.2 demonstrates the analytical lower bound for the system OP performance when different signal-to-interference power ratios (SIR) are utilized ($P/P_I=15,20,30\,$ dB). Our theoretical results match the Monte Carlo simulation results perfectly in medium to high SNR range even for small SIR (note that in cellular system, the practical SIR value to provide sufficient voice quality is greater than or equal to 18 dB [31]).

Figure 3.3 shows the system OP when the number of interference signals is N=6 and the SIR is $(P/P_I=30 \text{ dB})$. As can be observed, CCI significantly degrades the outage probability as the curves exhibit an error floor in the high SNR regime since the effect

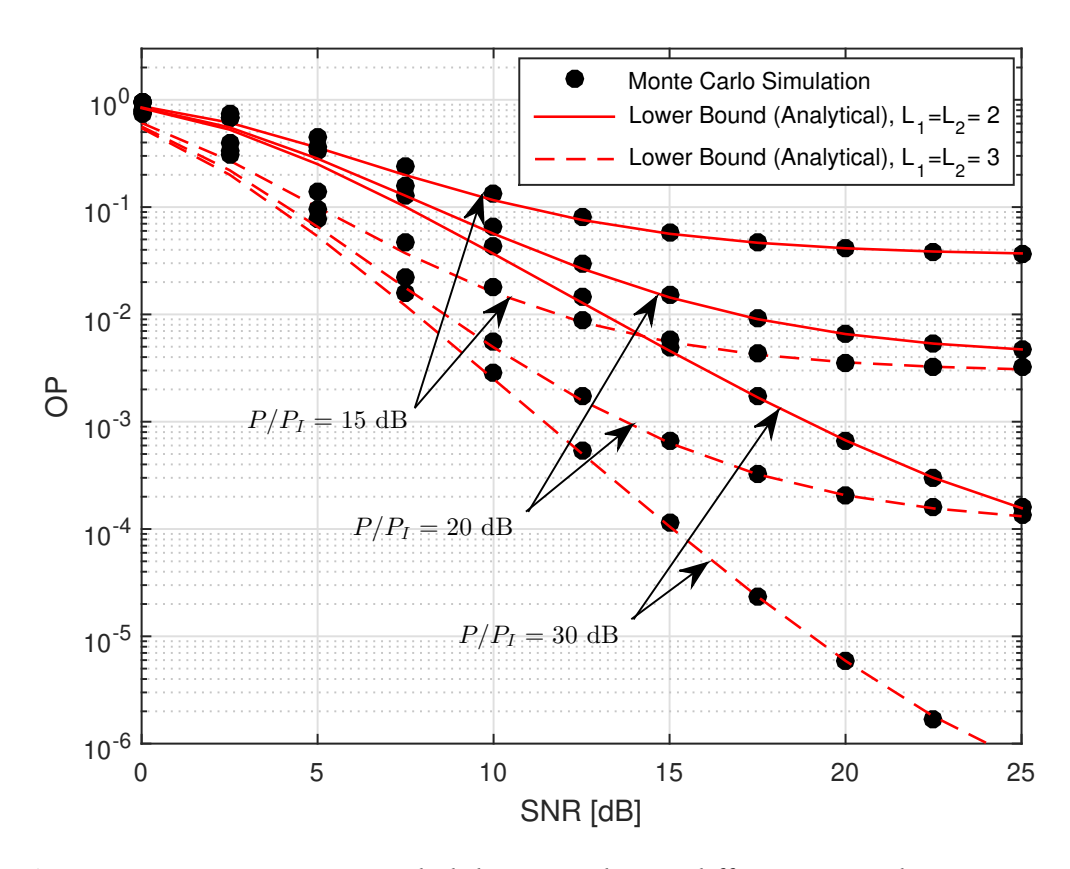


Figure 3.2 System outage probability considering different SIR values, $\gamma_{th} = 0$ dB and N = 6.

of interference becomes dominant compared to noise. In addition, to understand the effect of MRT on the performance, several number of antennas at S_1 and S_2 are selected as $(L_1, L_2) = (1, 1), (1, 2), (2, 2), (2, 3), (3, 3), (3, 4)$. As expected, for a fixed L_1 , increasing L_2 does not change the diversity gain e.g., $(L_1 = 1, L_2 = 1)$ and $(L_1 = 1, L_2 = 2)$ have the same diversity. Obviously, it can be inferred that employing MRT in AF-TWRN makes the system resilient against CCI and thus it is practically preferable to obtain 99% availability and more. Figure 3.4 illustrates the impact of the number of CCI signals on the system OP while $P/P_I = 30$ dB is kept constant and $L_1 = L_2 = 2$. As can be observed, by decreasing the number of CCI signals, the system OP decreases as well. When the SNR increases, the OP reaches to an error floor, while the error floor does not exist for the interference-free case.

Figure 3.5 illustrates the effect of the strength of CCI signals on the system OP. The number of CCI signals N=6 is kept constant and various interference powers ($P_I=0,7,10$ dB) are considered. It can be seen that the system OP increases when the interference power is increased. Besides, from Figures 3.4 and 3.5, it can be understood that the change of the number and/or the power of interfering signals do not affect the diversity order.

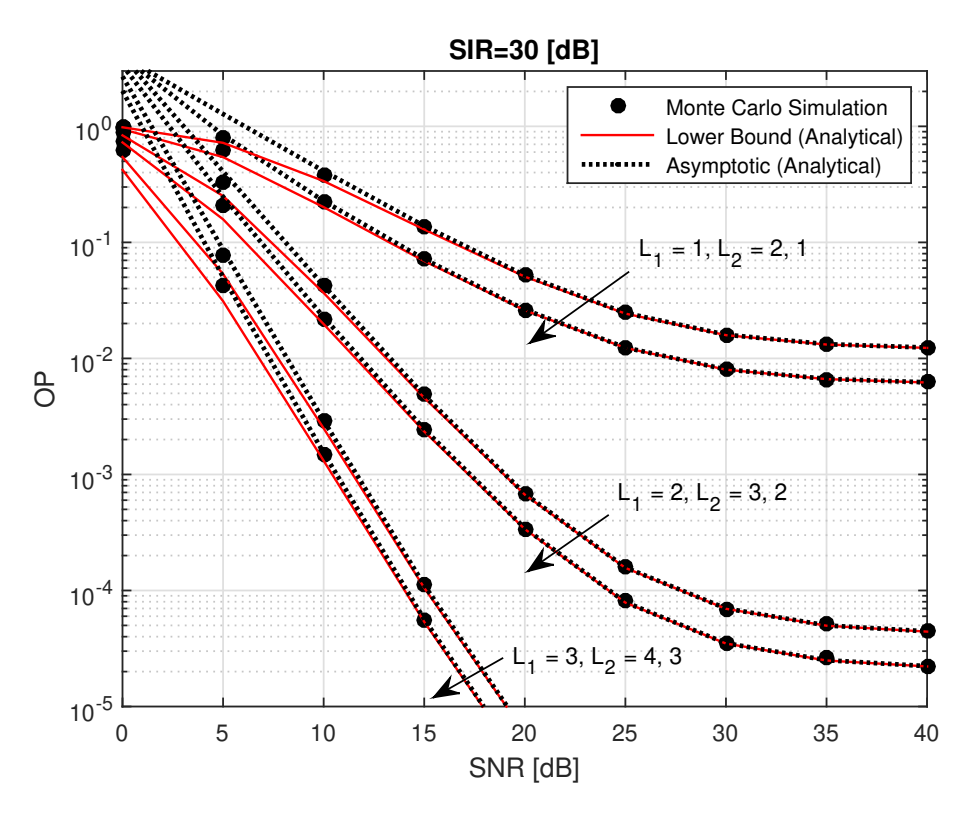


Figure 3.3 System outage probability of AF-TWRN with CCI for different number of antennas, $\gamma_{\rm th}=0$ dB.

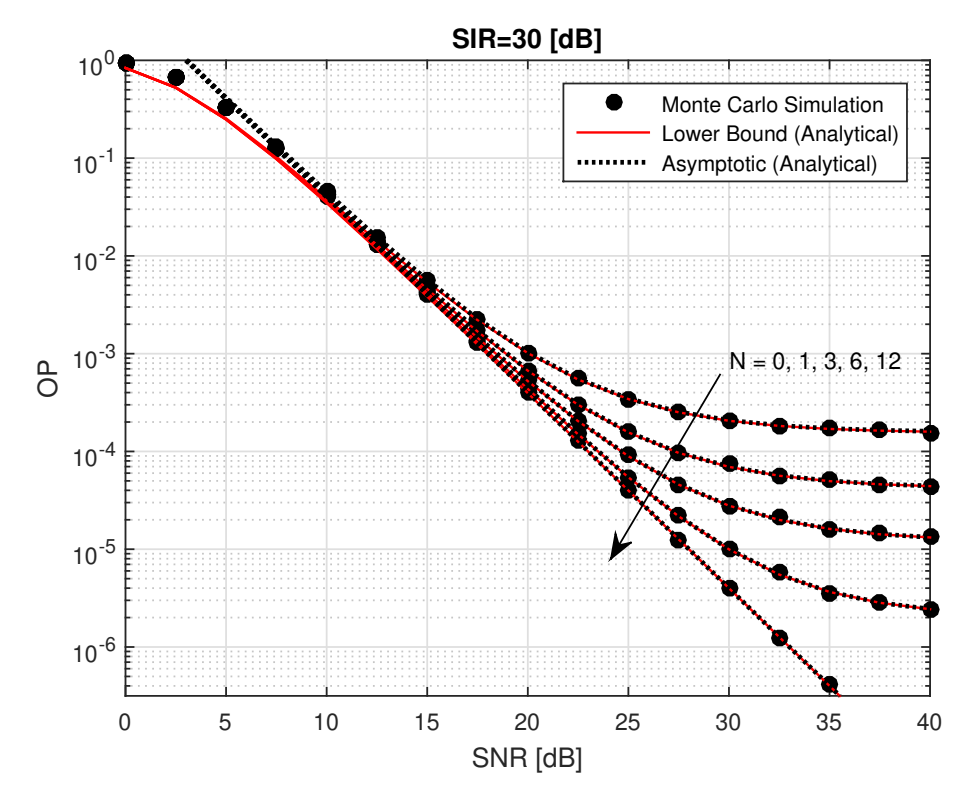


Figure 3.4 System outage probability of AF-TWRN with different numbers of co-channel interference signals, $\gamma_{\rm th}=0$ dB and $L_1=L_2=2$.

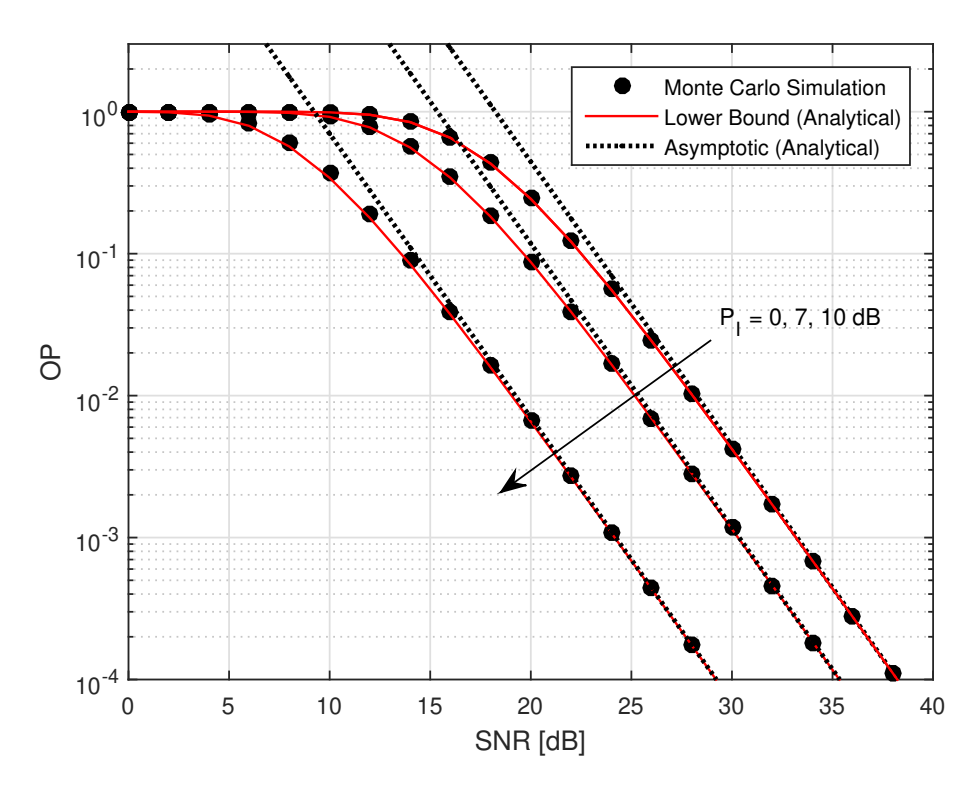


Figure 3.5 System outage probability with different values for the constant interference power, $\gamma_{\rm th}=0$ dB and $L_1=L_2=2$.

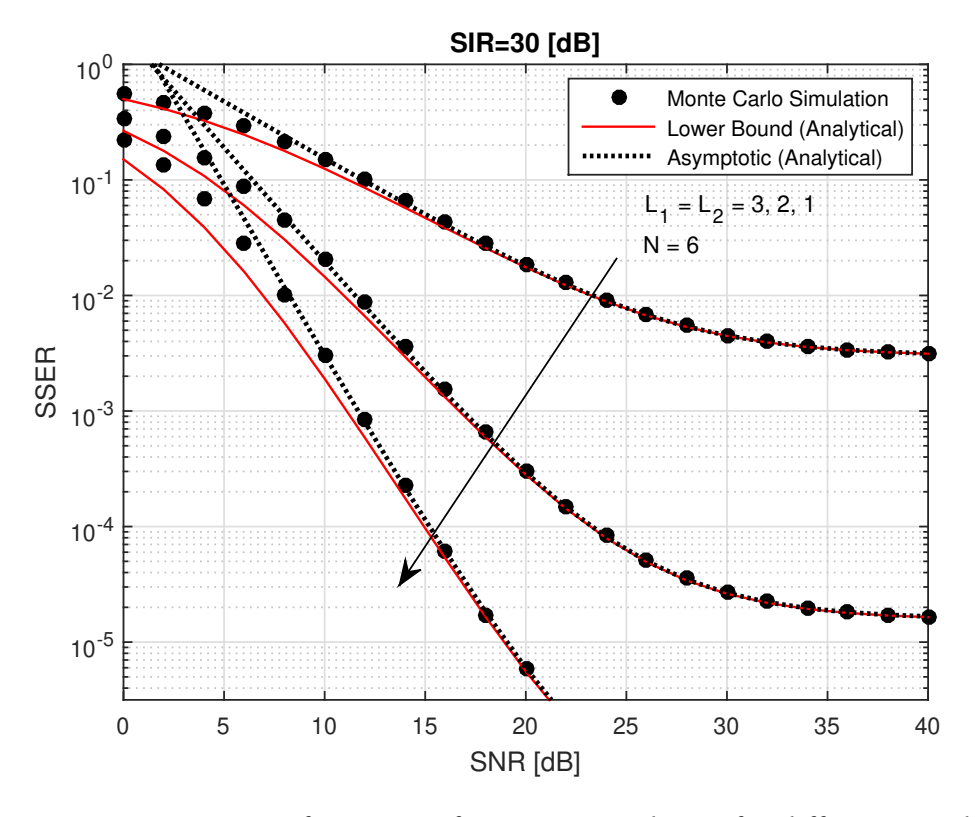


Figure 3.6 Sum SER performance of AF-TWRN with CCI for different number of antennas.

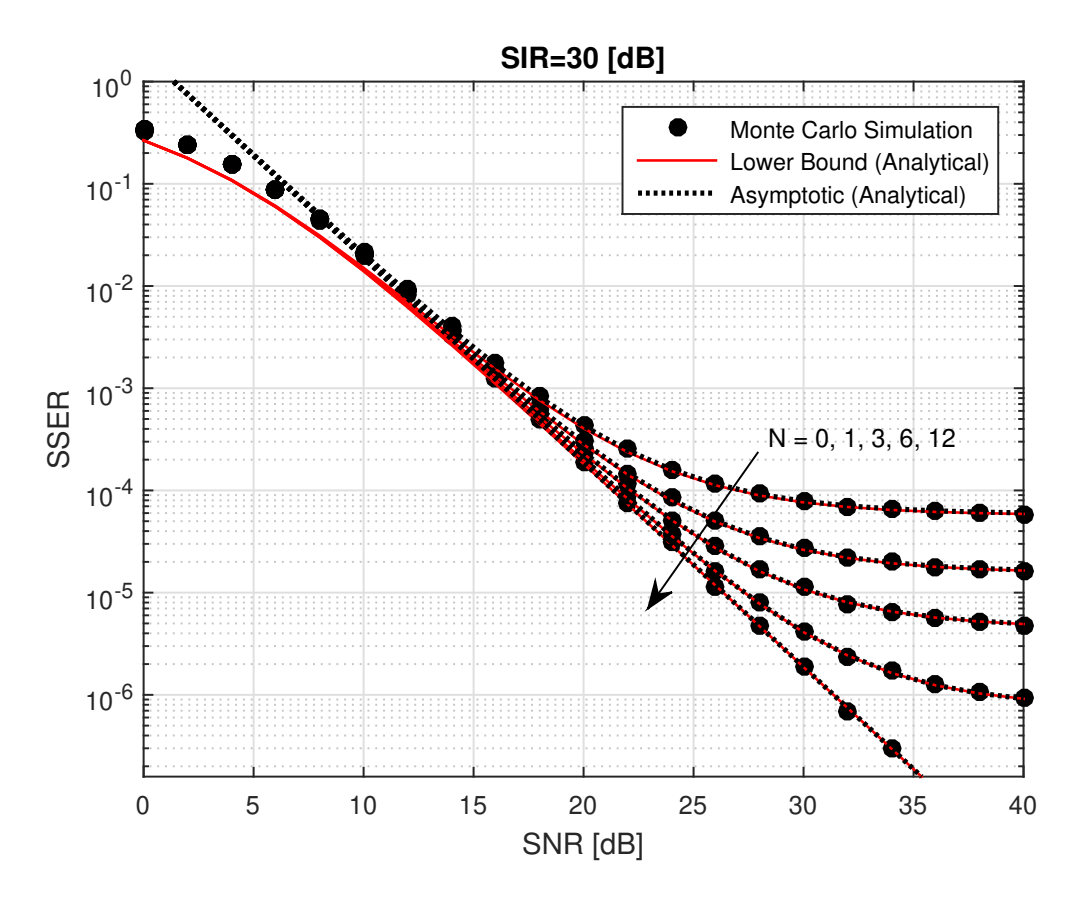


Figure 3.7 Sum SER performance of AF-TWRN with CCI for different number of interference signals, $L_1 = L_2 = 2$.

Figure 3.6 depicts the theoretical lower bound of the SSER for BPSK modulation (a = b = 1) with different antenna numbers for S_1 and S_2 . As can be observed, the SSER can be improved dramatically by employing MRT (the cases when $L_1 = L_2 = 2,3$) compared to the single antenna case (when $L_1 = L_2 = 1$). Specifically, MRT with 2 or 3 antennas at both sources can achieve $10^{-2.9}$ and 10^{-4} SSER respectively at 15 dB SNR compared to $10^{-1.5}$ SSER without MRT.

Figure 3.7 demonstrates the impact of the number of CCI signals on the SSER. When the number of CCI signals is decreased, the SSER performance becomes better as the number of CCI have a direct influence on the system array gain with no change in the diversity order.

Figure 3.8 shows the ergodic sum rate of the system for several number of CCI signals, antennas and different levels of interference power. Our analytical ESR upper bound denoted by (3.40) is tight compared to simulation results. Obviously, increasing the number and/or the power of the CCI signals will degrade the ESR performance. On the other hand, increasing the number of antennas will improve the performance.

Figure 3.9 presents the effect of both CCI and CEE on the system OP performance for

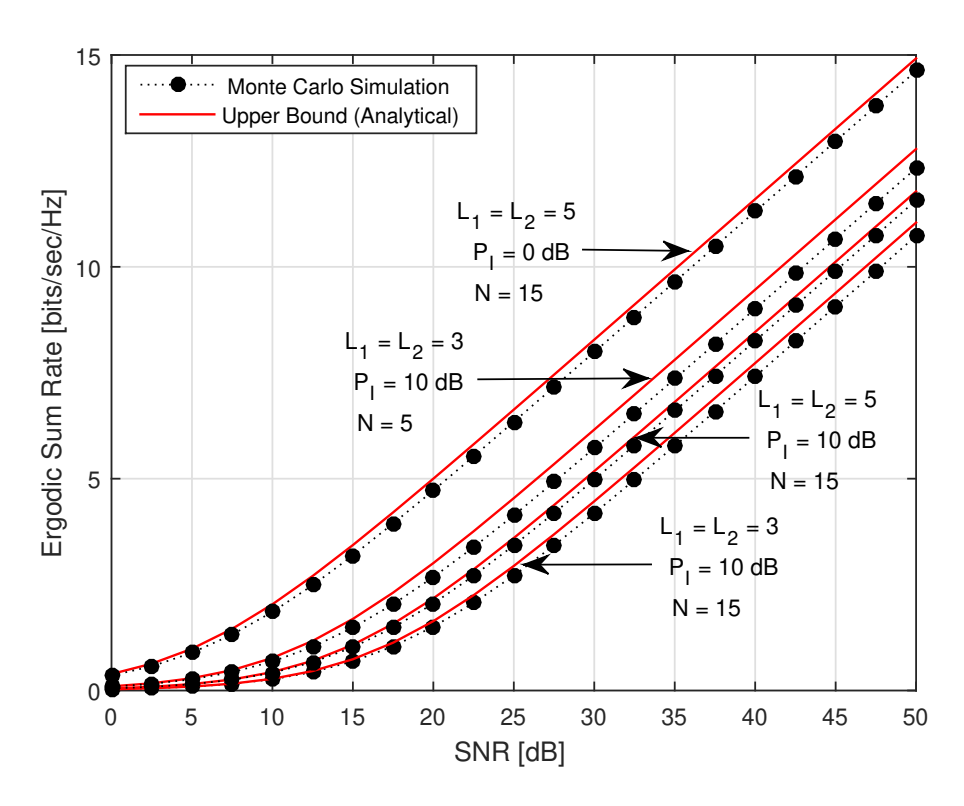


Figure 3.8 Achievable sum rate with different numbers of CCI Signals, power and different number of antennas.

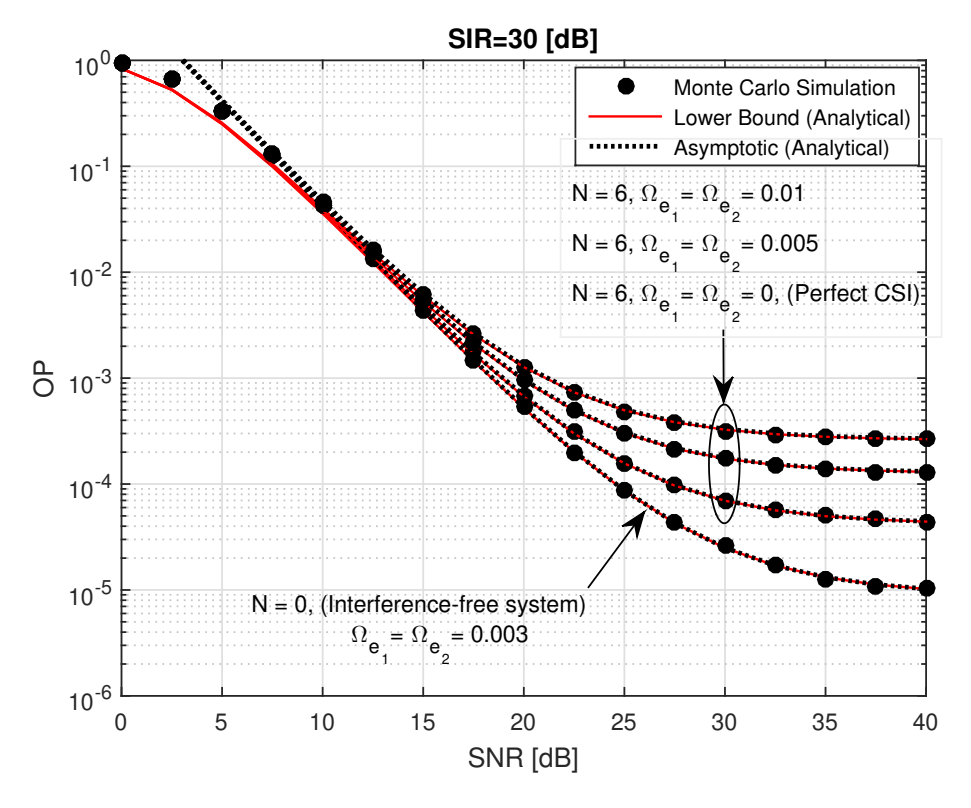


Figure 3.9 System outage probability of AF-TWRN with CCI and different CEE values, $\gamma_{\rm th}=0$ dB and $L_1=L_2=2$.

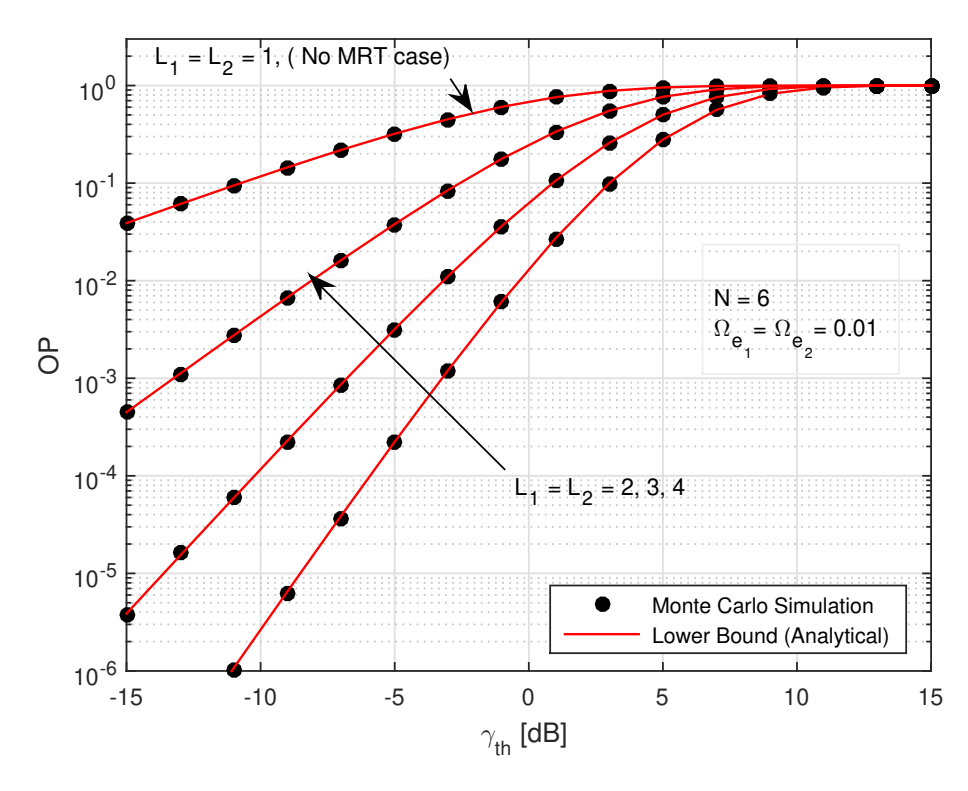


Figure 3.10 System outage probability vs SINR threshold for different number of antennas, $P_I = 10$ dB and $\Omega_{e_1} = \Omega_{e_2} = 0.01$.

various values of CEE where the analytical lower bound results are calculated by using expression (3.47) and the ratio between the signal and interference power is assumed to be constant ($P/P_I=30~\mathrm{dB}$). As can be seen from the figure, the OP becomes worse when CEE increases. To overcome this problem, the number of pilot symbols can be increased. More links can be deployed in the proposed system to make it robust against the CCI and CEE.

Figure 3.10 shows the impact of the number of antennas on OP where the noise power N_0 is normalized to unity where the transmit and interferer powers are fixed at P=20 dB and $P_I=10$ dB, respectively. Note that our analytical bounds are close to the exact results obtained by Monte Carlo simulations even at low SNRs when the interference power (see Figure 3.5) is assumed to be fixed. The plot indicates that the joint effect of CCI and CEE can be reduced considerably by utilizing MRT with increasing the number of antennas.

In Figure 3.11, the effect of imperfect channel estimation on the SSER performance is explored. As in Figure 3.6, SIR is assumed constant $(P/P_I=30 \text{ dB})$ and the single antenna case is compared with the multi-antenna case $(L_1=L_2=2)$ when the number of CCI signals is fixed (N=6) and the values of CEE is varied. Clearly, in both cases, increasing amount of estimation errors affect only the array gain, thus

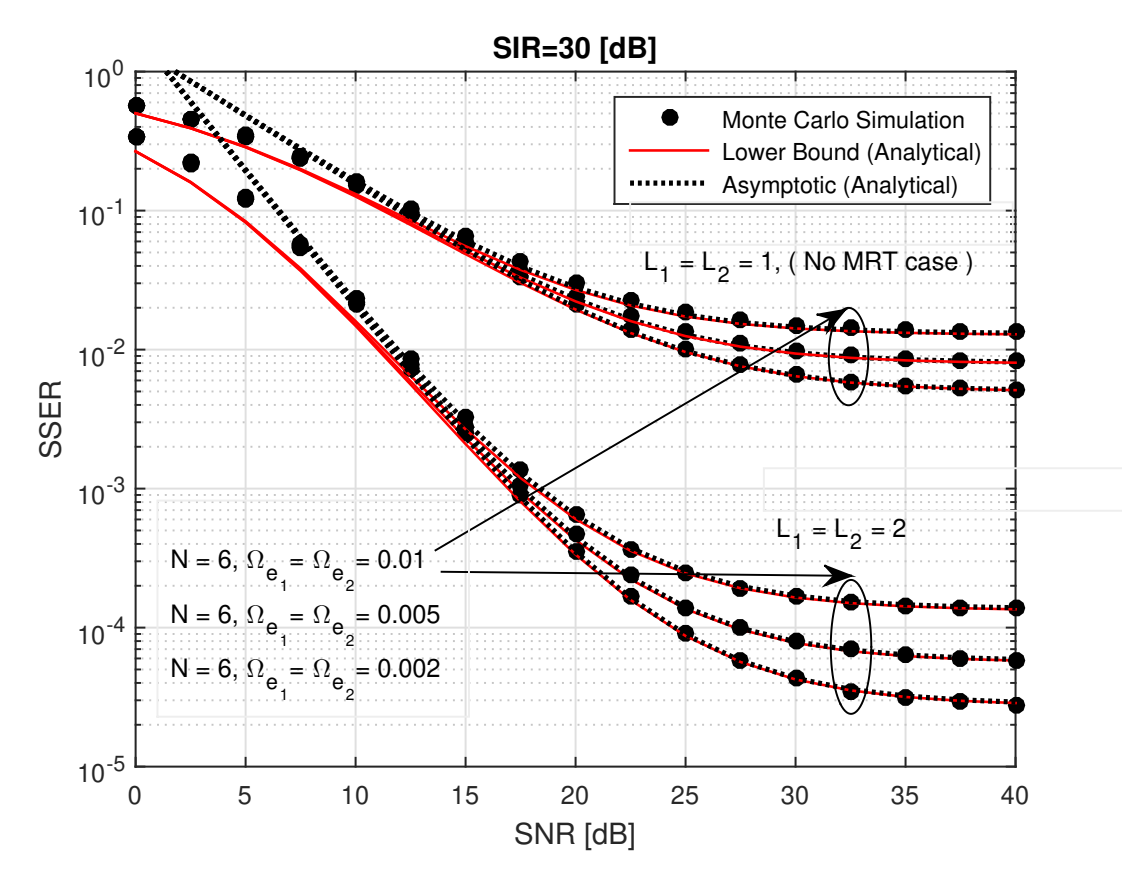


Figure 3.11 Sum SER performance of AF-TWRN with different number of antennas, different values of CEE, $P/P_I = 30$ dB and N = 6.

the SSER becomes worse. However, using more antennas with MRT increases the diversity gain and SSER considerably. Employing the low complexity MRT technique can be a practical solution for the performance degradation observed in TWRNs due to CCI, noise and CEE.

3.5 Chapter Summary

In this chapter, MRT technique is proposed as a solution for AF-TWRNs to suppress the performance loss caused by unavoidable CCI plus noise distortion at the single antenna relay receiver. After obtaining the upper bound of the cumulative distribution function of SINR, tight lower bound expressions of OP, SER and upper bound of system ergodic sum rate are derived and illustrated with extensive numerical examples. Moreover, the asymptotic behavior of the OP and SSER, the array and diversity gains are presented. Furthermore, the effect of imperfect CSI is also explored. Our derived expressions are validated for arbitrary signal-to-interference power ratios, numbers of co-channel interferers and a majority of modulation formats employed in the practical systems.

4

EXACT PERFORMANCE ANALYSIS OF MAXIMAL RATIO TRANSMISSION ON DECODE-AND-FORWARD RELAYING SYSTEM UNDER THE IMPACT OF CO-CHANNEL INTERFERENCE

Co-channel interference (CCI) in wireless networks is increasing and thus becoming a critical factor degrading the reliability and quality experienced since the valuable spectrum bands are shared by growing number of terminals. With the aim of improving the performance, this chapter analyzes the performance of maximal-ratio transmission (MRT) cooperative communication system over Nakagami-m fading channels in the presence of CCI. In particular, a dual-hop decode-and-forward relaying is investigated when multiple interferers affect the relay and the destination nodes. Firstly, the cumulative distribution function (CDF) and the probability density function (PDF) of the signal-to-interference-plus-noise ratio (SINR) are derived. Then, the exact expressions for the outage probability (OP), average bit error probability (ABEP), and ergodic capacity are obtained. Furthermore, asymptotic expressions for OP and ABEP are provided to get insights about the diversity and coding gains. Finally, simulation results are presented to validate our theoretical analysis.

4.1 Introduction

One-way relaying networks (OWRNs) can be widely used to increase capacity and coverage while decreasing power consumption [78, 79]. These benefits are quite desirable in emerging systems such as industrial wireless sensor networks (IWSNs) [80] and internet of things (IoT) [81]. Therefore, OWRNs has been studied in the literature recently. For example, Cai et al. [10] explore device-to-device communications while physical layer security (PLS) of OWRN is investigated in [11]. Furthermore, Solanki et al. [12] deals with the cognitive radio (CR), hardware impairment, and channel estimation error (CEE). Most of the research assume that

relays use amplify-and-forward (AF) method instead of decode-and-forward (DF) although DF technique can be more preferable in practice since it results in better reliability by eliminating noise enhancement in AF relays [50].

Co-channel interference (CCI) is a major factor that degrades the performance of wireless communication networks. For instance, In the next-generation cellular networks [82], CCI is expected to increase further since the number of users, sensors, IoT devices in the same cluster will be increasing while frequency bands are limited. Moreover, the number of the cells tends to increase in order to improve energy efficiency and reduce latency, thus, there will be more cells using the same frequency due to the frequency reuse that increase capacity [83]. Consequently, the influence of co-channel interference has been examined for both AF and DF relaying systems (e.g., [26, 84–89] and references therein). For instance, Al-Qahtani et al. [84] obtains the exact outage probability (OP) for AF-OWRN with single antenna nodes over Nakagami-m fading by considering CCI only at the relay and destination. Similarly, the OP performance of the dual-hop DF relaying system with CCI effect has been studied over Rayleigh [85–87], Nakagami-m [88], and κ - μ [89] fading channels. Besides, the ergodic capacity of AF relaying systems in the presence of interference over Nakagami-m fading for dual-hop [26], and multi-hop [27] are provided when all terminals are equipped with a single antenna.

The use of multiple-antenna techniques is well-known for achieving spatial diversity gains to increase reliability that is much needed especially when CCI becomes significant. However, due to the increased computational complexity at the receiver, only a few of multi-input multi-output (MIMO) techniques are preferable in practice. For example, the maximal ratio transmission (MRT) [3, 90] approach is simple and it can achieve full spatial diversity without increasing receiver complexity. Therefore, it is highly suitable for transmissions from base stations to the size and power-constrained mobile units and relays of one-way relaying network (OWRN). In the literature, the performance of MRT with the DF relaying has been investigated over Rayleigh fading [17] and Nakagami-m fading channels [18]. The error performance of the dual-hop AF relaying with MRT over Nakagami-m fading is presented in [19]. Similarly, Eylem et al. [20] derives an upper-bound on OP, lower-bound for error probability, and ergodic capacity for AF relaying system in the Rayleigh fading. Furthermore, an error probability of multi-hop DF relay networks with MRT over cascaded Nakagami-m fading channel is studied in [21]. All of the above MRT related works considered noise-limited scenarios and neglected the effects of co-channel interference.

Performance of OWRN with multi-antenna terminals exposed to co-channel

interference has been studied in [91–95]. Particularly, Yang et al. [91] proposed interference-limited AF single antenna relaying with multi-antenna source and destination using diversity-multiplexing trade-off (DMT) approach ¹. Lee et al. [92] provides the outage and the average bit error probabilities of AF OWRN over Rayleigh fading with CCI impact on the relay and destination while only the source is equipped with multiple antennas employing the orthogonal space-time block code (OSTBC). Zhong et al. [93] has studied the OP of dual-hop AF system over Rayleigh fading with single antenna terminals where only a single interferer is affecting the relay that use MRT. Furthermore, the outage probability [94], and the ergodic capacity [95] have been explored for an CCI exposed relaying with MRT over Rayleigh fading while single antenna source and destination are assumed to be free from CCI effects.

Throughout the development of wireless standards, mostly low complexity options are adopted since high complexity results in increased delay and hence lower throughput. The motivation for using MRT is mostly reducing the computational load for receiver of size and power limited user terminal which can also behave as relays in the future. Relays can also be used for extending the coverage without introducing much delay and power consumption. In addition, The above-mentioned works shows the background for MRT based OWRN research with CCI. Due to the mathematical difficulty of analyzing the general case, most of the existing studies have only analyzed outage probability and/or considered single antenna nodes and/or some CCI-free nodes. In this paper, a comprehensive performance analysis of a dual-hop DF OWRN over Nakagami-m fading channel where all transmitters employs MRT and all receivers are affected by multiple co-channel interferers. The main contributions of this chapter can be listed as follows:

- Signal-to-interference-plus-noise ratios of the first and second hop are provided considering multiple co-channel interference signals and noise at the relay and destination nods.
- The per-hop SINR random variable (RV) statistics are obtained in teams of the cumulative distribution function and the probability density function over Nakagami-m fading channels.
- The exact-form expressions of the outage, average bit error probabilities, and ergodic capacity are derived. Besides, the performance of interference-free system is included as a special case.

¹DMT has been proposed in [96] which considers two principal gains, diversity and multiplexing available in a slow-fading MIMO channel when the SNR $\rightarrow \infty$.

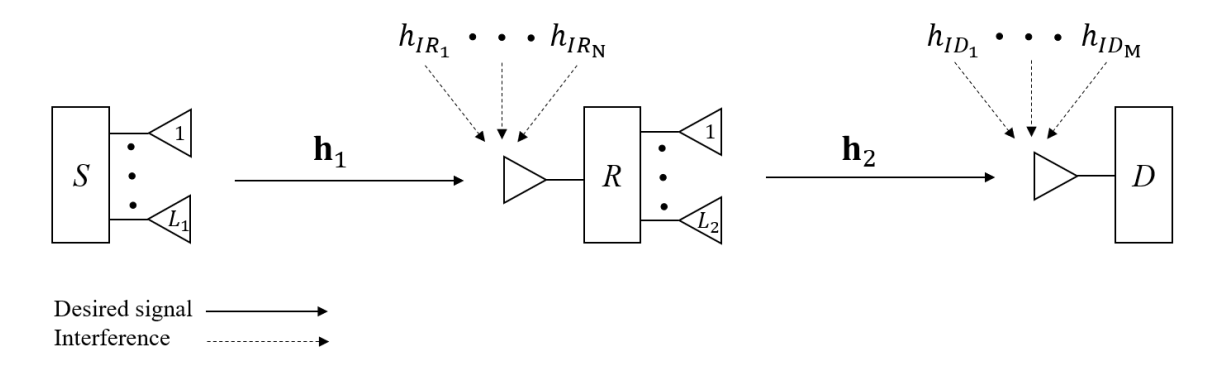


Figure 4.1 Block diagram of dual-hop maximal ratio transmission with CCI at the relay and destination.

- Asymptotic expressions of outage and bit error probabilities are presented, then, diversity and array gains are extracted.
- To verifying our derivations' correctness, numerical examples are presented and compared with Monte Carlo simulations and observe comparisons of different cases.

The rest of this chapter is organized as follows: Section 4.2 describes the system model. The performance analysis for the proposed system is presented in Section 4.4. Numerical examples are provided in Section 4.5 followed by the conclusions in Section 4.6.

4.2 System and Channel Models

The block diagram of the DF dual-hop relaying with MRT and CCI system model is shown in Figure 4.1. It is assumed that the communication between source to the destination takes place in two phases. In the first phase, the source node S transmits the information signal by employing MRT scheme [3] from L_1 antennas to the relay node R having a single receive antenna. The relay node receives the information signal plus additive white Gaussian noise (AWGN), as well as finite number of CCI signals from N interferers. In the second phase, the relay utilizes the decode-and-forward (DF) protocol to send the re-encoded MRT signal via its L_2 transmit antennas to the single antenna destination D which is also under the impact of CCI signals from M interferers. The direct link between source and destination is assumed to be unavailable as can be observed when severe path loss or shadowing exist. In addition, receivers are assumed to know the channel coefficient vectors \mathbf{h}_1 having size $L_1 \times 1$ at $S \to R$ link and \mathbf{h}_2 having size $L_2 \times 1$ between $R \to D$. Furthermore, h_{IRi} (i = 1, 2, ..., N) and h_{IDj} (j = 1, 2, ..., M) are channel coefficients from i-th and j-th interferers at R and D respectively which do not know their values, this can be considered a

"worst-case" scenario [97, 98]. Moreover, it is assumed that the CCI links at the relay and destination nodes have the same average interference-to-noise ratio (INR) similar to [99, 100]. Besides, all channels between the nodes and the interference signals are assumed to be independent and non-identically distributed (i.n.i.d) Nakagami-m RV. Received signals of the first and second hop, y_R and y_D respectively can be written as

$$y_{R} = \sqrt{P_{S}} \mathbf{h}_{1} \mathbf{w}_{1} x_{S} + \sqrt{P_{IR}} \sum_{i=1}^{N} h_{IRi} x_{IRi} + n_{R},$$
(4.1)

$$y_{D} = \sqrt{P_{R}} \mathbf{h}_{2} \mathbf{w}_{2} x_{R} + \sqrt{P_{ID}} \sum_{j=1}^{M} h_{IDj} x_{IDj} + n_{D},$$
(4.2)

where x_S , x_R , x_{IRi} , and x_{IDj} are the transmitted symbols from source, relay and i-th interferer of the relay, and j-th interferer for the destination, respectively, each having an average power normalized to unity. Consequently, \mathbf{w}_1 and \mathbf{w}_2 represent the MRT weight vectors of the first and second hop specified as $\mathbf{w}_1 = (\mathbf{h}_1^H/||\mathbf{h}_1||)$ and $\mathbf{w}_2 = (\mathbf{h}_2^H/||\mathbf{h}_2||)$, respectively. P_S and P_R are the source and relay permitted transmission power, respectively. P_{IR} and P_{ID} are the CCI power at the relay and destination nodes, respectively. Noise samples n_R and n_D at the relay and destination nodes are modeled as complex Gaussian RVs with zero mean and N_0 variance.

4.3 SINR Statistical Analysis

In this section, the SINR per hop, instantaneous SNR, instantaneous INR, and the system end-to-end (e2e) SINR are presented and then, exact e2e cumulative distribution function (CDF) and probability density function (PDF) of SINRs are derived.

Firstly, for the considered system, equivalent signal to interference plus noise ratios (SINRs) of the first and second hops, i.e., (γ_{SR}) and (γ_{RD}) RVs respectively, can be written as

$$\gamma_{SR} = \frac{\gamma_1}{\gamma_{IR} + 1},\tag{4.3}$$

$$\gamma_{RD} = \frac{\gamma_2}{\gamma_{ID} + 1},\tag{4.4}$$

where $\gamma_1 = P_S ||\mathbf{h}_1||^2/N_0$ and $\gamma_2 = P_R ||\mathbf{h}_2||^2/N_0$ are instantaneous desired SNRs at relay and destination, respectively. While, $\gamma_{IR} = P_{IR} \sum_{i=1}^N |h_{IRi}|^2/N_0$ and $\gamma_{ID} = P_{ID} \sum_{j=1}^M |h_{IDj}|^2/N_0$ are instantaneous interference-to-noise ratio (INR) at the relay and destination of first and second hop, respectively. To this end, in DF relaying system, end-to-end (e2e) SINR is dominated by the weakest SINR per-hop and it can be expressed as follows [101, 102]

$$\gamma_{e2e} = \min(\gamma_{SR}, \gamma_{RD}). \tag{4.5}$$

4.3.1 The CDFs Derivation

By using the e2e SINR expression, its CDF (for the $\gamma_{\rm e2e}$ RV) can be derived by using the following computation, [103]

$$F_{\gamma_{e2e}}(\gamma) = \Pr\left[\min\left(\gamma_{SR}, \gamma_{RD}\right) \leq \gamma\right]$$

$$= 1 - \Pr\left[\gamma_{SR} > \gamma\right] \Pr\left[\gamma_{RD} > \gamma\right]$$

$$\stackrel{(a)}{=} 1 - (1 - F_{\gamma_{SR}}(\gamma))(1 - F_{\gamma_{RD}}(\gamma))$$

$$\stackrel{(b)}{=} F_{\gamma_{SR}}(\gamma) + F_{\gamma_{RD}}(\gamma) - F_{\gamma_{SR}}(\gamma)F_{\gamma_{RD}}(\gamma),$$

$$(4.6)$$

where $F_{\gamma_{SR}}(\gamma)$ and $F_{\gamma_{RD}}(\gamma)$ are the CDFs of the first and second hop SINR, i.e., (γ_{SR}) and (γ_{RD}) respectively. In our proposed system, all channel coefficients of the desired and interference links are Nakagami-m distributed. Thus, the instantaneous SNRs (γ_1, γ_2) and INRs $(\gamma_{IR}, \gamma_{ID})$ of the first and second hop are central Chi-square distributed random variables with $2m_1L_1$, $2m_2L_2$, $2m_{IR}N$, and $2m_{ID}M$ degrees of freedom, respectively. Their probability density functions are given as [15, 102]

$$f_{\gamma_1}(x) = \left(\frac{m_1}{\bar{\gamma}_1}\right)^{m_1 L_1} \frac{x^{m_1 L_1 - 1}}{\Gamma(m_1 L_1)} \exp\left(-\frac{m_1}{\bar{\gamma}_1}x\right),\tag{4.7}$$

$$f_{\gamma_2}(y) = \left(\frac{m_2}{\bar{\gamma}_2}\right)^{m_2 L_2} \frac{y^{m_2 L_2 - 1}}{\Gamma(m_2 L_2)} \exp\left(-\frac{m_2}{\bar{\gamma}_2}y\right),$$
 (4.8)

$$f_{\gamma_{IR}}(z) = \left(\frac{m_{IR}}{\bar{\gamma}_{IR}}\right)^{m_{IR}N} \frac{z^{m_{IR}N-1}}{\Gamma(m_{IR}N)} \exp\left(-\frac{m_{IR}}{\bar{\gamma}_{IR}}z\right), \tag{4.9}$$

$$f_{\gamma_{ID}}(w) = \left(\frac{m_{ID}}{\bar{\gamma}_{ID}}\right)^{m_{ID}M} \frac{w^{m_{ID}M-1}}{\Gamma(m_{ID}M)} \exp\left(-\frac{m_{ID}}{\bar{\gamma}_{ID}}w\right), \tag{4.10}$$

where m_1 , m_2 , m_{IR} , and m_{ID} are the Nakagami-m fading severity parameters for the channels between source to the relay, relay to the destination, CCI signals to the relay, and CCI signals to the destination, respectively² where $\Gamma(\cdot)$ is the Gamma function ([69][eqn 8.339.1]). Besides, $\bar{\gamma}_1 = P_S/N_0$ and $\bar{\gamma}_2 = P_R/N_0$ are the average received SNRs at the relay and destination, respectively. In addition, $\bar{\gamma}_{IR} = P_{IR}/N_0$ and $\bar{\gamma}_{ID} = P_{ID}/N_0$ are the average interference to noise ratio (INR) at the relay and destination in the first and second hop, respectively. To this end, the CDF of the first hop SINR can be obtained as

$$F_{\gamma_{SR}}(\gamma) = 1 - \frac{\left(\frac{m_{IR}}{\bar{\gamma}_{IR}}\right)^{m_{IR}N} \exp\left(-\frac{m_1}{\bar{\gamma}_1}\gamma\right)}{\Gamma(m_{IR}N)} \sum_{n=0}^{m_1L_1-1} \sum_{k=0}^{n} \binom{n}{k} \left(\frac{m_1}{\bar{\gamma}_1}\gamma\right)^n \frac{(k+m_{IR}N-1)!}{n! \left(\frac{m_{IR}}{\bar{\gamma}_{IR}} + \frac{m_1}{\bar{\gamma}_1}\gamma\right)^{k+m_{IR}N}},$$
(4.11)

Proof. See Appendix C.

Furthermore, it is worth mentioning that for no-interference case, the CDF in (4.11) can be reduced to the well-known CDF of instantaneous SNR, i.e., γ_1 expression in [15, 104]

$$F_{\gamma_1}(x) = \frac{\Upsilon\left(m_1 L_1, \frac{m_1}{\bar{\gamma}_1} x\right)}{\Gamma(m_1 L_1)} = 1 - \exp\left(-\frac{m_1}{\bar{\gamma}_1} x\right) \sum_{n=0}^{m_1 L_1 - 1} \frac{\left(\frac{m_1}{\bar{\gamma}_1} x\right)^n}{n!},\tag{4.12}$$

where $\Upsilon(.,.)$ refers to the lower incomplete gamma function [69]. To obtain the CDF of the second hop SINR, i.e., $F_{\gamma_{RD}}(\gamma)$, Same derivation steps can be followed by exchanging the parameters $(m_1, m_{IR}, \bar{\gamma}_1, \bar{\gamma}_{IR}, L_1, N, \gamma_{SR})$ with the following parameters $(m_2, m_{ID}, \bar{\gamma}_2, \bar{\gamma}_{ID}, L_2, M, \gamma_{RD})$ respectively. Finally, the dual-hop e2e SINR CDF can be readily obtained by substituting the derived CDFs of SINR per-hop into (4.6).

²Note that our system analysis can be valid for many other fading channels readily by selecting a specific value for the fading severity parameter m, i.e., one-sided Gaussian (m = 1/2), Rayleigh (m = 1) and Rician with K factor ($m = (K + 1)^2/(2K + 1)$) distributions.

4.3.2 The PDFs derivation

The PDF of the SINR is another important function to compute the performance metrics of the system. The PDF $f_{\gamma_{SR}}(\gamma)$ of the SINR for the first hop can be calculated as

$$f_{\gamma_{SR}}(\gamma) = \frac{\left(\frac{m_1}{\bar{\gamma}_1}\right)^{m_1 L_1} \left(\frac{m_{IR}}{\bar{\gamma}_{IR}}\right)^{m_{IR}N} \gamma^{m_1 L_1 - 1} \exp\left(-\frac{m_1}{\bar{\gamma}_1}\gamma\right)}{\Gamma(m_1 L_1) \Gamma(m_{IR}N)} \sum_{n=0}^{m_1 L_1} {m_1 L_1 \choose n} \frac{(n + m_{IR}N - 1)!}{\left(\frac{m_{IR}}{\bar{\gamma}_{IR}} + \frac{m_1}{\bar{\gamma}_1}\gamma\right)^{n + m_{IR}N}},$$
(4.13)

Similarly, the PDF for the second hop SINR ($f_{\gamma_{RD}}(\gamma)$) can be readily obtained by using the corresponding channel parameters in (4.13).

4.4 Performance analysis

In this section, the performance analysis of a dual-hop multi-antenna DF with MRT transmission scheme under the impact of co-channel interference is presented. Specifically, the exact forms of OP, average error probability and ergodic capacity are derived. In addition, diversity and array gains are found after obtaining asymptotic expressions of AEP and OP.

4.4.1 Outage Probability

A decode-and-forward dual-hop relaying system is considered to be in outage when one of the two links is in outage. Mathematically, the exact OP can be determined as below by replacing the variable γ in the CDF of the system e2e SINR at expression (4.6), with the SINR threshold, i.e., γ_{th} ,

$$P_{out} = \Pr\left[\gamma_{e2e} \le \gamma_{th}\right] = F_{\gamma_{e2e}}(\gamma_{th}), \tag{4.14}$$

where the SINR threshold value can be selected as $\gamma_{th} = 2^{2R} - 1$, when *R* denotes the target data rate.

4.4.2 Average Bit Error Probability

As common in DF dual hop relaying, the average bit error probability (ABEP) of the system can be expressed as follows [90, 102],

$$P_{e2e}(e) = P_{SR}(e) + P_{RD}(e) - 2(P_{SR}(e) P_{RD}(e)), \tag{4.15}$$

where $P_{SR}(e)$ and $P_{RD}(e)$ denote error probabilities for the first and the second hop, respectively. In the literature, ABEP has been evaluated by using the well-known integrations based on CDF, PDF, or MGF of SINR[32]. In this study, the derived PDF in (4.13) is used to find the exact bit error probability per-hop using the following formula [54, 105]:

$$P_{SR}(e) = \int_0^\infty P_e(e|\gamma_{SR}) f_{\gamma_{SR}}(\gamma) d\gamma , \qquad (4.16)$$

where, $P_e(e|\gamma_{SR})$ is the conditional bit error probability for a given SINR γ_{SR} .

Corollary 4.1. The average error probability of the first hop dual-hop DF relaying system with MRT in the presence of CCI is obtained as

$$P_{SR}(e) = \frac{\alpha^{-m_1 L_1} \left(\frac{m_1}{\tilde{\gamma}_1}\right)^{m_1 L_1} \left(\frac{m_{IR}}{\tilde{\gamma}_{IR}}\right)^{m_{IR}N}}{2 \Gamma(\beta) \Gamma(m_1 L_1) \Gamma(m_{IR}N)} \sum_{n=0}^{m_1 L_1} {m_1 L_1 \choose n} \left(\frac{m_{IR}}{\tilde{\gamma}_{IR}}\right)^{-n-m_{IR}N} \times G_{2,1:0,1;1,1}^{0,2:1,0;1,1} \left(\begin{array}{c} \frac{m_1}{\alpha} \frac{1}{\tilde{\gamma}_{IR}} \\ \frac{m_1}{\alpha} \frac{\tilde{\gamma}_{IR}}{m_{IR}} \frac{1-m_1 L_1 - \beta : - ; 1-n-m_{IR}N}{1-m_1 L_1 - 1 : 0 ; 0} \right),$$

$$(4.17)$$

where α is a constant that depends on the type of modulation (e.g., 0.5 for frequency shift keying (FSK), 1 for phase shift keying (PSK)) and β is another constant depending on the detection scheme (0.5 for coherent detection, and 1 for non-coherent detection). Furthermore, $G_{2,1:0,1;1,1}^{0,2:1,0;1,1}(\cdot|\cdot)$ is the extended generalized bivariate Meijer G-function (EGBMGF) which can be computed efficiently by using Mathematica ([54] [Table II]).

By using similar steps, $P_{RD}(e)$ can be obtained, and then, ABEP for both hops can be substituted into (4.15) to attain the exact e2e average bit error probability.

4.4.3 Ergodic Capacity

The ergodic channel capacity for a dual-hop DF relaying system can be written as

$$C_{e2e} = \frac{1}{2} \min(\bar{C}_{SR}, \bar{C}_{RD}),$$
 (4.18)

where \bar{C}_{SR} and \bar{C}_{RD} denote the average ergodic capacities of the source to relay $S \to R$ and relay to destination $R \to D$ links, respectively. Furthermore, division by 2 comes from the fact that the e2e transmission requires two time slots.

Corollary 4.2. The first hop average ergodic capacity of the dual-hop decode-and-forward multi-antenna relaying system with MRT and co-channel interference can be derived as follows

$$\bar{C}_{SR} = \frac{\log(e)}{\Gamma(m_1 L_1) \Gamma(m_{IR} N)} \sum_{n=0}^{m_1 L_1} {m_1 L_1 \choose n} \left(\frac{m_{IR}}{\bar{\gamma}_{IR}}\right)^{-n} \times G_{1,0:1,1;2,2}^{0,1:1,1;1,2} \left(\begin{array}{c} \frac{\bar{\gamma}_{IR}}{m_{IR}} \\ \frac{\bar{\gamma}_{I}}{m_1} \end{array} \right| 1 - m_1 L_1 : 1 - n - m_{IR} N ; 1 , 1 \\ - : 0 : 1 , 0 \right).$$
(4.19)

Proof. See Appendix F.

The second hop average ergodic capacity can be derived by following similar steps, and then, \bar{C}_{SR} and \bar{C}_{RD} can be substituted into (4.18) to obtain the system ergodic capacity in exact form.

4.4.4 Asymptotic Analysis

In this subsection, in order to extract the diversity and array gains, P_{out} and $P_{sys}(e)$ expressions are simplified by considering high SNR values (i.e., $\bar{\gamma} \to \infty$). By using the Maclaurin series expansion of the exponential function [74], the PDF of γ_1 and γ_2 in (4.7) and (4.8) can be approximated respectively as

$$f_{\gamma_1}^{\infty}(x) \approx \left(\frac{m_1}{\bar{\gamma}_1}\right)^{m_1 L_1} \frac{x^{m_1 L_1 - 1}}{\Gamma(m_1 L_1)},$$
 (4.20)

$$f_{\gamma_2}^{\infty}(y) \approx \left(\frac{m_2}{\bar{\gamma}_2}\right)^{m_2 L_2} \frac{y^{m_2 L_2 - 1}}{\Gamma(m_2 L_2)}.$$
 (4.21)

Then, by integrating these PDFs with respect to x and y, CDFs can be written as follows

$$F_{\gamma_1}^{\infty}(x) \approx \frac{1}{(m_1 L_1)!} \left(\frac{m_1}{\bar{\gamma}_1} x\right)^{m_1 L_1},$$
 (4.22)

$$F_{\gamma_2}^{\infty}(y) \approx \frac{1}{(m_2 L_2)!} \left(\frac{m_2}{\bar{\gamma}_2} y\right)^{m_2 L_2}.$$
 (4.23)

To this end, the asymptotic CDF of the first hop SINR (γ_{SR}) (with $\bar{\gamma} \to \infty$) can be derived as

$$F_{\gamma_{SR}}^{\infty}(\gamma) = \int_{0}^{\infty} F_{\gamma_{1}}^{\infty}((z+1)\gamma) f_{\gamma_{IR}}(z) dz. \tag{4.24}$$

By substituting (4.22) and (4.9) into (4.24) by using ([69] [eqn 1.111 and 3.351.3]), $F_{\gamma_{SR}}^{\infty}(\gamma)$ can be computed as

$$F_{\gamma_{SR}}^{\infty}(\gamma) = \frac{\left(\frac{m_1}{\bar{\gamma}_1}\gamma\right)^{m_1L_1} \left(\frac{m_{IR}}{\bar{\gamma}_{IR}}\right)^{m_{IR}N}}{(m_1L_1)! \ \Gamma(m_{IR}N)} \sum_{n=0}^{m_1L_1} {m_1L_1 \choose n} \frac{(n+m_{IR}N-1)!}{\left(\frac{m_{IR}}{\bar{\gamma}_{IR}}\right)^{n+m_{IR}N}}.$$
 (4.25)

The asymptotic PDF of (γ_{SR}) RV, i.e., $f_{\gamma_{SR}}^{\infty}(\gamma)$ can be obtained as below after taking the derivative of the CDF in (4.25) with respect to γ ,

$$f_{\gamma_{SR}}^{\infty}(\gamma) = \frac{m_1 L_1 \, \gamma^{m_1 L_1 - 1} \left(\frac{m_1}{\tilde{\gamma}_1}\right)^{m_1 L_1} \left(\frac{m_{IR}}{\tilde{\gamma}_{IR}}\right)^{m_{IR}N}}{(m_1 L_1)! \, \Gamma(m_{IR}N)} \sum_{n=0}^{m_1 L_1} {m_1 L_1 \choose n} \frac{(n + m_{IR}N - 1)!}{\left(\frac{m_{IR}}{\tilde{\gamma}_{IR}}\right)^{n + m_{IR}N}}. \tag{4.26}$$

Similarly, $F_{\gamma_{RD}}^{\infty}(\gamma)$ and $f_{\gamma_{RD}}^{\infty}(\gamma)$ can be derived by following the above steps. Then, recall that step (b) in (4.6) can be simplified via neglecting the last multiplication term; $F_{\gamma_{e2e}}(\gamma) \approx F_{\gamma_{SR}}(\gamma) + F_{\gamma_{RD}}(\gamma)$. To this end, using this approximations with $F_{\gamma_{SR}}^{\infty}(\gamma)$ and

 $F_{\gamma_{RD}}^{\infty}(\gamma)$, the asymptotic CDF for (γ_{e2e}) RV can be written as

$$F_{\gamma_{e2e}}^{\infty}(\gamma) \approx \frac{\left(\frac{m_{1}}{\tilde{\gamma}_{1}}\gamma\right)^{m_{1}L_{1}}\left(\frac{m_{IR}}{\tilde{\gamma}_{IR}}\right)^{m_{IR}N}}{(m_{1}L_{1})! \ \Gamma(m_{IR}N)} \sum_{n=0}^{m_{1}L_{1}} {m_{1}L_{1} \choose n} \frac{(n+m_{IR}N-1)!}{\left(\frac{m_{IR}}{\tilde{\gamma}_{IR}}\right)^{n+m_{IR}N}} + \frac{\left(\frac{m_{2}}{\tilde{\gamma}_{2}}\gamma\right)^{m_{2}L_{2}}\left(\frac{m_{ID}}{\tilde{\gamma}_{ID}}\right)^{m_{ID}M}}{(m_{2}L_{2})! \ \Gamma(m_{ID}M)} \sum_{k=0}^{m_{2}L_{2}} {m_{2}L_{2} \choose k} \frac{(k+m_{ID}M-1)!}{\left(\frac{m_{ID}}{\tilde{\gamma}_{ID}}\right)^{k+m_{ID}M}}.$$

$$(4.27)$$

For the interference-free system, (4.27) becomes

$$F_{\gamma_{\text{e2e}}}^{\infty}(\gamma) \approx \frac{1}{(m_1 L_1)!} \left(\frac{m_1}{\bar{\gamma}_1} \gamma\right)^{m_1 L_1} + \frac{1}{(m_2 L_2)!} \left(\frac{m_2}{\bar{\gamma}_2} \gamma\right)^{m_2 L_2}. \tag{4.28}$$

Both ([55] [Prop. 5]) and (4.27) can be used by replacing γ with $\gamma_{\rm th}$ and assuming large value of $\bar{\gamma}$ in order to obtain the asymptotic system OP expression P_{out}^{∞} as

$$P_{out}^{\infty} = \mathcal{G}\left(\frac{\gamma_{\text{th}}}{\bar{\gamma}}\right)^{\min(m_1L_1, m_2L_2)} + \text{H.O.T.}, \tag{4.29}$$

where H.O.T denotes high order terms and the scaling factor \mathcal{G} is given as

$$\frac{g - \left(\frac{m_1^{m_1 L_1} \left(\frac{m_{IR}}{\bar{\gamma}_{IR}}\right)^{m_{IR}N}}{(m_1 L_1)! \ \Gamma(m_{IR}N)} \sum_{n=0}^{m_1 L_1} {m_1 L_1 \choose n} \Xi_1, \qquad m_1 L_1 < m_2 L_2\right) \\
\frac{m_1^{m_1 L_1} \left(\frac{m_{IR}}{\bar{\gamma}_{IR}}\right)^{m_{IR}N}}{(m_1 L_1)! \ \Gamma(m_{IR}N)} \sum_{n=0}^{m_1 L_1} {m_1 L_1 \choose n} \Xi_1 + \frac{m_2^{m_2 L_2} \left(\frac{m_{ID}}{\bar{\gamma}_{ID}}\right)^{m_{ID}M}}{(m_2 L_2)! \ \Gamma(m_{ID}M)} \sum_{k=0}^{m_2 L_2} {m_2 L_2 \choose k} \Xi_2, \qquad m_1 L_1 = m_2 L_2 \\
\frac{m_2^{m_2 L_2} \left(\frac{m_{ID}}{\bar{\gamma}_{ID}}\right)^{m_{ID}M}}{(m_2 L_2)! \ \Gamma(m_{ID}M)} \sum_{k=0}^{m_2 L_2} {m_2 L_2 \choose k} \Xi_2, \qquad m_1 L_1 > m_2 L_2, \\
\frac{m_2^{m_2 L_2} \left(\frac{m_{ID}}{\bar{\gamma}_{ID}}\right)^{m_{ID}M}}{(m_2 L_2)! \ \Gamma(m_{ID}M)} \sum_{k=0}^{m_2 L_2} {m_2 L_2 \choose k} \Xi_2, \qquad (4.30)$$

where Ξ_1 and Ξ_2 are $\frac{(n+m_{IR}N-1)!}{\left(\frac{m_{IR}}{\hat{\gamma}_{IR}}\right)^{n+m_{IR}N}}$ and $\frac{(k+m_{ID}M-1)!}{\left(\frac{m_{ID}}{\hat{\gamma}_{ID}}\right)^{k+m_{ID}M}}$ respectively.

Furthermore, by using $P_{out}^{\infty} \approx (G_a \bar{\gamma})^{-G_d}$ as described in [55], where G_d is the diversity

gain and G_a is the array gain can be found as

$$G_d = \min(m_1 L_1, m_2 L_2),$$

$$G_a = \frac{1}{\gamma_{th}} (\mathcal{G})^{-1/G_d}.$$
(4.31)

Similarly, in order to analyze the average BEP at high SNR, γ_{SR} in (4.16) can be substituted with the asymptotic PDF and then steps in the Appendix E. The corresponding integral can be solved with the help of ([69][eqn 7.811.4]). After mathematical simplifications, asymptotic expression of ABEP for the first hop can be derived as

$$P_{SR}^{\infty}(e) = \frac{\alpha^{-m_{1}L_{1}}m_{1}L_{1} \left(\frac{m_{1}}{\bar{\gamma}_{1}}\right)^{m_{1}L_{1}} \left(\frac{m_{IR}}{\bar{\gamma}_{IR}}\right)^{m_{IR}N}}{2 \Gamma(\beta) \Gamma(m_{IR}N) (m_{1}L_{1})!} \sum_{n=0}^{m_{1}L_{1}} {m_{1}L_{1} \choose n} \times \frac{(n+m_{IR}N-1)! \Gamma(m_{1}L_{1}) \Gamma(\beta+m_{1}L_{1})}{\left(\frac{m_{IR}}{\bar{\gamma}_{IR}}\right)^{n+m_{IR}N} \Gamma(1+m_{1}L_{1})}.$$
(4.32)

Having this result, the asymptotic ABEP of the second hop $P_{RD}^{\infty}(e)$ can be found similarly, and thus, the asymptotic e2e average BEP, $P_{e2e}^{\infty}(e)$ can be easily obtained by substituting $P_{SR}^{\infty}(e)$ and $P_{RD}^{\infty}(e)$ into (4.15).

4.5 Numerical Results and Discussion

In this section, OP, ABEP and ergodic capacity curves obtained by Monte Carlo simulations are presented to verify our analytical findings. 10^6 and 4×10^7 symbols and channel vectors are randomly generated to simulate the OP and ABEP, respectively. For simplicity, the source and the relay have been assumed to have equal transmit powers, i.e., $P_S = P_R$, and the relay and the destination are affected by the same number of interferers, i.e., N = M unless otherwise stated.

Figure 4.2 plots the outage probability simulation and analytical findings. In this figure, the system parameters are chosen as: $L_1 = L_2 = 1, 2, 3$, $m_1 = m_2 = 1$ (special case as Rayleigh distribution), $m_{IR} = m_{ID} = 0.5$ (special case as one-sided Gaussian distribution), $P_S/P_{IR} = P_R/P_{RD} = 30$ and $\gamma_{th} = 7$ dB. It can be recognized that increasing the number of antennas used in maximal ratio transmission results in

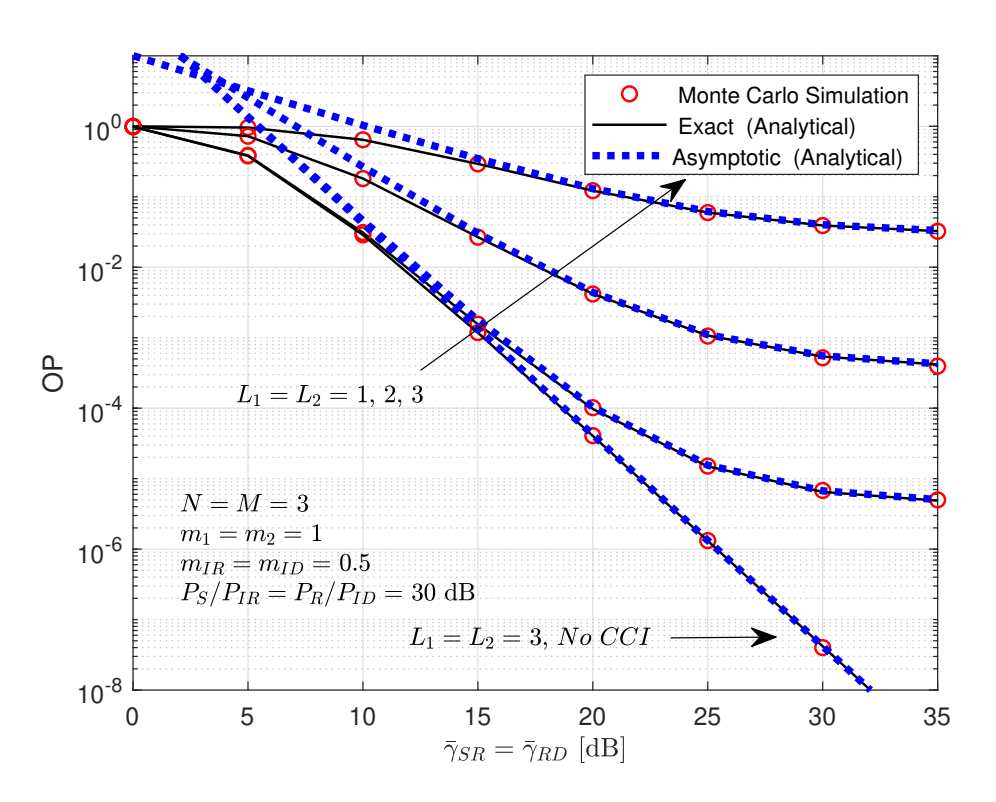


Figure 4.2 Outage probability as a function of average SNR for different number of antennas with constant signal-to-interference ratio.

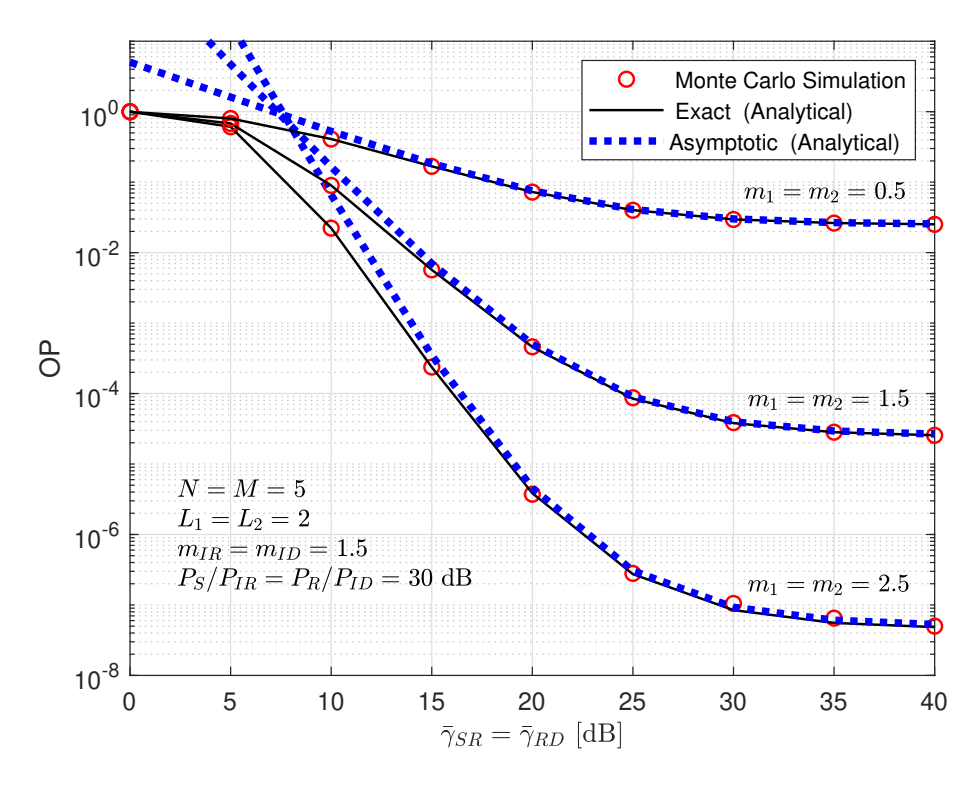


Figure 4.3 Outage probability as a function of average SNR for different Nakagami-m fading severity parameter with constant signal-to-interference ratio.

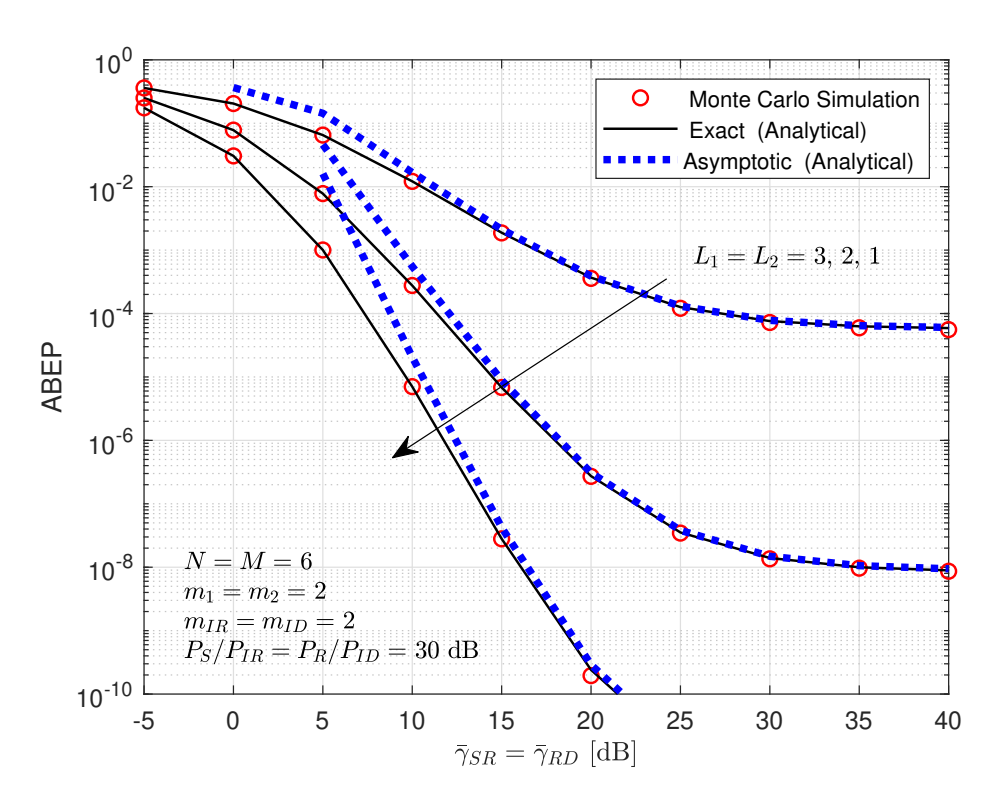


Figure 4.4 Average bit error probability as a function of average SNR for different number of antennas with constant signal-to-interference ratio.

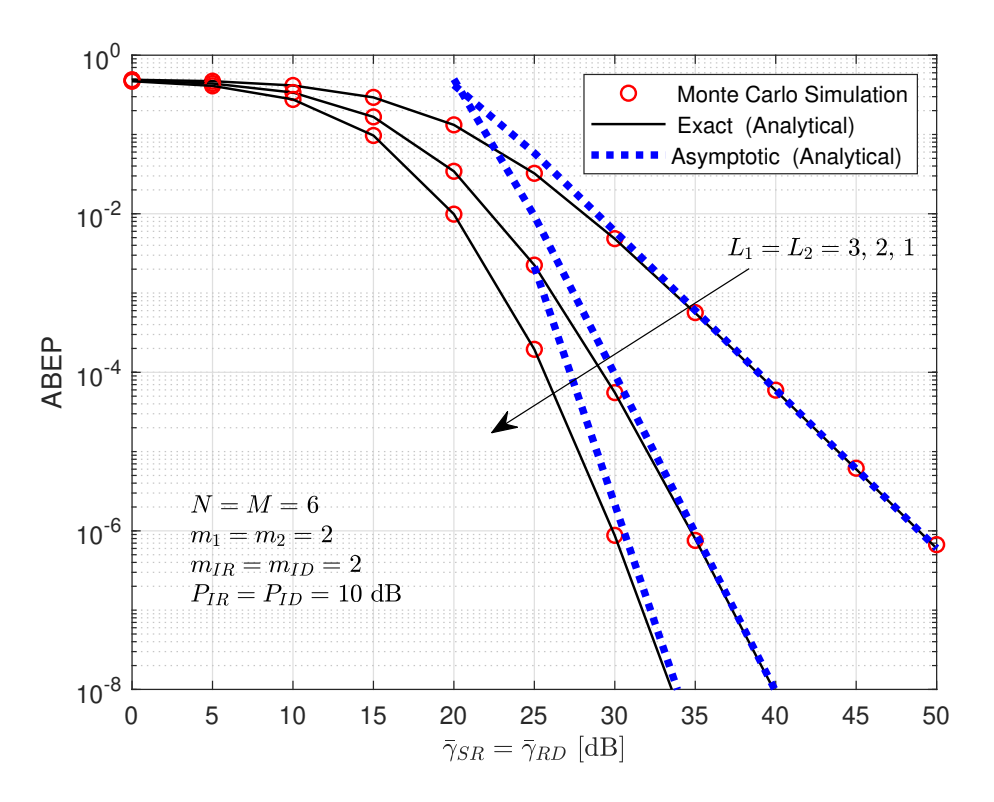


Figure 4.5 Average bit error probability as a function of average SNR for different number of antennas with constant interference power.

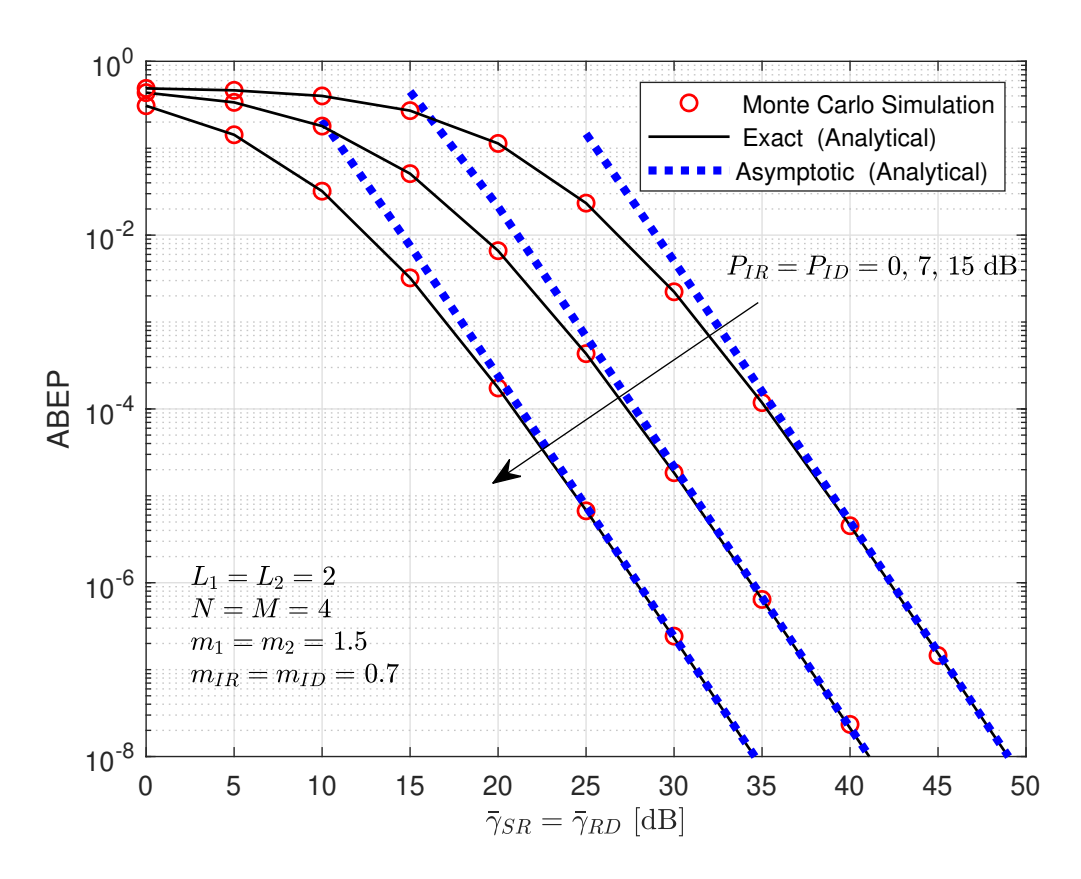


Figure 4.6 Average bit error probability as a function of average SNR with different values of the constant interference power.

better performance. Specifically, the diversity order is increased from one to three. However, as the power of desired signals are scaled with the power of interferers, the interference will dominate the OP at high SNR. Thus, the system diversity decreases down to zero, and an error floor occurs. The interference-free case does not have this phenomenon as can be seen.

Figure 4.3 illustrates the effect of fading severity on the OP performance. The network parameters are selected as: N=M=5, $L_1=L_2=2$, $m_{IR}=m_{RD}=1.5$, $P_S/P_{IR}=P_R/P_{RD}=30$ and $\gamma_{\rm th}=7$ dB. When fading parameter of the desired signals increases from $m_1=m_2=0.5, 1.5$ to 2.5, OP decreases from 0.0631, 1.9953 \times 10⁻⁴ to 1.9953 \times 10⁻⁶ at 20 dB SNRs. Moreover, according to (4.31), the diversity order raises from 1,3 to 5. Thus, it can inferred that the source and destination need less number of antennas for transmission when dual-hop links do not have severe fading.

Figure 4.4 and 4.5 compares the analytical results of average bit error probability for coherent binary phase shift keying (CBPSK) with Monte Carlo simulation. In both figures, the following network setting are used: $L_1 = L_2 = 1, 2, 3, N = M = 6, m_1 = m_2 = m_{IR} = m_{RD} = 2$. It can be seen that the analytical results, as

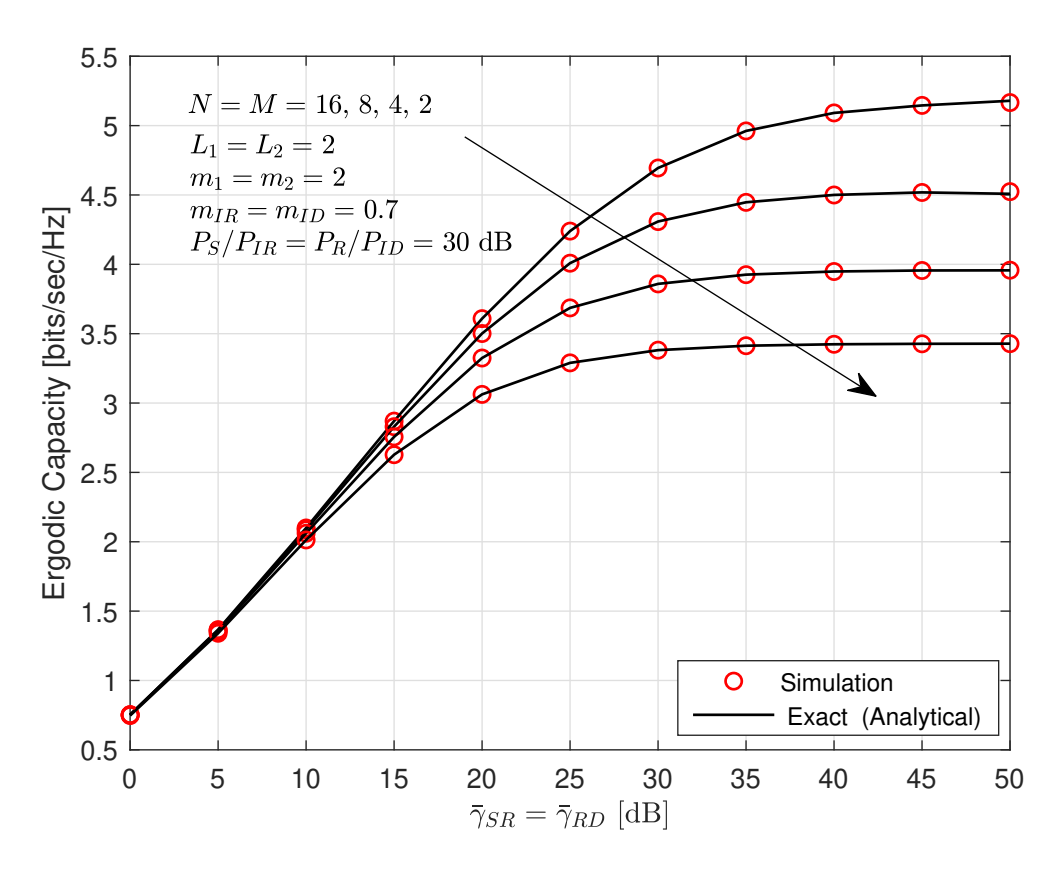


Figure 4.7 Ergodic capacity as a function of average SNR for different number of CCI signals with constant signal-to-interference ratio.

well as the asymptotic curves, perfectly fit with the simulations. Moreover, figure 4.4 demonstrates the benefits of using MRT to reduce the co-channel interference adverse effects on the ABEP performance. Similar to the outage probability, when the number of antennas increases from one to three, the amount of achievement in ABEP performance increases. Similarly, from figure 4.5, one can also notice that the ABEP decreases as the number of antennas increases. Furthermore, it is evident that the diversity order linearly increases from 2,4 to 6 when the number of antennas increases from $L_1 = L_2 = 1,2$ to 3. This figure also shows that when INR does not scale with the SNR, the system can still achieve full diversity gain.

Figure 4.6 shows the average bit error probability versus average SNR when a different value of the interference power is assumed ($P_{IR} = P_{RD} = 0,7,15$ dB) with the same number of antennas $L_1 = L_2 = 2$. The results reveal no error floor, which is due to the fact that the ratio of average INR over average SNR decreases when P_S increases and P_{IR} is fixed according to the asymptotic expression in (4.32). This is also valid for the second hop, thus, it improves the error performance. Furthermore, from these parallel curves of ABEP, one can further deduce that the interference power impacts the array gain but does not affect the diversity order as it still remains at three even

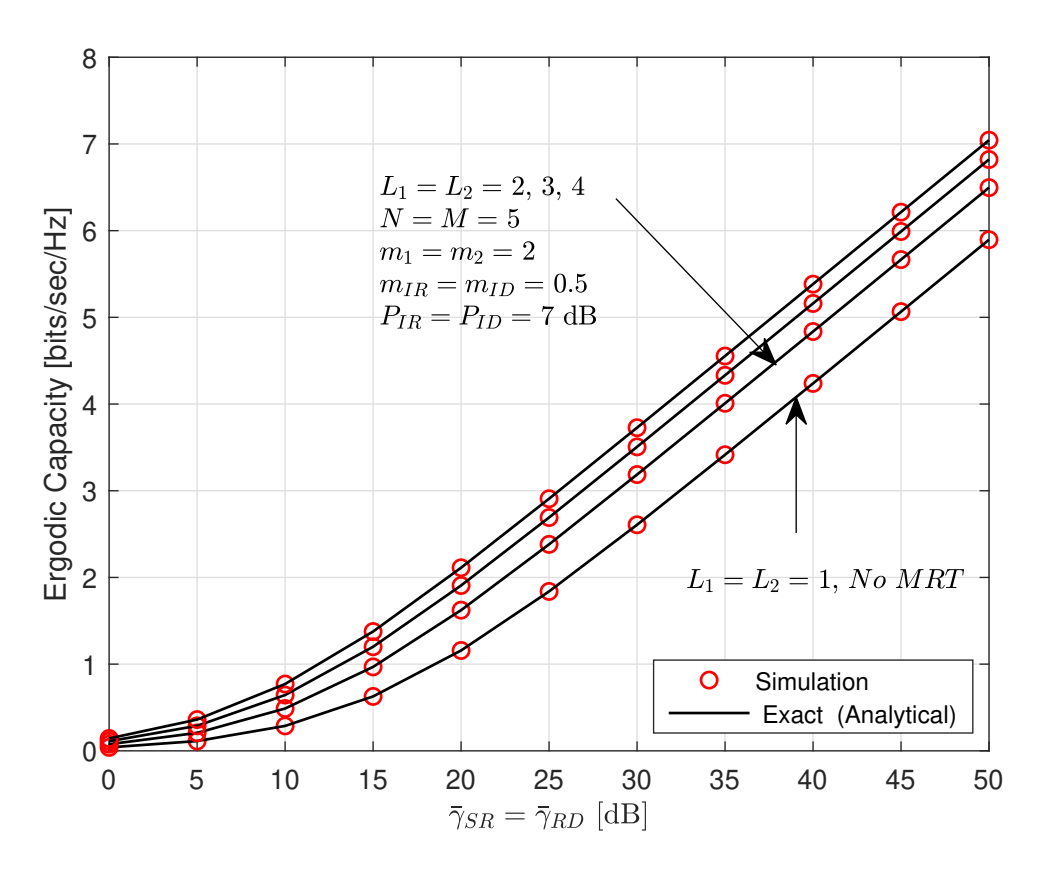


Figure 4.8 Ergodic capacity as a function of average SNR for different number of antennas with constant interference power.

when interference power increases.

Figure 4.7 shows the effect of number of CCI signals on ergodic capacity performance when the number of antennas are $L_1=L_2=2$, fading parameters for desired signals are $m_1=m_2=2$, and $m_{IR}=m_{RD}=0.7$ for interference signals. Besides, the signal to interference ratio is fixed for the first and second hop, i.e., $P_S/P_{IR}=P_R/P_{RD}=30$ dB. As expected, It can be observed that when the number of CCI signals increases, the ergodic capacity in the medium-to-high SNR (15-35 dB) region decreases. Besides, the ergodic capacity reaches saturation at values 5.2, 4.5, 4, and 3.4 bits/sec/Hz when the CCI numbers increase gradually from 2, 4, 8 to 16, respectively.

Finally, figure 4.8 illustrates the advantage of increasing the number of the antennas on the system ergodic capacity. In this figure, the following network parameter values are used: N=M=5, $m_1=m_2=2$, $m_{IR}=m_{RD}=0.5$ and $P_S/P_{IR}=P_R/P_{RD}=30$ dB. It can be observed that increasing the number of antennas for the source and destination from $L_1=L_2=1,2,3$ to 4, the MRT scheme results in capacity improvement. However, this gain is lower compared to the dramatic benefits gained in outage and error probabilities performance since the goal of MRT is reliability first.

4.6 Chapter Summary

Exact closed form error, outage probability and ergodic capacity performance of multi-antenna decode-and-forward dual-hop relaying system with MRT over Nakagami-m channels are derived and verified by simulation results. Due to unavoidable co-channel interference effect on the communication system, performance degradation can be overcome with the use of low complexity MRT scheme. Our numerical examples show that this technique can be a highly effective option when severe fading channels results in high outage rates undesired for next generation communication systems. Reliability and availability of the network can be increased by utilizing more antennas for MRT without increasing the receiver complexity.

EXACT PERFORMANCE ANALYSIS OF MAXIMAL RATIO TRANSMISSION WITH MULTI-HOP DECODE-AND-FORWARD INTERFERENCE-LIMITED RELAYING SYSTEM OVER WEIBULL FADING CHANNEL

In this chapter, the utilizing of maximum ratio transmission (MRT) technique with multi-antenna multi-hop decode-and-forward (DF) relaying networks is investigated to enhance system reliability by suppressing the performance loss due to co-channel interference (CCI). By considering the interference-limited system, the fading channel for the desired and interference signals are assumed follow Weibull distribution. Firstly, the statistics of the desired received signal power and the equivalent signal-to-interference ratio (SIR) per-hop are obtained in terms of probability density function (PDF), probability distribution function (CDF), and moment generating function (MGF). Then, exact expressions for outage probability (OP) and average error probability are derived. Besides, to fully understand the system behavior, asymptotic expressions with diversity and array gains are presented. Our results are perfectly matched with the Monte-Carlo simulations. They infer that MRT scheme can effectively mitigate the deteriorating effects of the co-channel interference as well as the multi-hop drawbacks.

5.1 Introduction

Multi-hop cooperative communication is a beneficial method that is commonly suggested to expand coverage with low transmitting power [106]. It is a possible approach to bypass the channel's extreme conditions that currently affect millimeter wave (mmWave) signals. On the other hand, undesired influences of multi-hop relaying are increased channel usage, overhead synchronization, and latency. Weibull distribution has been used as a quite effective model to describe the narrow and broad band small scale fading channels [107, 108]. Moreover, as a particular case,

the Weibull parameter can be adjusted so that it can be modeled as a lognormal distribution. Consequently, Weibull distribution can model the current 5G mmWave applications such as cellular communication and Internet of Things (IoT) [109].

Multi-hop single antenna relaying system over Weibull fading channel is investigated in [110], where the close-form symbol error rate (SER) is obtained for (M-QAM) transmissions. Soulimani et al. [111] studies the outage probability and channel capacity of the mmWave Weibull fading channel. The energy efficiency and error probability for detect-and-forward multi-hop single antenna relaying system with Weibull fading is explored in [112]. Furthermore, amplify-and-forward (AF) multi-hop relaying is considered in [113]; approximate performance indicators are obtained depending on the upper bound of per-hop SNR, which followed Weibull distribution. Recently, [114] provides only numerical results of SER for multi-hop relaying protocols in cognitive radio networks over Weibull fading channel.

The use of multiple-antenna techniques is well-known for achieving spatial diversity gains to increase reliability that is much needed especially when CCI becomes significant. Thus, multi-antenna direct link system with receiving diversity techniques under Weibull fading channel is demonstrated in [115]. Specifically, approximated SNR PDF following i.i.d Weibull fading channel is derived, then, OP and SER for L-branch MRC receiver are obtained. Similar PDF approximation method is followed in [116] to evaluate the performance of STBC transmission scheme. Furthermore, in [117], the approximate performance criterion of EGC, MRC and SC receivers over Weibull fading channel are provided. Da Costa et al. [118], proposes an approximate approach to derive the PDF of sum of correlated Weibull RVs, which consider essential to examine the performance of MRC receiver. Likewise, in [119], a unified method to approximate the PDF of generalized fading sums of i.n.i.d. α - μ , η - μ , and κ - μ RVs, included a special case to represent Wiebull distribution are derived.

The papers above give background and understanding of this research topic. In general, the sum of multiple random variables is the essential key point to investigate the performance of MRT and MRC (similarly, the arbitrary number of CCI). Besides, the ratio of two RVs is another challenge to evaluate CCI studies. To the best of the author's knowledge, the sum and ratio of Weibull RVs do not present in literature. However, the majority of previous studies have only analyzed a noise-limited system with single antenna nodes or direct link with limited cases (i.e., integer Weibull parameter, i.i.d random variable, etc.). The rest of the other works, used the approximated PDF of the sum or ratio (approximated by Padé approximation method, or approximate the weibull PDF to a simpler distribution and estimate the parameter by moment based estimation method, or assuming large number of weibull RVs, then approximate

the PDF of the sum as normal distribution PDF using Gaussian limit theorem). An insight investigation for MRT (nor MRC) based multi-hop DF relaying with CCI has not been investigated yet. In this study, with the motivation of having a reliable and low complexity communication system, we propose the MRT transmission technique for reducing CCI and dual-hop performance degradation. For this system over i.n.i.d Weibull fading channel, the main contributions of this paper can be listed as follows:

- Signal-to-interference ratios (SIR) of the per-hop are provided, considering the co-channel interference signal at all receiver nods.
- The exact cumulative distribution function, probability density function, and moment generating of the sum of squared (i.n.i.d) Weibull fading channel RV (for the desired per-hop signal power distribution) are derived.
- The exact per-hop SIR random variable (ratio of two weibull RVs) statistics are obtained in teams of the cumulative distribution function, probability density function over (i.n.i.d) Weibull fading channels.
- The new exact analytical expressions of the per-hop and e2e system outage, average bit error probabilities are derived. Besides, the performance of the interference-free system is presented as a special case.
- Asymptotic expressions of outage and bit error probabilities are provided to obtain the diversity and array gains.
- Numerical examples are presented using Monte Carlo simulations to verify our results and observe the effect of system parameters.

The remainder of the chapter is organized as follows. System and channel models are described in Section 5.2. In Section 5.3, the cumulative distribution function (CDF), probability density function (PDF), moment generating function (MGF) of the SIR for each node and end-to-end (e2e) system are obtained. Moreover, OP, ABEP expressions are derived in section 5.4. Section 5.5 presents the numerical examples obtained by Monte Carlo simulations. Finally, conclusions are summarized in Section 5.6.

5.2 System and Channel Models

In this chapter, MRT based multi-hop decode-and-forward (DF) relaying Interference-limited networks is considered, as shown in figure 5.1. When the source ($S \equiv R_0$) with L_0 transmit antenna communicate with the destination ($D \equiv R_N$) has a single receive antenna, with the help of the intermediate (N-1) DF

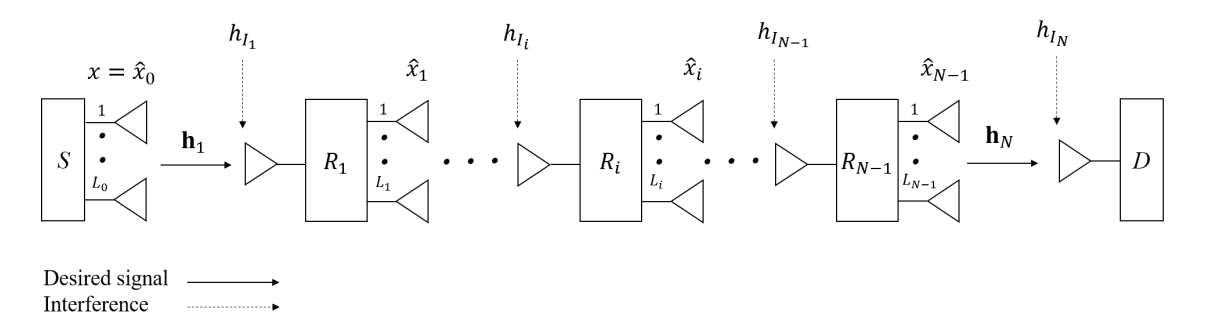


Figure 5.1 Block diagram of MRT based multi-antenna multi-hop decode-and-forward (DF) relaying networks with co-channel interference

relay nodes $(R_i, i = 1, ..., N-1)$ each has single receive antenna and L_i transmit antennas. Without loss of generality, all nodes are operating in half-duplex mode and MRT scheme is employed by all transmitter nodes in the system to maximize the received power at the receivers [3]. Furthermore, each i-th receiver node in the network is impaired by a single dominant interferer from an external source¹. For instance, as the interference power dominate the noise variance, such that the impact of noise is negligible. Moreover, the receiver nodes can receive the information signal from the previous adjacent transmitter, i.e., there is no direct link between S and R. This assumption is valid due to high path loss and deep fading. In addition, all the channels between the nodes and the interference signals, are subject to independent and non-identically distributed (i.n.i.d) Weibull fading channels. To this end, the received signal at the i-th receiver node (i = 1, ..., N) can be expressed as follows

$$y_i = \sqrt{P_{i-1}} \mathbf{h}_i \mathbf{w}_i \ \hat{x}_{i-1} + \sqrt{P_{I_i}} \ h_{I_i} x_{I_i}, \tag{5.1}$$

where \mathbf{h}_i is the $(L_{i-1} \times 1)$ desired channel vector between the transceiver nodes. \mathbf{w}_i is the MRT weight vector which constructed as $\mathbf{w}_i = (\mathbf{h}_i^H / \|\mathbf{h}_i\|)$ [3]. In addition, \hat{x}_i is the desired unit energy information symbol (note that $\hat{x}_0 = x$ is the source transmitted symbol). Moreover, x_{I_i} and h_{I_i} are the interference unit energy symbol and channel coefficient at i-th receiver node, respectively. The transmit power of i-th transmitter node denoted as P_i^2 , while P_{I_i} is the interference power at i-th receiver node, respectively. Furthermore, $y_N = y$ is the received signal at the destination node.

¹It is worth mentioning that the assumption of a single dominant interfere still of practical interest and importance. For example, in a well planned cellular network, it is very likely that the system will be subjected to a single dominant interferer [120–123].

²Note that our analysis are readily cover the mmWave by substation $\sqrt{P_{i-1}} = \sqrt{\frac{P_{i-1} B_i}{\xi_i}}$ in (5.1), where the path-loss $\xi_i[dB] = a + 10b \log_{10}(d_i)$, d_i is the distance between the adjacent nodes, a and b are given in ([124][Table 1]) for 28GHz and 73GHz mmWave bands. B_i denote the blockage probability from the 3GPP model [125] given as $B_i = \min(\frac{18}{d_i}, 1)(1 - \exp(\frac{-d_i}{63})) + \exp(\frac{-d_i}{63})$, for urban areas, and $B_i = \exp(\frac{-d_i}{200})$, for suburban areas. Similar substitution have to include P_{I_i} with corresponding parameters.

5.3 SIR Statistical Analysis

In this section, the end-to-end (e2e) system SIR is presented, then, its cumulative distribution function (CDF) and probability density function (PDF) are obtained.

According to (5.1), the equivalent instantaneous signal-to-interference ratio (SIR) at the *i*-th received node, named (γ_{eq_i} , i = 1, ..., N) can be given as

$$\gamma_{\text{eq}_i} = \frac{P_{i-1} ||\mathbf{h}_i||^2}{P_{I_i} |h_{I_i}|^2} = \frac{\gamma_{D_i}}{\gamma_{I_i}},$$
(5.2)

where $\|\mathbf{h}_i\|^2$ and $|h_{I_i}|^2$ are the desired and interference signals channel gain, respectively. Consequently, in the multi-hop relaying networks, the end-to-end (e2e) SIR is dominated by the weakest *i*-th hop equivalent SIR. Thus, by using the order statistic, e2e SIR RV (named γ_{e2e}) can be expressed as

$$\gamma_{e2e} = \min(\gamma_{eq_i}, \dots, \gamma_{eq_N}). \tag{5.3}$$

Thus, the CDF and PDF for γ_{e2e} can be given respectively by using the following formulas [126, 127]

$$F_{\gamma_{e2e}}(\gamma) = \Pr\left[\min\left(\gamma_{eq_i}, \dots, \gamma_{eq_N}\right) \leq \gamma\right]$$

$$= 1 - \prod_{i=1}^{N} \left(1 - F_{\gamma_{eq_i}}(\gamma)\right),$$
(5.4)

$$f_{\gamma_{\text{e2e}}}(\gamma) = \sum_{i=1}^{N} f_{\gamma_{\text{eq}_i}}(\gamma) \prod_{\substack{j=1\\j\neq i}}^{N} \left(1 - F_{\gamma_{\text{eq}_i}}(\gamma)\right). \tag{5.5}$$

5.3.1 The CDFs Derivation

In this subsection, the *i*-th hop desired received signal and equivalent SIR (i.e., γ_{D_i} and γ_{eq_i} , i = 1,...,N) cumulative distribution function (CDF) are obtained in exact form.

Firstly, since the decode-and-forward scheme at the relay nodes is assumed, the statistic derivation steps for any particular i-th receiver nodes SIR will be similar to the

other hops in the system by using the corresponding per-hop entities to that particular hop. To avoid confusion and make the calculation simpler and more tractable, a simple representations for the PDF, MGF, and CDF equation entities, (i.e. we use L, P, P_I , \mathbf{h} , h_I , γ_D , γ_I and γ_{eq} instead of L_i , P_{i-1} , P_{I_i} , \mathbf{h}_i , h_{I_i} , γ_{D_i} , γ_{I_i} , and γ_{eq_i} respectively) are used unless otherwise stated.

As we mentioned in the system model section, the elements of the transmitted channel vector ($\mathbf{h} = [h_1, ..., h_L]^T$) and the interference channel coefficient (h_I) are i.n.i.d random variables follows the Weibull distribution, their PDF can be respectively given as follows [32]:

$$f_h(x) = \beta \left(\frac{\omega}{\sigma^2}\right)^{\frac{\beta}{2}} x^{\beta - 1} \exp\left(-\left(\frac{\omega}{\sigma^2}x^2\right)^{\frac{\beta}{2}}\right),\tag{5.6}$$

$$f_{h_I}(z) = \beta_I \left(\frac{\omega_I}{\sigma_I^2}\right)^{\frac{\beta_I}{2}} z^{\beta_I - 1} \exp\left(-\left(\frac{\omega_I}{\sigma_I^2}z^2\right)^{\frac{\beta_I}{2}}\right), \tag{5.7}$$

where the parameters $\omega = \Gamma\left(1+\frac{2}{\beta}\right)$, $\omega_I = \Gamma\left(1+\frac{2}{\beta_I}\right)$, $(\beta > 0)$ and $(\beta_I > 0)$ are Weibull fading parameter for the desired and inteference channel, respectively³. Moreover, $(\sigma^2 = \mathrm{E}[h^2])$ and $(\sigma_I^2 = \mathrm{E}[h_I^2])$ are the channel coefficient mean-square values, both are normalized to one in this chapter. The PDF of $(\gamma_I = P_I |h_I|^2)$ can be readily founded by using the function of the random variable as ([32] [eqn 2.3])

$$f_{\gamma_I}(z) = \frac{\beta_I}{2} \left(\frac{\omega_I}{\bar{P}_I} \right)^{\frac{\beta_I}{2}} z^{\frac{\beta_I}{2} - 1} \exp\left(-\left(\frac{\omega_I}{\bar{P}_I} z \right)^{\frac{\beta_I}{2}} \right), \tag{5.8}$$

where \bar{P}_l is the average received interference power per symbol. On other hand, in order to find the statistics of $(\gamma_D = P ||\mathbf{h}||^2 = \sum_{l=1}^L P |h_l|^2)$, the random variable $(\gamma_l = P ||h_l|^2)$ is introduced as the instantaneous received signal power from the l-th transmit antenna and its PDF can be written as

$$f_{\gamma_l}(x) = \frac{\beta_l}{2} \left(\frac{\omega_l}{\bar{P}}\right)^{\frac{\beta_l}{2}} x^{\frac{\beta_l}{2} - 1} \exp\left(-\left(\frac{\omega_l}{\bar{P}}x\right)^{\frac{\beta_l}{2}}\right),\tag{5.9}$$

where \bar{P} is the average received power per transmitted symbol. The moment

³As β increases, the severity of the fading decreases. In the special case when $\beta = 1$, Weibull distribution becomes an exponential distribution, and for $\beta = 2$ proposed channel becomes Rayleigh distribution [35]

generating function (MGF) of γ_l can be derived as follows

$$M_{\gamma_l}(s) = \int_0^\infty \exp(-sx) f_{\gamma_l}(x) dx, \qquad (5.10)$$

by substitution the PDF of γ_l into (5.10) yields

$$M_{\gamma_l}(s) = \frac{\beta_l}{2} \left(\frac{\omega_l}{\bar{p}}\right)^{\frac{\beta_l}{2}} \int_0^\infty \exp\left(-sx\right) x^{\frac{\beta_l}{2} - 1} \exp\left(-\left(\frac{\omega_l}{\bar{p}}x\right)^{\frac{\beta_l}{2}}\right) dx. \tag{5.11}$$

To solving the above integral, firstly, ([128] [eqn 1.39]) is used to express the exponential function which has complex argument in terms of H-function as

$$M_{\gamma_l}(s) = \frac{\beta_l}{2} \left(\frac{\omega_l}{\bar{P}} \right)^{\frac{\beta_l}{2}} \int_0^{\infty} \exp(-sx) \, x^{\frac{\beta_l}{2} - 1} \, H_{0,1}^{1,0} \left[\left(\frac{\omega_l}{\bar{P}} x \right)^{\frac{\beta_l}{2}} \right] - \left(0, 1 \right) \, dx, \quad (5.12)$$

then, taking advantage of Laplace transform of H-function in ([128] [eqn 2.19]) to solve the resultant integral in (5.12) as

$$M_{\gamma_l}(s) = \frac{\beta_l}{2} \left(\frac{\omega_l}{\bar{P}}\right)^{\frac{\beta_l}{2}} s^{-\frac{\beta_l}{2}} H_{1,1}^{1,1} \left[\left(\frac{\omega_l}{\bar{P}} s\right)^{\frac{\beta_l}{2}} \middle| \left(1 - \frac{\beta_l}{2}, \frac{\beta_l}{2}\right) \right], \tag{5.13}$$

by invoke ([129] [Pro. 2.3, 2.4 and 2.5]) respectively, the MGF of γ_l can be written in a simple form as

$$M_{\gamma_{l}}(s) = \frac{\beta_{l}}{2} \left(\frac{\omega_{l}}{\bar{P}}\right)^{\frac{\beta_{l}}{2}} s^{-\frac{\beta_{l}}{2}} H_{1,1}^{1,1} \left[\left(\frac{\bar{P}}{\omega_{l}} s\right)^{\frac{\beta_{l}}{2}} \middle| \begin{array}{c} (1,1) \\ \left(\frac{\beta_{l}}{2}, \frac{\beta_{l}}{2}\right) \end{array} \right]$$

$$= \left(\frac{\omega_{l}}{\bar{P}}\right)^{\frac{\beta_{l}}{2}} s^{-\frac{\beta_{l}}{2}} H_{1,1}^{1,1} \left[\frac{\bar{P}}{\omega_{l}} s \middle| \begin{array}{c} (1, \frac{2}{\beta_{l}}) \\ \left(\frac{\beta_{l}}{2}, 1\right) \end{array} \right]$$

$$= H_{1,1}^{1,1} \left[\frac{\bar{P}}{\omega_{l}} s \middle| \begin{array}{c} (0, \frac{2}{\beta_{l}}) \\ (0, 1) \end{array} \right],$$
(5.14)

To this end, since the signals from transmitting antennas are assumed independent,

the moment generating function of $(\gamma_D = \sum_{l=1}^{L} \gamma_l)$ can be derived as

$$M_{\gamma_D}(s) = \prod_{l=1}^{L} M_{\gamma_l}(s) = \prod_{l=1}^{L} H_{1,1}^{1,1} \left[\frac{\bar{P}}{\omega_l} s \, \middle| \, \begin{array}{c} (0, \frac{2}{\beta_l}) \\ (0, 1) \end{array} \right], \tag{5.15}$$

In order to evaluate the product of multiple H-function in (5.15), a similar idea in ([130][eqn 10]) is used. We start with the representation of the H-functions in terms of Mellin-Barnes integrals by following the H-function definition below.

Definition 5.1. The H-function is expressed by means of a Mellin–Barnes type integral as following

$$H_{p,q}^{m,n} \left[\zeta \left| \frac{(a_{j}, A_{j})_{j=1:p}}{(b_{j}, B_{j})_{j=1:q}} \right. \right] = \frac{1}{2\pi i} \int_{\mathcal{L}} \frac{\prod_{j=1}^{m} \Gamma(b_{j} + B_{j}t) \prod_{j=1}^{n} \Gamma(1 - a_{j} - A_{j}t)}{\prod_{j=n+1}^{p} \Gamma(a_{j} + A_{j}t) \prod_{j=m+1}^{q} \Gamma(1 - b_{j} - B_{j}t)} \zeta^{-t} dt$$
(5.16)

Then, for the guarantee of mathematical tractability, two transmit antennas are assumed (i.e., L=2). By using (5.15) with the help of (5.16), the MGF of γ_D can be given as follows

$$M_{\gamma_{D}}(s) = \frac{1}{(2\pi i)^{2}} \int_{\mathcal{L}_{1}} \int_{\mathcal{L}_{2}} \Gamma(t_{1}) \Gamma\left(1 - \frac{2}{\beta_{1}}t_{1}\right) \Gamma(t_{2}) \Gamma\left(1 - \frac{2}{\beta_{2}}t_{2}\right) \left(\frac{\bar{P}}{\omega_{1}}s\right)^{-t_{1}} \left(\frac{\bar{P}}{\omega_{2}}s\right)^{-t_{2}} \times dt_{2} dt_{1}.$$
(5.17)

To this end, the CDF of $\gamma_{\it D}$ can be derived straightforwardly by perform the inverse

Laplace transform on the $(M_{\gamma_D}(s)/s)$ as

$$F_{\gamma_{D}}(x) = \frac{1}{(2\pi i)^{3}} \int_{\sigma - i\infty}^{\sigma + i\infty} \frac{\exp(sx)}{s} \int_{\mathscr{L}_{1}} \int_{\mathscr{L}_{2}} \Gamma(t_{1}) \Gamma\left(1 - \frac{2}{\beta_{1}}t_{1}\right) \Gamma(t_{2}) \Gamma\left(1 - \frac{2}{\beta_{2}}t_{2}\right)$$

$$\times \left(\frac{\bar{P}}{\omega_{1}}s\right)^{-t_{1}} \left(\frac{\bar{P}}{\omega_{2}}s\right)^{-t_{2}} dt_{2} dt_{1} ds. \tag{5.18}$$

By interchanging the order of the contour integration with some arrangement we obtain

$$F_{\gamma_{D}}(x) = \frac{1}{(2\pi i)^{3}} \int_{\mathcal{L}_{1}} \int_{\mathcal{L}_{2}} \Gamma(t_{1}) \Gamma\left(1 - \frac{2}{\beta_{1}}t_{1}\right) \Gamma(t_{2}) \Gamma\left(1 - \frac{2}{\beta_{2}}t_{2}\right) \left(\frac{\bar{P}}{\omega_{1}}\right)^{-t_{1}} \left(\frac{\bar{P}}{\omega_{2}}\right)^{-t_{2}}$$

$$\times \int_{\sigma - i\infty}^{\sigma + i\infty} \frac{\exp(sx) s^{-(t_{1} + t_{2})}}{s} ds dt_{2} dt_{1},$$
(5.19)

where the innermost integral with respect to s has a solution as

$$\frac{1}{(2\pi i)} \int_{\sigma-i\infty}^{\sigma+i\infty} \frac{\exp(sx) \, s^{-(t_1+t_2)}}{s} \, ds = \frac{x^{t_1+t_2}}{\Gamma(1+t_1+t_2)}. \tag{5.20}$$

By using the solution in (5.20), the CDF of γ_D can be attained in integral form as follows

$$F_{\gamma_{D}}(x) = \frac{1}{(2\pi i)^{2}} \int_{\mathcal{L}_{1}} \int_{\mathcal{L}_{2}} \frac{\Gamma(t_{1}) \ \Gamma(1 - \frac{2}{\beta_{1}}t_{1}) \ \Gamma(t_{2}) \ \Gamma(1 - \frac{2}{\beta_{2}}t_{2})}{\Gamma(1 + t_{1} + t_{2})} \left(\frac{\bar{p}}{\omega_{1} x}\right)^{-t_{1}} \left(\frac{\bar{p}}{\omega_{2} x}\right)^{-t_{2}} \times dt_{2} dt_{1},$$
(5.21)

Furthermore, It is recognized that (5.21) can be re-represented in terms of the multivariate H-function and generalized for any number of transmit antenna as be

given in (5.23) after the multivariate H-function definition.

Definition 5.2. The multivariate H-function is defined in terms of multiple Mellin–Barnes contour type integral as

$$H_{p,q:[p_{l},q_{l}]_{l=1:L}}^{0,n:[m_{l},n_{l}]_{l=1:L}} \begin{bmatrix} \zeta_{1} \\ \vdots \\ \zeta_{L} \end{bmatrix} \begin{pmatrix} c_{j}: \left\{C_{j}^{(l)}\right\}_{l=1:L} \end{pmatrix}_{j=1:p} \begin{bmatrix} \left(a_{j}^{(l)},A_{j}^{(l)}\right)_{j=1:p_{l}} \\ \left(b_{j}^{(l)},B_{j}^{(l)}\right)_{j=1:q_{l}} \end{bmatrix}_{l=1:L}$$

$$= \frac{1}{(2\pi i)^{L}} \int_{\mathcal{L}_{1}} \cdots \int_{\mathcal{L}_{L}} \Xi(t_{1},\ldots,t_{L}) \prod_{l=1}^{L} \left(\phi_{l}(t_{l})\zeta_{l}^{-t_{l}}\right) dt_{1},\ldots,dt_{L}$$

$$(5.22)$$

where $\Xi(t_1,\ldots,t_L)$ and $\phi_l(t_l)$ are defined respectively as

$$\begin{split} \Xi(t_1,\ldots,t_L) = & \frac{\prod\limits_{j=1}^n \Gamma\left(1-c_j - \sum\limits_{l=1}^L C_j^{(l)} t_l\right)}{\prod\limits_{j=n+1}^p \Gamma\left(c_j + \sum\limits_{l=1}^L C_j^{(l)} t_l\right) \prod\limits_{j=1}^q \Gamma\left(1-d_j - \sum\limits_{l=1}^L D_j^{(l)} t_l\right)} \\ \phi_l(t_l) = & \frac{\prod\limits_{j=1}^{m_l} \Gamma\left(b_j^{(l)} + B_j^{(l)} t_l\right) \prod\limits_{j=1}^{n_l} \Gamma\left(1-a_j^{(l)} - A_j^{(l)} t_l\right)}{\prod\limits_{j=n_l+1}^{p_l} \Gamma\left(a_j^{(l)} + A_j^{(l)} t_l\right) \prod\limits_{j=m_l+1}^{q_l} \Gamma\left(1-b_j^{(l)} - B_j^{(l)} t_l\right)}, \quad l=1,\ldots,L. \end{split}$$

Proof. See ([128] [Appendix A.1]) and ([131] [eqn 28, 29a, 29b and 30]) ■

$$F_{\gamma_{D}}(x) = H_{1,0:[1,1]_{l=1:L}}^{0,0:[1,1]_{l=1:L}} \begin{bmatrix} \frac{\bar{p}}{\omega_{l} x} \\ \vdots \\ \frac{\bar{p}}{\omega_{l} x} \end{bmatrix} (1;\{1\}_{l=1:L}) : \begin{bmatrix} \left(0, \frac{2}{\beta_{l}}\right) \\ (0,1) \end{bmatrix}_{l=1:L}$$
(5.23)

We want to mention here that these exact CDF expression is, to the best of our knowledge, the most accurate and general expression ever presented in the literature to investigate the MRT under (i.n.i.d) Weibull fading channels. The CDF of the equivalent received signal-to-interference ratio (SIR) at the i-th node (i.e., γ_{eq} in (5.2)) in our considered system can be derived as

$$F_{\gamma_{eq}}(x) = \Pr[\gamma_{eq} < x]$$

$$= \Pr\left[\frac{\gamma_D}{\gamma_I} < x\right]$$

$$= \int_0^\infty \Pr[\gamma_D < z \ x] f_{\gamma_I}(z) dz$$

$$= \int_0^\infty F_{\gamma_D}(z \ x) f_{\gamma_I}(z) dz,$$
(5.24)

by substituting the CDF of γ_D from (5.21), and the PDF of γ_I from (5.8) into (5.24) with some parameters arrangement, we get the integral bellow

$$F_{\gamma_{\text{eq}}}(x) = \frac{\beta_{I}}{2} \left(\frac{\omega_{I}}{\bar{P}_{I}}\right)^{\frac{\beta_{I}}{2}} \frac{1}{(2\pi i)^{2}} \int_{0}^{\infty} \int_{\mathcal{L}_{1}} \int_{\mathcal{L}_{2}}^{\infty} \frac{\Gamma(t_{1}) \ \Gamma\left(1 - \frac{2}{\beta_{1}}t_{1}\right) \ \Gamma(t_{2}) \ \Gamma\left(1 - \frac{2}{\beta_{2}}t_{2}\right)}{\Gamma(1 + t_{1} + t_{2})} \times \left(\frac{\bar{P}}{\omega_{1} \ z \ x}\right)^{-t_{1}} \left(\frac{\bar{P}}{\omega_{2} \ z \ x}\right)^{-t_{2}} \ dt_{2} \ dt_{1} \ z^{\frac{\beta_{I}}{2} - 1} \exp\left(-\left(\frac{\omega_{I}}{\bar{P}_{I}}z\right)^{\frac{\beta_{I}}{2}}\right) \ dz.$$
(5.25)

Now, interchanging the order of the real and contour integrals (which is permissible given the absolute convergence of the involved integrals) and re-arrange the parameters, we obtain

$$F_{\gamma_{eq}}(x) = \frac{\beta_{I}}{2} \left(\frac{\omega_{I}}{\bar{P}_{I}}\right)^{\frac{\beta_{I}}{2}} \frac{1}{(2\pi i)^{2}} \int_{\mathcal{L}_{2}} \frac{\Gamma(t_{1}) \Gamma(1 - \frac{2}{\beta_{1}}t_{1}) \Gamma(t_{2}) \Gamma(1 - \frac{2}{\beta_{2}}t_{2})}{\Gamma(1 + t_{1} + t_{2})} \times \left(\frac{\bar{P}}{\omega_{1} x}\right)^{-t_{1}} \left(\frac{\bar{P}}{\omega_{2} x}\right)^{-t_{2}} \int_{0}^{\infty} z^{\frac{\beta_{I}}{2} + t_{1} + t_{2} - 1} \exp\left(-\left(\frac{\omega_{I}}{\bar{P}_{I}}z\right)^{\frac{\beta_{I}}{2}}\right) dz dt_{2} dt_{1},$$
(5.26)

using change of variable $u = \left(\frac{\omega_l}{\bar{p}_l}z\right)^{\frac{\bar{p}_l}{2}}$, with the help of ([69] [eqn 8.339.1]) and some mathematical manipulations. The integral I_1 in (5.26) can be solved as

$$I_{1} = \left(\frac{\omega_{I}}{\bar{P}_{I}}\right)^{-\frac{\beta_{I}}{2}} \left(\frac{\beta_{I}}{2}\right)^{-1} \left(\frac{\omega_{I}}{\bar{P}_{I}}\right)^{-(t_{1}+t_{2})} \Gamma\left(1 + \frac{2}{\beta_{I}}t_{1} + \frac{2}{\beta_{I}}t_{2}\right), \tag{5.27}$$

by perfectly substituting (5.27) into (5.26) with some arrangement, the following

integral formula can be attained

$$F_{\gamma_{eq}}(x) = \frac{1}{(2\pi i)^{2}} \int_{\mathcal{L}_{1}} \int_{\mathcal{L}_{2}} \frac{\Gamma\left(1 + \frac{2}{\beta_{I}}t_{1} + \frac{2}{\beta_{I}}t_{2}\right) \Gamma(t_{1}) \Gamma\left(1 - \frac{2}{\beta_{1}}t_{1}\right) \Gamma(t_{2}) \Gamma\left(1 - \frac{2}{\beta_{2}}t_{2}\right)}{\Gamma(1 + t_{1} + t_{2})} \times \left(\frac{\omega_{I} \bar{P}}{\omega_{1} \bar{P}_{I} x}\right)^{-t_{1}} \left(\frac{\omega_{I} \bar{P}}{\omega_{2} \bar{P}_{I} x}\right)^{-t_{2}} dt_{2} dt_{1}.$$
(5.28)

Then, the CDF of SIR in above can be re-expressed and generalized to any number of transmit antenna in terms of the multivariate H-function by using (5.22) along with ([129] [Pro. 2.3]) (to switch the order of H-function, thus faster integration convergence is achieved especially with the small β_I value), as follows

$$F_{\gamma_{\text{eq}}}(x) = H_{1,1:[1,1]_{l=1:L}}^{0,1:[1,1]_{l=1:L}} \begin{bmatrix} \frac{\omega_{l} \ \bar{P}_{l} \ x}{\omega_{l} \ \bar{P}} \\ \vdots \\ \frac{\omega_{L} \ \bar{P}_{l} \ x}{\omega_{l} \ \bar{P}} \end{bmatrix} \begin{pmatrix} 0; \left\{\frac{2}{\beta_{l}}\right\}_{l=1:L} \end{pmatrix} : \begin{bmatrix} (1,1) \\ (1,\frac{2}{\beta_{l}}) \end{bmatrix}_{l=1:L}$$
(5.29)

Finally, by substituting (5.29) into (5.4). The e2e SIR probability distribution function expression can be attained in exact form.

5.3.2 The PDFs Derivation

The PDFs of γ_D and γ_{eq} can be obtained by following the same procedures that followed to derive the CDF. Starting with taking the inverse Laplace transform of $(M_{\gamma_D}(s))$ in (5.17).

$$f_{\gamma_{D}}(x) = \frac{1}{(2\pi i)^{3}} \int_{\sigma - i\infty}^{\sigma + i\infty} \exp(sx) \iint_{\mathcal{L}_{1}} \Gamma(t_{1}) \Gamma\left(1 - \frac{2}{\beta_{1}}t_{1}\right) \Gamma(t_{2}) \Gamma\left(1 - \frac{2}{\beta_{2}}t_{2}\right)$$

$$\times \left(\frac{\bar{P}}{\omega_{1}}s\right)^{-t_{1}} \left(\frac{\bar{P}}{\omega_{2}}s\right)^{-t_{2}} dt_{2} dt_{1} ds,$$
(5.30)

switching the order of the integration and re-arrange the parameters

$$f_{\gamma_{D}}(x) = \frac{1}{(2\pi i)^{3}} \int_{\mathcal{L}_{1}} \int_{\mathcal{L}_{2}} \Gamma(t_{1}) \Gamma\left(1 - \frac{2}{\beta_{1}}t_{1}\right) \Gamma(t_{2}) \Gamma\left(1 - \frac{2}{\beta_{2}}t_{2}\right) \left(\frac{\bar{P}}{\omega_{1}}\right)^{-t_{1}} \left(\frac{\bar{P}}{\omega_{2}}\right)^{-t_{2}}$$

$$\times \int_{\sigma - i\infty}^{\sigma + i\infty} \exp(sx) s^{-(t_{1} + t_{2})} ds dt_{2} dt_{1},$$

$$(5.31)$$

the inner integral with respect to s can be written as

$$\frac{1}{(2\pi i)} \int_{\sigma - i\infty}^{\sigma + i\infty} \exp(sx) \, s^{-(t_1 + t_2)} \, ds = \frac{x^{-1 + t_1 + t_2}}{\Gamma(t_1 + t_2)},\tag{5.32}$$

then, by substituting this result into (5.31), the PDF of γ_D is resulted in integral form as follows

$$f_{\gamma_{D}}(x) = \frac{1}{(2\pi i)^{2}} \int_{\mathcal{L}_{1}} \int_{\mathcal{L}_{2}} \frac{\Gamma(t_{1}) \ \Gamma(1 - \frac{2}{\beta_{1}}t_{1}) \ \Gamma(t_{2}) \ \Gamma(1 - \frac{2}{\beta_{2}}t_{2})}{x \ \Gamma(t_{1} + t_{2})} \left(\frac{\bar{p}}{\omega_{1} \ x}\right)^{-t_{1}} \left(\frac{\bar{p}}{\omega_{2} \ x}\right)^{-t_{2}} \times dt_{2} dt_{1}.$$
(5.33)

Finally, with the help of (5.22), we can re-expressed the integrals in above as follows

$$f_{\gamma_{D}}(x) = \frac{1}{x} H_{1,0:[1,1]_{l=1:L}}^{0,0:[1,1]_{l=1:L}} \begin{bmatrix} \frac{\bar{p}}{\omega_{l} x} \\ \vdots \\ \frac{\bar{p}}{\omega_{L} x} \end{bmatrix} (0;\{1\}_{l=1:L}) : \begin{bmatrix} \left(0, \frac{2}{\beta_{l}}\right) \\ \left(0, 1\right) \end{bmatrix}_{l=1:L}$$
(5.34)

On other hand, to obtain the PDF of the received SIR at the i-th node, we can use the following formula

$$f_{\gamma_{\text{eq}}}(x) = \int_{0}^{\infty} z \, f_{\gamma_{D}}(z \, x) \, f_{\gamma_{I}}(z) \, dz, \qquad (5.35)$$

by substituting the PDFs of γ_D and γ_I from (5.33) and (5.8) respectively, into (5.35). Then, similar derivation steps that is used to derive the CDF are followed. The PDF of the i-th hop equivalent SIR can be resulted in integral and multivariate H-function forms, respectively as below

$$f_{\gamma_{eq}}(x) = \frac{1}{(2\pi i)^{2}} \int_{\mathcal{L}_{1}} \int_{\mathcal{L}_{2}} \frac{\Gamma\left(1 + \frac{2}{\beta_{I}}t_{1} + \frac{2}{\beta_{I}}t_{2}\right) \Gamma(t_{1}) \Gamma\left(1 - \frac{2}{\beta_{1}}t_{1}\right) \Gamma(t_{2}) \Gamma\left(1 - \frac{2}{\beta_{2}}t_{2}\right)}{x \Gamma(t_{1} + t_{2})} \times \left(\frac{\omega_{I} \bar{P}}{\omega_{1} \bar{P}_{I} x}\right)^{-t_{1}} \left(\frac{\omega_{I} \bar{P}}{\omega_{2} \bar{P}_{I} x}\right)^{-t_{2}} dt_{2} dt_{1},$$
(5.36)

$$f_{\gamma_{\text{eq}}}(x) = \frac{1}{x} H_{1,1:[1,1]_{l=1:L}}^{0,1:[1,1]_{l=1:L}} \begin{bmatrix} \frac{\omega_{l} \ \bar{P}_{l} \ x}{\omega_{l} \ \bar{P}} \\ \vdots \\ \frac{\omega_{L} \ \bar{P}_{l} \ x}{\omega_{l} \ \bar{P}} \end{bmatrix} \begin{pmatrix} 0; \left\{ \frac{2}{\beta_{l}} \right\}_{l=1:L} \right) : \begin{bmatrix} (1,1) \\ (1,\frac{2}{\beta_{l}}) \end{bmatrix}_{l=1:L} \end{bmatrix}.$$
 (5.37)

Then, by substituting (5.37) into (5.5). The exact expression of the e2e SIR probability density function can be obtained.

5.4 Performance analysis

In this section, first, the e2e system outage probability (OP) is obtained. Then the exact form average bit error probability (ABEP), for the system and for the per-hop node are derived.

5.4.1 Outage Probability

For our multi-hop cooperation network with co-channel interference model, the system be in outage if at least one of the i-th hop be outage. This outage event might happen when the signal-to-interference ratio (SIR) drops below a specific SIR threshold, ($\gamma_{\rm th}$), that is required for satisfying a certain quality of service (QoS) metric. Mathematically, OP of the system is the CDF of the e2e SIR ,($\gamma_{\rm e2e}$) RV, evaluated at $\gamma_{\rm th}$,

$$P_{out} = \Pr[\gamma_{e2e} \le \gamma_{th}] = F_{\gamma_{e2e}}(\gamma_{th}). \tag{5.38}$$

5.4.2 Average Bit Error Probability

Average bit error probability (ABEP) is one of the most important performance metric that used to understand the system behavior. For multi-hop relaying networks, the e2e ABEP can be given as [132]

$$P_{e2e}(e) = \sum_{i=1}^{N} \bar{P}_i(e) \prod_{j=i+1}^{N} (1 - 2\bar{P}_j(e)), \qquad (5.39)$$

where $(\bar{P}_i(e), i = 1,...,N)$ denotes the average bit error probability per-hop. Furthermore, for the most binary modulations, the average bit error probability is expressed as follows ([54][eqn 12])

$$\bar{P}(e) = \frac{a^b}{2\Gamma(b)} \int_0^\infty \gamma^{b-1} \exp(-a\gamma) F_{\gamma_{eq}}(\gamma) d\gamma, \qquad (5.40)$$

where (*a*) is a constant depends on the type of modulation (e.g., 0.5 for frequency shift keying (FSK), 1 for phase shift keying (PSK)) and (*b*) is another constant, depending on the detection scheme (0.5 for coherent detection, and 1 for non-coherent detection).

Now by changing x by γ in our derived CDF per-hop (i.e., $F_{\gamma_{eq}}(x)$ in (5.28)), then, substituting it in (5.40) with switching the order of the real and contour integrals with some manipulations, we get the following integral formula

$$\bar{P}(e) = \frac{a^{b}}{2\Gamma(b) (2\pi i)^{2}} \int_{\mathcal{L}_{1}} \int_{\mathcal{L}_{2}} \frac{\Gamma\left(1 + \frac{2}{\beta_{I}}t_{1} + \frac{2}{\beta_{I}}t_{2}\right) \Gamma(t_{1}) \Gamma\left(1 - \frac{2}{\beta_{1}}t_{1}\right) \Gamma(t_{2}) \Gamma\left(1 - \frac{2}{\beta_{2}}t_{2}\right)}{\Gamma(1 + t_{1} + t_{2})}$$

$$\times \left(\frac{\omega_{I} \bar{P}}{\omega_{1} \bar{P}_{I}}\right)^{-t_{1}} \left(\frac{\omega_{I} \bar{P}}{\omega_{2} \bar{P}_{I}}\right)^{-t_{2}} \int_{0}^{\infty} \gamma^{b+t_{1}+t_{2}-1} \exp(-a\gamma) d\gamma dt_{2} dt_{1}.$$

$$(5.41)$$

In the innermost integral with respect to γ , using change of variable $u = a\gamma$, and with the help of ([69] [eqn 8.339.1]) and some mathematical arrangements. The per-hop

ABEP can be obtained in integral form as

$$\bar{P}(e) = \frac{1}{2\Gamma(b) (2\pi i)^{2}} \int_{\mathcal{L}_{1}} \int_{\mathcal{L}_{2}} \frac{\Gamma\left(1 + \frac{2}{\beta_{I}}t_{1} + \frac{2}{\beta_{I}}t_{2}\right) \Gamma(b + t_{1} + t_{2}) \Gamma(t_{1}) \Gamma\left(1 - \frac{2}{\beta_{1}}t_{1}\right)}{\Gamma(1 + t_{1} + t_{2})} \times \Gamma(t_{2}) \Gamma\left(1 - \frac{2}{\beta_{2}}t_{2}\right) \left(\frac{a \omega_{I} \bar{P}}{\omega_{1} \bar{P}_{I}}\right)^{-t_{1}} \left(\frac{a \omega_{I} \bar{P}}{\omega_{2} \bar{P}_{I}}\right)^{-t_{2}} dt_{2} dt_{1}.$$
(5.42)

To this end, by using the definition of the multivariate H-function, we can generalize our derivations and provide the exact ABEP per-hop with MRT for any number of transmit antennas as follows

$$\bar{P}(e) = \frac{1}{2\Gamma(b)} H_{2,1:[1,1]_{l=1:L}}^{0,2:[1,1]_{l=1:L}} \begin{bmatrix} \frac{\omega_{l} \ \bar{P}_{l}}{a \ \omega_{l} \ \bar{P}} \\ \vdots \\ \frac{\omega_{L} \ \bar{P}_{l}}{a \ \omega_{l} \ \bar{P}} \end{bmatrix} \begin{pmatrix} 0; \left\{ \frac{2}{\beta_{l}} \right\}_{l=1:L}, (1-b; \{1\}_{l=1:L}) : \begin{bmatrix} (1,1) \\ (1,\frac{2}{\beta_{l}}) \end{bmatrix}_{l=1:L} \\ (0; \{1\}_{l=1:L}) : (5.43)$$

By substituting (5.43) into (5.39), the exact e2e average bit error probability for multi-antenna multi-hop DF relaying networks with CCI can be attained.

5.4.3 Asymptotic Analysis

In this subsection, our derived exact expressions for per-hop outage and average error probabilities in (5.29) and (5.43) respectively do not express the insight of the system behaviour (e.g., diversity and array gains). Thus, by assuming high received power values (i.e., $\bar{P} \to \infty$), along with using the asymptotic expansion of H-function ([129] [Theo. 1.11]), we can compute the residue of the effective poles of Mellin–Barnes contour integrals. Consequently, (5.29) and (5.43) can be approximated respectively as

$$F_{\gamma_{\text{eq}}}^{\infty}(\gamma_{\text{th}}) \approx \frac{\Gamma\left(1 + \sum_{l=1}^{L} \frac{\beta_{l}}{\beta_{l}}\right)}{\Gamma\left(1 + \sum_{l=1}^{L} \frac{\beta_{l}}{\beta_{l}}\right)} \prod_{l=1}^{L} \Gamma\left(\frac{\beta_{l}}{2}\right) \left(\frac{\beta_{l}}{2}\right) \left(\frac{\omega_{l} \ \bar{P}_{I} \ \gamma_{\text{th}}}{\omega_{I} \ \bar{P}}\right)^{\frac{\beta_{l}}{2}}, \tag{5.44}$$

$$\bar{P}^{\infty}(e) \approx \frac{\Gamma\left(1 + \sum_{l=1}^{L} \frac{\beta_{l}}{\beta_{l}}\right) \Gamma\left(b + \sum_{l=1}^{L} \frac{\beta_{l}}{2}\right)}{2\Gamma(b) \Gamma\left(1 + \sum_{l=1}^{L} \frac{\beta_{l}}{2}\right)} \prod_{l=1}^{L} \Gamma\left(\frac{\beta_{l}}{2}\right) \left(\frac{\beta_{l}}{2}\right) \left(\frac{\omega_{l} \ \bar{P}_{l}}{a \ \omega_{l} \ \bar{P}}\right)^{\frac{\beta_{l}}{2}}. \quad (5.45)$$

Similarly, at the high SIR, the e2e system outage and average error probabilities in (5.4) and (5.39) can be approximated respectively as

$$F_{\gamma_{e2e}}(\gamma_{th}) = \Pr\left[\min\left(\gamma_{eq_{i}}, \dots, \gamma_{eq_{N}}\right) \leq \gamma_{th}\right]$$

$$= 1 - \prod_{i=1}^{N} \left(1 - F_{\gamma_{eq_{i}}}(\gamma_{th})\right)$$

$$\approx \sum_{i=1}^{N} F_{\gamma_{eq_{i}}}^{\infty}(\gamma_{th}),$$
(5.46)

$$P_{e2e}(e) = \sum_{i=1}^{N} \bar{P}_{i}(e) \prod_{j=i+1}^{N} (1 - 2\bar{P}_{j}(e))$$

$$\approx \sum_{i=1}^{N} \bar{P}_{i}^{\infty}(e).$$
(5.47)

Finally, by substituting (5.44) into (5.46), and (5.45) into (5.47), respectively, a simple but very useful e2e system outage and average error probabilities expressions can be attained.

5.5 Numerical Results and Discussion

In this section, numerical examples for our derived expressions of outage and average error probability are presented and validated by Monte-Carlo simulations. For simplicity, a balanced system parameters for all nodes are used to avoid confusion by many symbols (i.e., we use L, P, P_I , β and β_I instead of L_i , P_{i-1} , P_{I_i} , β_{l_i} and β_{I_i} , respectively). Maximum 10^6 and 4×10^7 iterations are used to gets the simulation results for OP and ABEP (in high diversity order), respectively. Firstly, our derivation results reflect a perfect convergence with the Monte-Carlo simulations. Besides, there is no built-in function to compute the multivariate H-function in MATLAB, MATHEMATICA nor Maple, thus, numerical integration is used with the help of

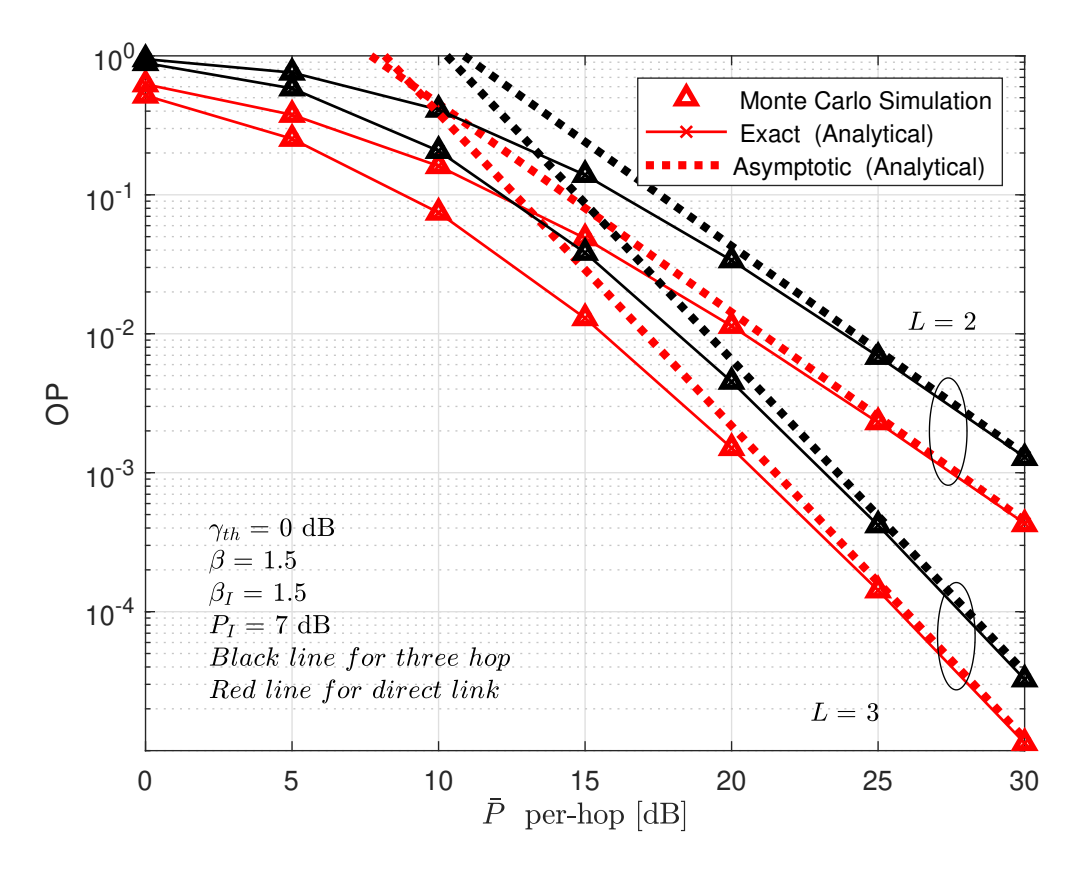


Figure 5.2 Outage probability versus average per-hop signal power for the direct and multi-hop cooperative links, N = 1, 3.

MATLAB program.

In Figure 5.2, the outage probability versus average received power per-hop is presented. Two cases are considered; direct link and cooperative with three hops. The system settings are chosen as: zero signal-to-interference threshold, ($P_I = 7 \, \mathrm{dB}$) at the first and second relay nodes, ($\beta = \beta_I = 1.5$), and the number of antenna is assumed two and three, respectively, for both cases. By increasing the number of antennas with MRT, high performance gain is achieved in both cases, as the diversity order increased from (1.5) to (2.25). Moreover, it is observed that the multi-hop transmission has bad influence on the OP, specifically, the array gain (i.e., the red and black curve are still parallel even with the increase of the diversity order by adding one more antenna).

Figure 5.3 plots the outage probability as a function of average received power per-hop (\bar{P}) , to investigate the influence of the fading severity on the system performance. Thus, the Weibull parameter for the desired channels are specified as $\beta=1,1.5,2$ (Note that 1 and 2 are the special cases of Weibull channel to represent Exponential and Rayleigh distributions, respectively). The other system parameters are chosen as: (L=2), $(\beta_I=0.5)$, (N=3), $(P_I=10)$ and $(\gamma_{\rm th}=-3)$ dB). It can be recognized

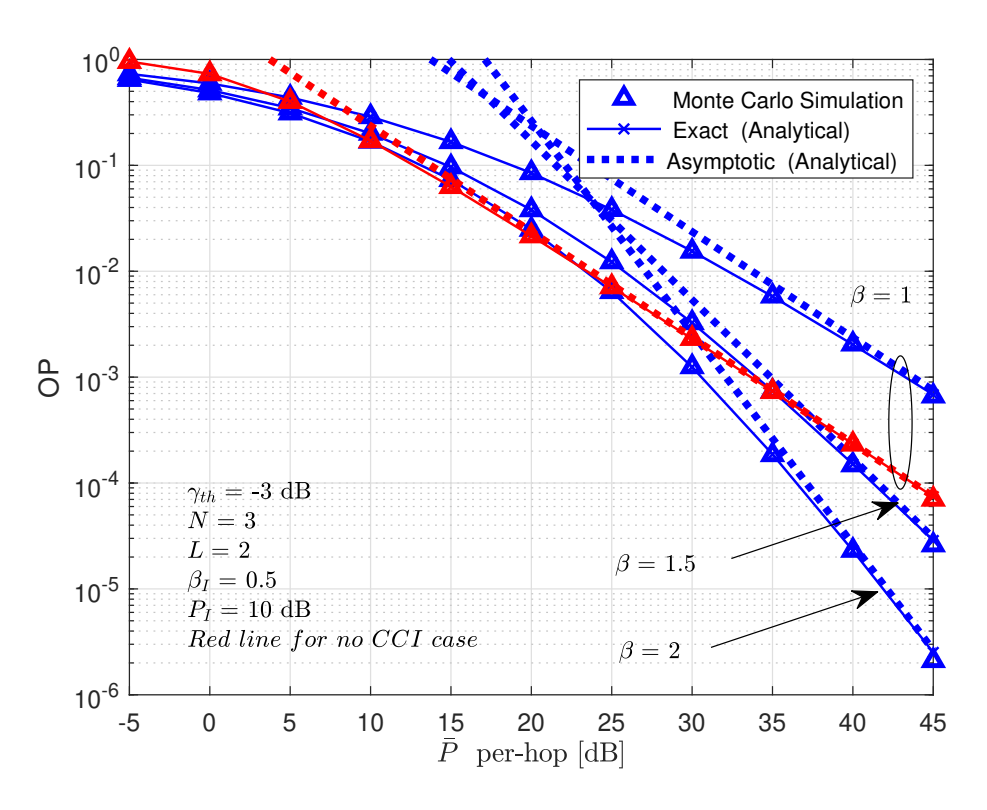


Figure 5.3 Outage probability versus average per-hop signal power for the multi-hop with different fading parameter values, N = 3.

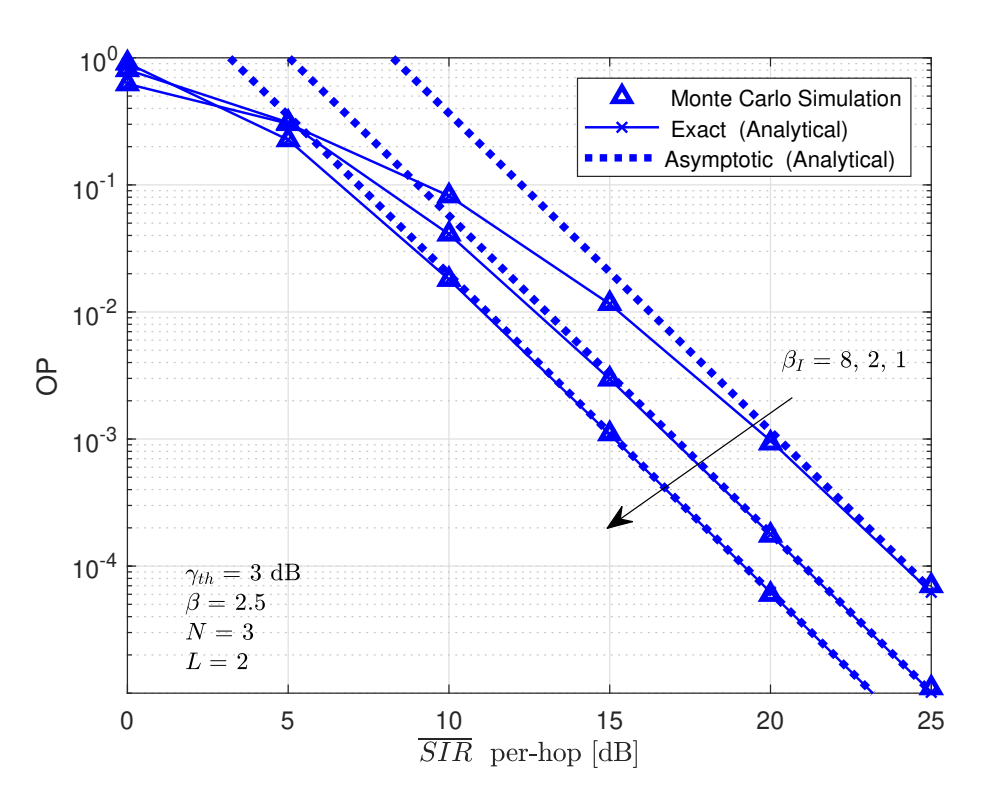


Figure 5.4 Outage probability versus per-hop average signal-to-interference ratio for the multi-hop with different interference fading parameter values, N = 3.

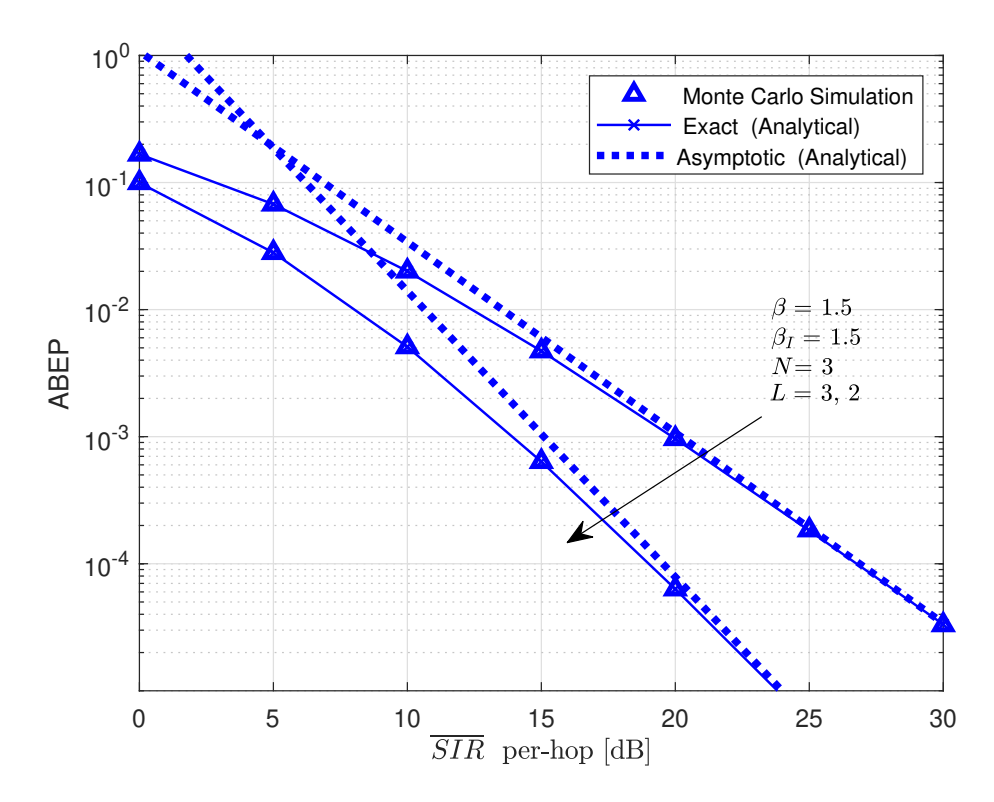


Figure 5.5 Average bit error probability versus per-hop average signal-to-interference ratio for the multi-hop with different number of antennas, N = 3.

that choosing the Weibull parameter as ($\beta = 1, 1.5, 2$), and keeping the number of antennas as two, results in better performance. Specifically, the diversity order is increased from one to two. The other interesting observation is that the two curves with different colors (interference-limited and free interference cases) having ($\beta = 1$), are parallel at high power, i.e., no diversity change between the two cases.

Figure 5.4 shows the relation between the interference channel severity parameters (β_I) and the system outage probability. In this figure, OP versus SIR per-hop is plotted with network parameter values: N=3, $\beta=2.5$, L=2 and $\gamma_{th}=3$ dB. It can be observed that when increasing Weibull channel parameter of the interference signal as $(\beta_I=1,2,8)$ at all receivers in the system, better OP performance can be obtained. However, this performance benefit is in terms of array gain only, as the diversity order is fixed to (2.5). This observation supports the one in figure (5.3), that the interference has no impact on the system diversity gain utterly.

Figure 5.5, illustrates our derived exact and asymptotic ABEP expressions compared with Monte Carlo simulation. When the ABEP for coherent binary phase shift keying (CBPSK) plotted as a function of signal-to-interference ratio per-hop, the system parameters are assumed as: three hops (N=3), Weibull fading severity parameters ($\beta=\beta_I=1.5$), the number of antenna for each transmitter (L=2,3),

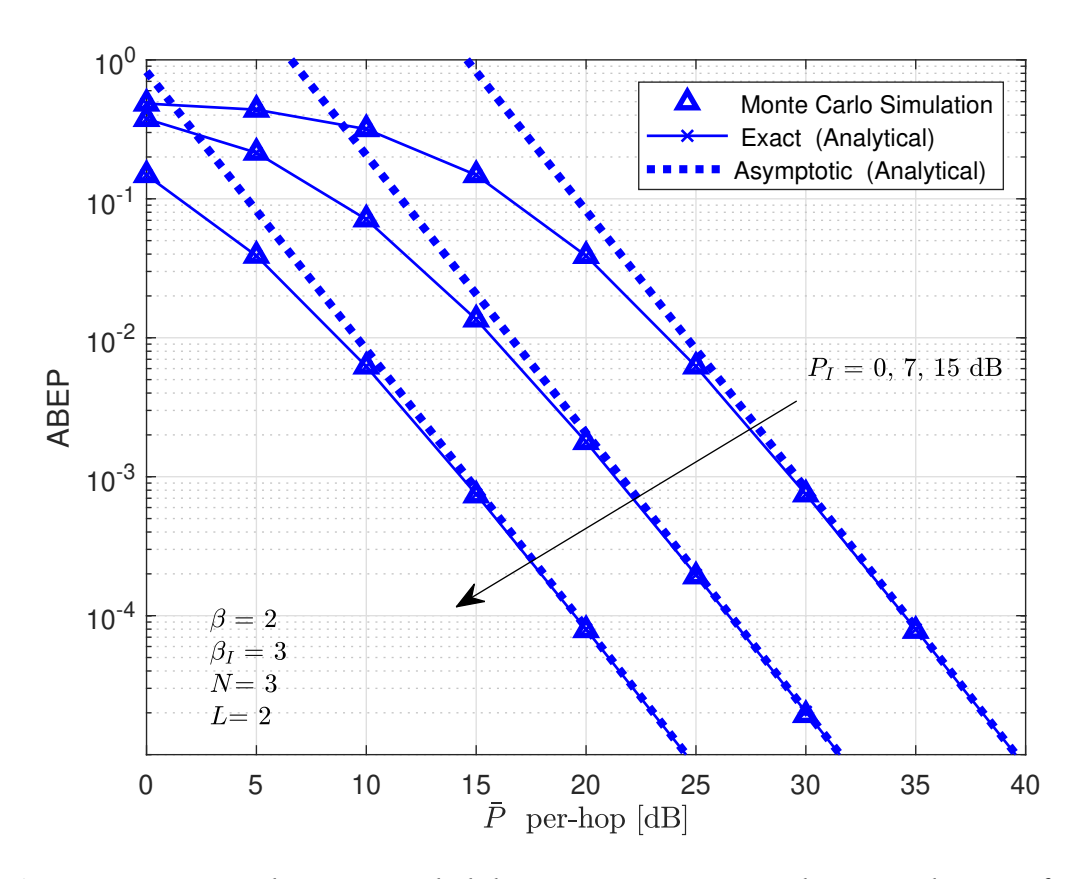


Figure 5.6 Average bit error probability versus average per-hop signal power for the multi-hop with different interference power values, N = 3.

respectively. One can notice that the ABEP decreases as the number of antennas increases. Furthermore, it is evident that the diversity order increases from (1.5) to (2.25) when the number of antennas increases from (2) to (3). In contrast, the ABEP decreases from (10^{-3}) to $(10^{-4.5})$ at 20 dB SIR.

Figure 5.6 demonstrates the average bit error probability as a function of average received power per-hop (\bar{P}) , when different interference power values are assumed $(P_I=0,7,15 \text{ dB})$ with the same number of antennas for all transmitter (L=2) in the system. Besides, three hops are used (N=3), and the Weibull fading severity parameters are considered as $(\beta=2)$ and $(\beta_I=3)$ for the desired and interference signals, respectively. The results clearly show that changing the interference power does not affect the diversity order, which remains at two according to our asymptotic result in (5.45). However, when the interference power increases, the array gain deteriorates and consistently the ABEP increases. Thus, more antenna with MRT is a solution to recoup the system degraded by CCI.

5.6 Chapter Summary

In this chapter, the performance analysis of multi-antenna multi-hop decode-and-forward relaying over Weibull fading channels with maximal ratio transmission (MRT) is investigated. With the assumption of interference-limited scenario, the exact expressions for the probability of outage and error are obtained and confirmed by simulation results. In addition, asymptotic results are provided to understand the effects of the channel severity as well as the number of transmit antennas on the system behaviour. It can be deduced that it is still possible with the aid of low complexity MRT to achieve high link reliability even with the existence of CCI and degrading influence of multiple hops.

6 RESULTS AND DISCUSSION

This thesis investigates the use of maximal ratio transmission to improve the reliability of cooperative relay networks, which have attracted considerable interest recently due to their numerous advantages and practical usages. Specifically, we studied the two-way, one-way and multi-hop relaying networks under co-channel interference with the help of the popular low complexity MRT technique. All of the theoretical results are validated by numerical simulations and summaries of each scenario are stated below.

6.1 Conclusions

MRT technique is proposed as a solution for AF-TWRNs to suppress the performance loss caused by unavoidable CCI plus noise distortion at the single antenna relay receiver. After obtaining the upper bound of the cumulative distribution function of SINR, tight lower bound expressions of OP, SER and upper bound of system ergodic sum rate are derived and illustrated with extensive numerical examples. Moreover, the asymptotic behavior of the OP and SSER, the array and diversity gains are presented. Furthermore, the effect of imperfect CSI is also explored. Our derived expressions are validated for arbitrary signal-to-interference power ratios, numbers of co-channel interferers, and most modulation formats employed in the practical systems. The new proposed system can be highly desirable since using MRT allows employing low complexity relays for coverage extension and reliability enhancement in cellular, WiFi, sensor networks.

In addition, Exact closed-form error, outage probability and ergodic capacity of multi-antenna decode-and-forward dual-hop relaying with maximal ratio transmission over Nakagami-m channels are derived when unavoidable co-channel interference effect on the receivers is taken into account. Theoretical results and numerical examples show that performance degradation due to interference can be overcome using low complexity MRT approach at the transmitters. Since the use of wireless

relaying is going to increase in next-generation communication networks, the considered system can be highly useful when the number of interferers can increase arbitrarily, and new massive MIMO base stations can utilize MRT to reduce outage rates to satisfy the quality of service requirements. The reliability and availability of the network can be improved by employing more antennas for MRT without increasing the receiver complexity, which can be especially useful for small devices in IoT and sensor networks.

Finally, Maximal ratio transmission is utilized to overcome the multi-hop relaying network limitations (in terms of increased channel use, coordination overhead, and delay) in addition to co-channel interference terrible influences. Specifically, an exact form outage and error probability of multi-antenna multi-hop decode-and-forward relaying with MRT over Weibull channels are derived and verified by simulation results. Due to unavoidable CCI, performance degradation can be overcome with the use of low complexity MRT approach. Our numerical examples show that this technique can be a highly effective option when severe fading channels results in high outage rates that is undesirable next-generation communication systems. The network's reliability and availability can be increased by utilizing more antennas for MRT without increasing the receiver complexity. This system model under critical Weibull channel has lots of applications in feature generation, e.g., Millimeter wave (mmWave) Internet of things (IoT), Vehicle-to-everything (V2X), and wireless sensor networks (WSN).

6.2 Future Works

Some suggestions about future works based on this thesis are given as follows:

- 1- Through our thesis analyses, mostly the statistics of the ratios of two RVs are derived to evaluate the co-channel interference effects. Recall that the performance analysis of a number of emerging wireless communication topics, including either non-orthogonal multiple access (NOMA), interference-limited scenarios, spectrum sharing cognitive radio, full-duplex, or physical-layer security networks are totally dependent in their performance investigations on the statistic of the ratio of two RVs. Consequently, one can adopt MRT with a multiple-antenna system in all the above-mentioned topics.
- 2- The developed techniques in chapter five, can be used to study the MRT performance in a multi-hop free-space optical (FSO) cooperative network to reinforce the reliability of cooperating link when Exponential Weibull or double Weibull fading channel is assumed.

3- It is also interesting to investigate the performance of MRT with a hybrid FSO/RF two-way relaying network scenario with the assumption of two sources having multiple transmit apertures and multiple transmit antennas, respectively and a relay node equipment with single receive photo-detector, transmit aperture, and antenna, respectively.

- [1] T. Gucluoglu, Reduced complexity algorithms for space-time coded systems over frequency selective fading channels. Arizona State University, 2006.
- [2] E. Telatar, "Capacity of multi-antenna gaussian channels," *European transactions on telecommunications*, vol. 10, no. 6, pp. 585–595, 1999.
- [3] T. K. Y. Lo, "Maximum ratio transmission," *IEEE Transactions on Communications*, vol. 47, no. 10, pp. 1458–1461, Oct. 1999.
- [4] Z. Chen, J. Yuan, B. Vucetic, "Analysis of transmit antenna selection/maximal-ratio combining in rayleigh fading channels," *IEEE Transactions on Vehicular Technology*, vol. 54, no. 4, pp. 1312–1321, 2005.
- [5] A. Sendonaris, E. Erkip, B. Aazhang, "User cooperation diversity. part i. system description," *IEEE transactions on communications*, vol. 51, no. 11, pp. 1927– 1938, Nov. 2003.
- [6] —, "User cooperation diversity. part ii. implementation aspects and performance analysis," *IEEE Transactions on communications*, vol. 51, no. 11, pp. 1939–1948, Nov. 2003.
- [7] A. H. Bastami, S. Habibi, "Cognitive mimo two-way relay network: Joint optimal relay selection and spectrum allocation," *IEEE Transactions on Vehicular Technology*, vol. 67, no. 7, pp. 5937–5952, Jul. 2018.
- [8] X. Yue, Y. Liu, S. Kang, A. Nallanathan, Y. Chen, "Modeling and analysis of two-way relay non-orthogonal multiple access systems," *IEEE Transactions on Communications*, vol. 66, no. 9, pp. 3784–3796, Sep. 2018.
- [9] K. Guo, D. Guo, B. Zhang, "Performance analysis of two-way multi-antenna multi-relay networks with hardware impairments," *IEEE Access*, vol. 5, pp. 15 971–15 980, Aug. 2017.
- [10] Y. Cai, Y. Ni, J. Zhang, S. Zhao, H. Zhu, "Energy efficiency and spectrum efficiency in underlay device-to-device communications enabled cellular networks," *China Communications*, vol. 16, no. 4, pp. 16–34, Apr. 2019.
- [11] Q. Guo, W. Feng, "Joint relay and eavesdropper selection strategy against multiple eavesdroppers over nakagami-*m* fading channels in cooperative decode-and-forward relay networks," *IEEE Access*, vol. 7, pp. 37980–37988, Mar. 2019.
- [12] S. Solanki, P. K. Upadhyay, D. B. da Costa, P. S. Bithas, A. G. Kanatas, "Performance analysis of cognitive relay networks with rf hardware impairments and cees in the presence of primary users' interference," *IEEE Transactions on Cognitive Communications and Networking*, vol. 4, no. 2, pp. 406–421, Jun. 2018.

- [13] N. Yang, P. L. Yeoh, M. Elkashlan, I. B. Collings, Z. Chen, "Two-way relaying with multi-antenna sources: Beamforming and antenna selection," *IEEE Transactions on Vehicular Technology*, vol. 61, no. 9, pp. 3996–4008, Nov. 2012.
- [14] S. Yadav, P. K. Upadhyay, S. Prakriya, "Performance evaluation and optimization for two-way relaying with multi-antenna sources," *IEEE Transactions on Vehicular Technology*, vol. 63, no. 6, pp. 2982–2989, Jul. 2014.
- [15] E. Erdoğan, T. Güçlüoğlu, "Performance analysis of maximal ratio transmission with relay selection in two-way relay networks over nakagami-m fading channels," *Wireless Personal Communications*, vol. 88, no. 2, pp. 185–201, May 2016.
- [16] K. Guo, D. Guo, B. Zhang, "Performance analysis of two-way multi-antenna multi-relay networks with hardware impairments," *IEEE Access*, vol. 5, pp. 15 971–15 980, Aug. 2017.
- [17] L. Yang, Q. T. Zhang, "Outage performance of mimo relay channels with maximal ratio transmission," *Electronics Letters*, vol. 45, no. 5, pp. 273–274, Feb. 2009.
- [18] M. Arti, M. R. Bhatnagar, "Performance analysis of hop-by-hop beamforming and combining in df mimo relay system over nakagami-m fading channels," *IEEE communications letters*, vol. 17, no. 11, pp. 2080–2083, Sep. 2013.
- [19] —, "Maximal ratio transmission in af mimo relay systems over nakagami-*m* fading channels," *IEEE Transactions on Vehicular Technology*, vol. 64, no. 5, pp. 1895–1903, Jul. 2014.
- [20] E. Erdogan, T. Gucluoglu, "Dual-hop amplify-and-forward multi-relay maximum ratio transmission," *Journal of Communications and Networks*, vol. 18, no. 1, pp. 19–26, Feb. 2016.
- [21] H. Ilhan, "End-to-end ser of mrt/mrc and sc in multi-hop wireless sensor networks," *Wireless Networks*, pp. 1–11, Mar. 2020.
- [22] S. S. Ikki, S. Aissa, "Performance analysis of two-way amplify-and-forward relaying in the presence of co-channel interferences," *IEEE Transactions on Communications*, vol. 60, no. 4, pp. 933–939, Apr. 2012.
- [23] D. B. da Costa, H. Ding, M. D. Yacoub, J. Ge, "Two-way relaying in interference-limited af cooperative networks over nakagami- *m* fading," *IEEE Transactions on Vehicular Technology*, vol. 61, no. 8, pp. 3766–3771, Oct. 2012.
- [24] E. Soleimani-Nasab, M. Matthaiou, M. Ardebilipour, G. K. Karagiannidis, "Two-way af relaying in the presence of co-channel interference," *IEEE Transactions on Communications*, vol. 61, no. 8, pp. 3156–3169, Aug. 2013.
- [25] L. Yang, K. Qaraqe, E. Serpedin, M. Alouini, "Performance analysis of amplify-and-forward two-way relaying with co-channel interference and channel estimation error," *IEEE Transactions on Communications*, vol. 61, no. 6, pp. 2221–2231, Jun. 2013.
- [26] I. Trigui, S. Affes, A. Stephenne, "On the ergodic capacity of amplify-and-forward relay channels with interference in nakagami-m fading," *IEEE transactions on communications*, vol. 61, no. 8, pp. 3136–3145, Apr. 2013.

- [27] I. Trigui, S. Affes, A. Stephenne, "Ergodic capacity analysis for interference-limited af multi-hop relaying channels in nakagami-m fading," *IEEE transactions on communications*, vol. 61, no. 7, pp. 2726–2734, May 2013.
- [28] A. Goldsmith, Wireless communications. Cambridge university press, 2005.
- [29] K. Hari, "Channel models for wireless communication systems," in *Wireless Network Design*, Springer, 2011, pp. 47–64.
- [30] S. R. Saunders, A. Aragón-Zavala, *Antennas and propagation for wireless communication systems*. John Wiley & Sons, 2007.
- [31] T. Rappaport, "Wireless communications: Principles and practice," 6th ed., Prentice Hall PTR, Upper Saddle River, NJ, USA, 2002.
- [32] M. K. Simon, M.-S. Alouini, *Digital communication over fading channels*. 2th ed. John Wiley & Sons, 2005, vol. 95.
- [33] M. Nakagami, "The m-distribution—a general formula of intensity distribution of rapid fading," in *Statistical methods in radio wave propagation*, Elsevier, 1960, pp. 3–36.
- [34] C. Kabiri, "On the performance of underlay cognitive radio networks with interference constraints and relaying," Ph.D. dissertation, Blekinge Institute of Technology, 2015.
- [35] A. M. Cvetkovic, G. T. Djordjevic, M. C. Stefanovic, "Performance analysis of dual switched diversity over correlated weibull fading channels with co-channel interference," *International Journal of Communication Systems*, vol. 24, no. 9, pp. 1183–1195, 2011.
- [36] Available online: http://5gmobile.fel.cvut.cz/img/activities/5GMvision, 08.png.
- [37] M.-S. Alouini, A. Goldsmith, "Area spectral efficiency of cellular mobile radio systems," in 1997 IEEE 47th Vehicular Technology Conference. Technology in Motion, IEEE, vol. 2, 1997, pp. 652–656.
- [38] P. Gupta, P. R. Kumar, "The capacity of wireless networks," *IEEE Transactions on information theory*, vol. 46, no. 2, pp. 388–404, 2000.
- [39] 3GPP, Technical Specification Group Radio Access Network; Physical layer aspects for evolved Universal Terrestrial Radio Access. (E-UTRA), 3rd ed., March 2011.
- [40] R. K. Saha, C. Aswakul, "A tractable analytical model for interference characterization and minimum distance enforcement to reuse resources in three-dimensional in-building dense small cell networks," *International Journal of Communication Systems*, vol. 30, no. 11, e3240, Jul. 2017.
- [41] R. K. Saha, "On maximizing energy and spectral efficiencies using small cells in 5g and beyond networks," *Sensors*, vol. 20, no. 6, p. 1676, Jan. 2020.
- [42] L. Lei, E. Lagunas, S. Chatzinotas, B. Ottersten, "Noma aided interference management for full-duplex self-backhauling hetnets," *IEEE Communications Letters*, vol. 22, no. 8, pp. 1696–1699, Aug. 2018.
- [43] A. Ghasemi, E. S. Sousa, "Spectrum sensing in cognitive radio networks: Requirements, challenges and design trade-offs," *IEEE Communications Magazine*, vol. 46, no. 4, pp. 32–39, Apr. 2008.

- [44] X. Xia, D. Zhang, K. Xu, Y. Xu, "A comparative study on interference-limited two-way transmission protocols," *Journal of Communications and Networks*, vol. 18, no. 3, pp. 351–363, Jun. 2016.
- [45] E. S. Sousa, J. A. Silvester, "Optimum transmission ranges in a direct-sequence spread-spectrum multihop packet radio network," *IEEE journal on selected areas in communications*, vol. 8, no. 5, pp. 762–771, 1990.
- [46] P. Cardieri, "Modeling interference in wireless ad hoc networks," *IEEE Communications Surveys & Tutorials*, vol. 12, no. 4, pp. 551–572, 2010.
- [47] J. Chen, M. Ding, Q. Zhang, "Interference statistics and performance analysis of mimo ad hoc networks in binomial fields," *IEEE transactions on vehicular technology*, vol. 61, no. 5, pp. 2033–2043, 2012.
- [48] F. Baccelli, B. Błaszczyszyn, *Stochastic geometry and wireless networks*. Now Publishers Inc, 2010, vol. 1.
- [49] H. Boujemâa, "Static hybrid amplify and forward (af) and decode and forward (df) relaying for cooperative systems," *Physical Communication*, vol. 4, no. 3, pp. 196–205, 2011.
- [50] S.-Q. Huang, H.-H. Chen, M.-Y. Lee, "Mixed af and df cooperative relay systems and their performance bounds analyses," *Wireless Communications and Mobile Computing*, vol. 14, no. 13, pp. 1204–1218, 2014.
- [51] N. Kong, T. Eng, L. B. Milstein, "A selection combining scheme for rake receivers," in *Proceedings of ICUPC'95-4th IEEE International Conference on Universal Personal Communications*, IEEE, 1995, pp. 426–430.
- [52] M. Kang, M.-S. Alouini, "A comparative study on the performance of mimo mrc systems with and without co-channel interference," in *IEEE International Conference on Communications*, 2003. ICC'03., IEEE, vol. 3, 2003, pp. 2154–2158.
- [53] K. S. Ahn, "Performance analysis of mimo-mrc systems with channel estimation error in the presence of cochannel interferences," *IEEE Signal Processing Letters*, vol. 15, pp. 445–448, 2008.
- [54] I. S. Ansari, S. Al-Ahmadi, F. Yilmaz, M. Alouini, H. Yanikomeroglu, "A new formula for the ber of binary modulations with dual-branch selection over generalized-k composite fading channels," *IEEE Transactions on Communications*, vol. 59, no. 10, pp. 2654–2658, Oct. 2011.
- [55] Zhengdao Wang, G. B. Giannakis, "A simple and general parameterization quantifying performance in fading channels," *IEEE Transactions on Communications*, vol. 51, no. 8, pp. 1389–1398, Aug. 2003.
- [56] M. K. Shukla, S. Yadav, N. Purohit, "Performance evaluation and optimization of traffic-aware cellular multiuser two-way relay networks over nakagami-m fading," *IEEE Systems Journal*, vol. 12, no. 2, pp. 1933–1944, Jun. 2018.
- [57] B. Rankov, A. Wittneben, "Spectral efficient protocols for half-duplex fading relay channels," *IEEE Journal on Selected Areas in Communications*, vol. 25, no. 2, pp. 379–389, Feb. 2007.

- [58] P. Popovski, H. Yomo, "Wireless network coding by amplify-and-forward for bi-directional traffic flows," *IEEE Communications Letters*, vol. 11, no. 1, pp. 16–18, Jan. 2007.
- [59] K. M. Rabie, B. Adebisi, M. Alouini, "Half-duplex and full-duplex af and df relaying with energy-harvesting in log-normal fading," *IEEE Transactions on Green Communications and Networking*, vol. 1, no. 4, pp. 468–480, Dec. 2017.
- [60] C. Peng, F. Li, H. Liu, "Wireless energy harvesting two-way relay networks with hardware impairments," *Sensors*, vol. 17, no. 11, 2017.
- [61] K. Guo, K. An, B. Zhang, D. Guo, "Performance analysis of two-way satellite multi-terrestrial relay networks with hardware impairments," *Sensors*, vol. 18, no. 5, 2018.
- [62] C. Sun, K. Liu, D. Zheng, W. Ai, "Secure communication for two-way relay networks with imperfect csi," *Entropy*, vol. 19, no. 10, 2017.
- [63] X. Liang, S. Jin, W. Wang, X. Gao, K. Wong, "Outage probability of amplify-and-forward two-way relay interference-limited systems," *IEEE Transactions on Vehicular Technology*, vol. 61, no. 7, pp. 3038–3049, Sep. 2012.
- [64] X. Liang, S. Jin, X. Gao, K. Wong, "Outage performance for decode-and-forward two-way relay network with multiple interferers and noisy relay," *IEEE Transactions on Communications*, vol. 61, no. 2, pp. 521–531, Feb. 2013.
- [65] X. Xia, D. Zhang, K. Xu, Y. Xu, "Interference-limited two-way df relaying: Symbol-error-rate analysis and comparison," *IEEE Transactions on Vehicular Technology*, vol. 63, no. 7, pp. 3474–3480, Sep. 2014.
- [66] M. K. Shukla, S. Yadav, N. Purohit, "Cellular multiuser two-way relay network with cochannel interference and channel estimation error: Performance analysis and optimization," *IEEE Transactions on Vehicular Technology*, vol. 67, no. 4, pp. 3431–3446, Apr. 2018.
- [67] E. Erdoğan, T. Güçlüoğlu, "Simple outage probability bound for two-way relay networks with joint antenna and relay selection over nakagami-m fading channels," *Electronics Letters*, vol. 51, no. 5, pp. 415–417, Feb. 2015.
- [68] M. O. Hasna, M. Alouini, "End-to-end performance of transmission systems with relays over rayleigh-fading channels," *IEEE Transactions on Wireless Communications*, vol. 2, no. 6, pp. 1126–1131, Nov. 2003.
- [69] I. Gradshteyn, I. Ryzhik, "Table of integrals, series, and products," 7th ed., Elsevier Academic Press, New York, NY, USA, 2005.
- [70] X. Xu, Y. Cai, C. Cai, W. Yang, "Overall outage probability of two-way amplify-and-forward relaying in nakagami-m fading channels," in 2011 International Conference on Wireless Communications and Signal Processing (WCSP), IEEE, Nov. 2011, pp. 1–4.
- [71] H. Guo, J. Ge, H. Ding, "Symbol error probability of two-way amplify-and-forward relaying," *IEEE Communications Letters*, vol. 15, no. 1, pp. 22–24, Nov. 2010.

- [72] Y. L. R. H. Y. Louie, B. Vucetic, "Practical physical layer network coding for two-way relay channels: Performance analysis and comparison," *IEEE Transactions on Wireless Communications*, vol. 9, no. 2, pp. 764–777, Feb. 2010.
- [73] O. Frank, "Nist handbook of mathematical functions," Cambridge University Press, New York, NY, USA, 2010.
- [74] Y. Huang, F. Al-Qahtani, C. Zhong, Q. Wu, J. Wang, H. Alnuweiri, "Performance analysis of multiuser multiple antenna relaying networks with co-channel interference and feedback delay," *IEEE Transactions on Communications*, vol. 62, no. 1, pp. 59–73, Jan. 2014.
- [75] P. V. Mieghem, "Performance analysis of communications networks and systems," Cambridge University Press, New York, NY, USA, 2006.
- [76] C. Wang, T. C. Liu, X. Dong, "Impact of channel estimation error on the performance of amplify-and-forward two-way relaying," *IEEE Transactions on Vehicular Technology*, vol. 61, no. 3, pp. 1197–1207, Mar. 2012.
- [77] L. Wang, Y. Cai, W. Yang, "On the finite-snr dmt of two-way af relaying with imperfect csi," *IEEE Wireless Communications Letters*, vol. 1, no. 3, pp. 161–164, Jun. 2012.
- [78] A. Nosratinia, T. E. Hunter, A. Hedayat, "Cooperative communication in wireless networks," *IEEE communications Magazine*, vol. 42, no. 10, pp. 74–80, Oct. 2004.
- [79] J. N. Laneman, D. N. Tse, G. W. Wornell, "Cooperative diversity in wireless networks: Efficient protocols and outage behavior," *IEEE Transactions on Information theory*, vol. 50, no. 12, pp. 3062–3080, Nov. 2004.
- [80] N. T. Tuan, D.-S. Kim, J.-M. Lee, "On the performance of cooperative transmission schemes in industrial wireless sensor networks," *IEEE Transactions on Industrial Informatics*, vol. 14, no. 9, pp. 4007–4018, Sep. 2018.
- [81] S. Jain, R. Bose, "Rateless-code-based secure cooperative transmission scheme for industrial iot," *IEEE Internet of Things Journal*, vol. 7, no. 7, pp. 6550–6565, Jul. 2020.
- [82] X. Zhao, D. Pompili, "Multi-cell interference management scheme for next-generation cellular networks," *IEEE Transactions on Communications*, vol. 68, no. 2, pp. 1200–1212, Dec. 2019.
- [83] B. Li, J. Zhou, Y. Zou, F. Wang, "Closed-form secrecy outage analysis of cellular downlink systems in the presence of co-channel interference," *IEEE Transactions on Wireless Communications*, vol. 17, no. 7, pp. 4721–4734, Jul. 2018.
- [84] F. S. Al-Qahtani, J. Yang, R. M. Radaydeh, C. Zhong, H. Alnuweiri, "Exact outage analysis of dual-hop fixed-gain af relaying with cci under dissimilar nakagami-m fading," *IEEE Communications Letters*, vol. 16, no. 11, pp. 1756–1759, Oct. 2012.
- [85] S. Choi, M.-S. Alouini, S. S. Nam, "Impact of co-channel interference on the outage performance under multiple type ii relay environments," *IEEE Access*, vol. 5, pp. 26201–26210, Nov. 2017.

- [86] A. M. Salhab, F. Al-Qahtani, S. A. Zummo, H. Alnuweiri, "Outage analysis of nth-best df relay systems in the presence of cci over rayleigh fading channels," *IEEE communications letters*, vol. 17, no. 4, pp. 697–700, Feb. 2013.
- [87] N.-E. Wu, H.-J. Li, "Performance analysis of snr-based decode-and-forward opportunistic relaying in the presence of cochannel interference," *IEEE Transactions on Vehicular Technology*, vol. 65, no. 9, pp. 7244–7257, Jan. 2013.
- [88] D. B. da Costa, H. Ding, J. Ge, "Interference-limited relaying transmissions in dual-hop cooperative networks over nakagami-m fading," *IEEE Communications Letters*, vol. 15, no. 5, pp. 503–505, Mar. 2011.
- [89] L. Zhang, W. Yang, J. Zhang, Y. Li, "Outage probability analysis of relay systems over κ - μ fading channels," *China Communications*, vol. 11, no. 10, pp. 60–66, Nov. 2014.
- [90] D. B. da Costa, S. Aissa, "Dual-hop decode-and-forward relaying systems with relay selection and maximal-ratio schemes," *Electronics letters*, vol. 45, no. 9, pp. 460–461, Apr. 2009.
- [91] W. Yang, Y. Cai, X. Xu, "Interference-limited mimo relaying systems over nakagami-m fading channels," *Electronics letters*, vol. 48, no. 11, pp. 660–662, May 2012.
- [92] K.-C. Lee, C.-P. Li, T.-Y. Wang, H.-J. Li, "Performance analysis of dual-hop amplify-and-forward systems with multiple antennas and co-channel interference," *IEEE transactions on wireless communications*, vol. 13, no. 6, pp. 3070–3087, May 2014.
- [93] C. Zhong, H. A. Suraweera, A. Huang, Z. Zhang, C. Yuen, "Outage probability of dual-hop multiple antenna af relaying systems with interference," *IEEE Transactions on Communications*, vol. 61, no. 1, pp. 108–119, Nov. 2012.
- [94] G. Zhu, C. Zhong, H. A. Suraweera, Z. Zhang, C. Yuen, "Outage probability of dual-hop multiple antenna af systems with linear processing in the presence of co-channel interference," *IEEE Transactions on Wireless Communications*, vol. 13, no. 4, pp. 2308–2321, Mar. 2014.
- [95] G. Zhu, C. Zhong, H. A. Suraweera, Z. Zhang, C. Yuen, R. Yin, "Ergodic capacity comparison of different relay precoding schemes in dual-hop af systems with co-channel interference," *IEEE Transactions on Communications*, vol. 62, no. 7, pp. 2314–2328, Jun. 2014.
- [96] L. Zheng, D. N. C. Tse, "Diversity and multiplexing: A fundamental tradeoff in multiple-antenna channels," *IEEE Transactions on information theory*, vol. 49, no. 5, pp. 1073–1096, May 2003.
- [97] Y. Li, L. Zhang, L. J. Cimini, H. Zhang, "Statistical analysis of mimo beamforming with co-channel unequal-power mimo interferers under path-loss and rayleigh fading," *IEEE Transactions on Signal Processing*, vol. 59, no. 8, pp. 3738–3748, Aug. 2011.
- [98] L. Zhang, Y. Li, L. J. Cimini, "Statistical performance analysis for mimo beamforming and stbc when co-channel interferers use arbitrary mimo modes," *IEEE Transactions on Communications*, vol. 60, no. 10, pp. 2926–2937, Oct. 2012.

- [99] S. S. Ikki, P. Ubaidulla, S. Aissa, "Performance study and optimization of cooperative diversity networks with co-channel interference," *IEEE Transactions on Wireless Communications*, vol. 13, no. 1, pp. 14–23, Jan. 2014.
- [100] J. A. Hussein, S. S. Ikki, S. Boussakta, C. C. Tsimenidis, "Performance analysis of opportunistic scheduling in dual-hop multiuser underlay cognitive network in the presence of cochannel interference," *IEEE Transactions on Vehicular Technology*, vol. 65, no. 10, pp. 8163–8176, Oct. 2016.
- [101] I. Lee, J. Kim, D. Kim, "Outage performance of heterogeneous mimo relaying in ostbc transmission over spatially correlated nakagami fading channels," *IEEE Communications Letters*, vol. 15, no. 3, pp. 284–286, Mar. 2011.
- [102] J. A. Hussein, S. Boussakta, S. S. Ikki, "Performance study of a ucrn over nakagami- *m* fading channels in the presence of cci," *IEEE Transactions on Cognitive Communications and Networking*, vol. 3, no. 4, pp. 752–765, Dec. 2017.
- [103] A. Aladwani, E. Erdogan, T. Gucluoglu, "Impact of co-channel interference on two-way relaying networks with maximal ratio transmission," *Electronics*, vol. 8, no. 4, p. 392, Apr. 2019.
- [104] Y. Sahin, E. Erdogan, T. Gucluoglu, "Performance analysis of two way decode and forward relay network with maximum ratio transmission," *Physical Communication*, vol. 32, pp. 75–80, 2019.
- [105] F. Yilmaz, M.-S. Alouini, "A novel unified expression for the capacity and bit error probability of wireless communication systems over generalized fading channels," *IEEE Transactions on Communications*, vol. 60, no. 7, pp. 1862–1876, 2012.
- [106] H. Li, M. Lott, M. Weckerle, W. Zirwas, E. Schulz, "Multihop communications in future mobile radio networks," in *The 13th IEEE International Symposium on Personal, Indoor and Mobile Radio Communications*, IEEE, vol. 1, Sep. 2002, pp. 54–58.
- [107] H. Yang, P. F. Smulders, M. H. Herben, "Channel characteristics and transmission performance for various channel configurations at 60 ghz," *EURASIP Journal on Wireless Communications and Networking*, vol. 2007, pp. 1–15, Dec. 2007.
- [108] J. Reig, M.-T. Martinez-Inglés, L. Rubio, V.-M. Rodrigo-Peñarrocha, J.-M. Molina-Garcia-Pardo, "Fading evaluation in the 60 ghz band in line-of-sight conditions," *International Journal of Antennas and Propagation*, vol. 2014, Aug. 2014.
- [109] A. Ghosh, A. Maeder, M. Baker, D. Chandramouli, "5g evolution: A view on 5g cellular technology beyond 3gpp release 15," *IEEE Access*, vol. 7, pp. 127 639–127 651, Sep. 2019.
- [110] A. Soulimani, M. Benjillali, H. Chergui, D. B. da Costa, "Performance analysis of m-qam multihop relaying over mmwave weibull fading channels," *CoRR*, 2016.
- [111] —, "On multihop weibull-fading communications: Performance analysis framework and applications," *arXiv preprint arXiv:1610.08535*, 2016.

- [112] A. Soulimani, M. Benjillali, H. Chergui, "Energy-efficient multihop schemes over weibull-fading channels: Performance analysis and optimization," in 2017 13th International Wireless Communications and Mobile Computing Conference (IWCMC), IEEE, Jun. 2017, pp. 2009–2014.
- [113] S. Ikki, M. H. Ahmed, "Performance of multi-hop relaying systems over weibull fading channels," in *New technologies, mobility and security*, Springer, 2007, pp. 31–38.
- [114] G. Pandeeswari, M. Suganthi, R. Asokan, "Performance of single hop and multi hop relaying protocols in cognitive radio networks over weibull fading channel," *Journal of Ambient Intelligence and Humanized Computing*, pp. 1–7, Feb. 2020.
- [115] A. Bessate, F. El Bouanani, "A very tight approximate results of mrc receivers over independent weibull fading channels," *Physical Communication*, vol. 21, pp. 30–40, Dec. 2016.
- [116] F. El Bouanani, A. Bessate, "A comparative study on the performance of mimo-stbc subject to weibull fading channels," *International Journal of Communication Systems*, vol. 31, no. 13, e3731, Sep. 2018.
- [117] F. El Bouanani, H. Ben-Azza, "Efficient performance evaluation for egc, mrc and sc receivers over weibull multipath fading channel," in *International Conference on Cognitive Radio Oriented Wireless Networks*, Springer, Apr. 2015, pp. 346–357.
- [118] F. El Bouanani, D. B. da Costa, "Accurate closed-form approximations for the sum of correlated weibull random variables," *IEEE Wireless Communications Letters*, vol. 7, no. 4, pp. 498–501, Jan. 2018.
- [119] V. Perim, J. D. V. Sánchez, J. C. S. Santos Filho, "Asymptotically exact approximations to generalized fading sum statistics," *IEEE Transactions on Wireless Communications*, vol. 19, no. 1, pp. 205–217, Oct. 2019.
- [120] G. Zhu, C. Zhong, H. A. Suraweera, Z. Zhang, C. Yuen, "Outage probability of dual-hop multiple antenna af systems with linear processing in the presence of co-channel interference," *IEEE Transactions on Wireless Communications*, vol. 13, no. 4, pp. 2308–2321, Apr. 2014.
- [121] A. Shah, A. M. Haimovich, M. K. Simon, M. .-. Alouini, "Exact bit-error probability for optimum combining with a rayleigh fading gaussian cochannel interferer," *IEEE Transactions on Communications*, vol. 48, no. 6, pp. 908–912, Jun. 2000.
- [122] T. V. Poon, N. C. Beaulieu, "Error performance analysis of a jointly optimal single-cochannel-interferer bpsk receiver," *IEEE Transactions on Communications*, vol. 52, no. 7, pp. 1051–1054, Jul. 2004.
- [123] A. M. Rabiei, N. C. Beaulieu, "A simple, intuitive expression for the ber of a jointly optimal single cochannel interferer bpsk receiver," *IEEE Communications Letters*, vol. 9, no. 3, pp. 201–203, Mar. 2005.
- [124] M. R. Akdeniz, Y. Liu, M. K. Samimi, S. Sun, S. Rangan, T. S. Rappaport, E. Erkip, "Millimeter wave channel modeling and cellular capacity evaluation," *IEEE journal on selected areas in communications*, vol. 32, no. 6, pp. 1164–1179, Jun. 2014.

- [125] 3GPP, Study on 3D channel model for LTE. Technical report 36.873 v12.5.1, 201, 2017.
- [126] O. S. Badarneh, D. B. Da Costa, M. Benjillali, M.-S. Alouini, "Ratio of products of fluctuating two-ray variates," *IEEE Communications Letters*, vol. 23, no. 11, pp. 1944–1948, Aug. 2019.
- [127] E. Mekić, M. Stefanović, P. Spalević, N. Sekulović, A. Stanković, "Statistical analysis of ratio of random variables and its application in performance analysis of multihop wireless transmissions," *Mathematical Problems in Engineering*, vol. 2012, Jan. 2012.
- [128] A. M. Mathai, R. K. Saxena, H. J. Haubold, *The H-function: theory and applications*. Springer Science & Business Media, Oct. 2009.
- [129] A. A. Kilbas, H-transforms: Theory and Applications. CRC Press, Mar. 2004.
- [130] H. Chergui, M. Benjillali, M.-S. Alouini, "Rician k-factor-based analysis of xlos service probability in 5g outdoor ultra-dense networks," *IEEE Wireless Communications Letters*, vol. 8, no. 2, pp. 428–431, Oct. 2018.
- [131] H. R. Alhennawi, M. M. El Ayadi, M. H. Ismail, H.-A. M. Mourad, "Closed-form exact and asymptotic expressions for the symbol error rate and capacity of the *h*-function fading channel," *IEEE Transactions on Vehicular Technology*, vol. 65, no. 4, pp. 1957–1974, Apr. 2015.
- [132] E. Morgado, I. Mora-Jiménez, J. J. Vinagre, J. Ramos, A. J. Caamaño, "End-to-end average ber in multihop wireless networks over fading channels," *IEEE transactions on wireless communications*, vol. 9, no. 8, pp. 2478–2487, Jul. 2010.
- [133] A. Prudnikov, Y. Brychkov, O. Marichev, "Integrals and series, volume 3," Gordon and Breach, New York, NY, USA, 1990.
- [134] Available online: http://functions.wolfram.com/06.06.26.0005.01.
- [135] Available online: http://functions.wolfram.com/07.34.21.0081.01.
- [136] V. Adamchik, O. Marichev, "The algorithm for calculating integrals of hypergeometric type functions and its realization in reduce system," in *Proceedings of the international symposium on Symbolic and algebraic computation*, Jul. 1990, pp. 212–224.
- [137] Available online: http://functions.wolfram.com/07.34.22.0007.01.

A Derivation of (3.20)

To begin with, recall that $\tilde{\gamma}_1 = \gamma_2/(\gamma_I + 2)$ and $\tilde{\gamma}_2 = \gamma_1/(\gamma_I + 2)$. Besides, step (a) of (3.19) is

$$F_{\gamma_{e,2e}^{\text{up}}}(\gamma) = \mathbb{E}_{\gamma_I} \left[1 - (1 - F_{\tilde{\gamma}_1}(\gamma))(1 - F_{\tilde{\gamma}_2}(\gamma)) \right], \tag{A.1}$$

where $(1 - F_{\tilde{\gamma}_1}(\gamma)) = \Pr[\gamma_2 > (\gamma_I + 2)\gamma]$ and $(1 - F_{\tilde{\gamma}_2}(\gamma)) = \Pr[\gamma_1 > (\gamma_I + 2)\gamma]$ are the complementary distribution function of $\tilde{\gamma}_1$ and $\tilde{\gamma}_2$ respectively. By substituting the CDFs of γ_1 and γ_2 from (3.9) and (3.10), (A.1) can be written as

$$F_{\gamma_{\text{e2e}}^{\text{up}}}(\gamma) = \mathbb{E}_{\gamma_I} \left[1 - \left(\sum_{w=0}^{L_2 - 1} \frac{e^{-(z+2)\gamma/\Omega_2}}{w!} \left(\frac{(z+2)\gamma}{\Omega_2} \right)^w \right) \left(\sum_{m=0}^{L_1 - 1} \frac{e^{-(z+2)\gamma/\Omega_1}}{m!} \left(\frac{(z+2)\gamma}{\Omega_1} \right)^m \right) \right]. \tag{A.2}$$

Then by averaging over the PDF of γ_I in (3.11) yields

$$F_{\gamma_{\text{e2e}}^{\text{up}}}(\gamma) = 1 - \int_{0}^{\infty} \sum_{w=0}^{L_2 - 1} \frac{e^{-(z+2)\gamma/\Omega_2}}{w!} \left(\frac{(z+2)\gamma}{\Omega_2}\right)^w \sum_{m=0}^{L_1 - 1} \frac{e^{-(z+2)\gamma/\Omega_1}}{m!} \left(\frac{(z+2)\gamma}{\Omega_1}\right)^m \frac{z^{N-1}e^{-z/\Omega_I}}{\Omega_I^N \Gamma(N)} dz.$$
(A.3)

The CDF expression can be further simplified by making substitution t = z/2, and using some simple algebraic manipulations.

$$F_{\gamma_{e2e}^{up}}(\gamma) = 1 - \sum_{m=0}^{L_1 - 1} \sum_{w=0}^{L_2 - 1} \frac{e^{-\frac{2\gamma}{\Omega_1}} e^{-\frac{2\gamma}{\Omega_2}}}{m! w! \Gamma(N)} \left(\frac{2\gamma}{\Omega_1}\right)^m \left(\frac{2\gamma}{\Omega_2}\right)^w \left(\frac{2}{\Omega_I}\right)^N \times \int_{0}^{\infty} t^{N-1} (t+1)^{m+w} e^{-\left(\frac{2\gamma}{\Omega_1} + \frac{2\gamma}{\Omega_2} + \frac{2}{\Omega_I}\right)t} dt,$$
(A.4)

where the above integral is solved by utilizing ([69] [eqn 9.211.4]) to obtain the desired closed form result as in (3.20).

B Derivation of (3.41)

The statistical mean values of $\gamma_{S_1}^{\rm up}$ and $\gamma_{S_2}^{\rm up}$ can be determined by using the CDF-based method as

$$\mathbb{E}[\gamma_{S_i}^{\text{up}}] = \int_0^\infty (1 - F_{\gamma_{S_i}^{\text{up}}}(\gamma)) d\gamma, \ i = 1, 2.$$
(B.1)

After applying the identity ([73][eqn 13.2.8]) on (3.14) and (3.15), the Tricomi confluent hypergeometric function is expanded to a finite sum series as

$$F_{\gamma_{S_i}^{\text{up}}}(\gamma) = 1 - \sum_{m=0}^{L_i - 1} \sum_{w=0}^{L_j - 1} \frac{e^{-\frac{\gamma}{\Omega_i}} e^{-\frac{2\gamma}{\Omega_j}}}{m!w!} \left(\frac{\gamma}{\Omega_i}\right)^m \left(\frac{2\gamma}{\Omega_j}\right)^w \left(\frac{2}{\Omega_I}\right)^N \sum_{n=0}^w {w \choose n} \frac{\Gamma(N+n)}{\Gamma(N)} \left(\frac{2\gamma}{\Omega_j} + \frac{2}{\Omega_I}\right)^{-N-n}.$$
(B.2)

Now, by substituting (B.2) into (B.1) yields

$$\mathbb{E}[\gamma_{S_i}^{\text{up}}] = \frac{1}{\Gamma(N)} \sum_{m=0}^{L_i - 1} \sum_{w=0}^{L_j - 1} \sum_{n=0}^{w} {w \choose n} \left(\frac{1}{\Omega_i}\right)^m \left(\frac{1}{\Omega_j}\right)^w \frac{\Gamma(N+n)}{m!w!} \left(\frac{2}{\Omega_I}\right)^{-n} \times \int_{0}^{\infty} \gamma^{m+w} \left(\frac{\Omega_I \gamma}{\Omega_j} + 1\right)^{-N-n} e^{-\left(\frac{1}{\Omega_i} + \frac{2}{\Omega_j}\right)\gamma} d\gamma,$$
(B.3)

to solving the resulting integral, ([133] [eqn 8.4.2.5 and 8.4.3.1]) are used to express

its integrands in terms of Meijer's G-functions as

$$\left(\frac{\Omega_{I}}{\Omega_{j}}\gamma + 1\right)^{-N-n} = \frac{1}{\Gamma(N+n)} G_{1,1}^{1,1} \left(\frac{\Omega_{I}}{\Omega_{j}}\gamma|_{0}^{1-N-n}\right),$$

$$e^{-\left(\frac{1}{\Omega_{i}} + \frac{2}{\Omega_{j}}\right)\gamma} = G_{0,1}^{1,0} \left(\left(\frac{1}{\Omega_{i}} + \frac{2}{\Omega_{j}}\right)\gamma|_{0}^{-}\right).$$
(B.4)

To this end, knowing that the Mellin transform of the product of two Meijer's G-functions is also a Meijer's G-function by using ([133] [2.24.1.1]) and with some basic mathematical simplifications, a closed-form expression for the statistical mean values of $\gamma_{S_1}^{\rm up}$ and $\gamma_{S_2}^{\rm up}$ can be attained as in (3.41).

In this Appendix, the derivation of the unconditional CDF of the first hop SINR RV (γ_{SR}) is given. Firstly, by using (4.3), the CDF can be written as

$$F_{\gamma_{SR}}(\gamma) = \Pr[\gamma_{SR} < \gamma] = \Pr\left[\frac{\gamma_1}{\gamma_{IR} + 1} < \gamma\right],\tag{C.1}$$

and then, by taking expectation with the help of the PDF of (γ_{IR}) , unconditional CDF becomes

$$F_{\gamma_{SR}}(\gamma) = \int_0^\infty \Pr\left[\frac{\gamma_1}{z+1} < \gamma\right] f_{\gamma_{IR}}(z) dz$$

$$= \int_0^\infty F_{\gamma_1}((z+1) \gamma) f_{\gamma_{IR}}(z) dz.$$
(C.2)

After substituting the CDF of the instantaneous SNR at the relay, i.e., γ_1 , CDF from (4.12) and (4.9) into (C.2), the following integral can be obtained

$$F_{\gamma_{IR}}(\gamma) = 1 - \frac{\left(\frac{m_{IR}}{\bar{\gamma}_{IR}}\right)^{m_{IR}N} \exp\left(-\frac{m_1}{\bar{\gamma}_1}\gamma\right) \sum_{n=0}^{m_1L_1-1} \frac{\left(\frac{m_1}{\bar{\gamma}_1}\gamma\right)^n}{n!}$$

$$\times \int_0^\infty (z+1)^n z^{m_{IR}N-1} \exp\left(-\left(\frac{m_{IR}}{\bar{\gamma}_{IR}} + \frac{m_1}{\bar{\gamma}_1}\gamma\right)z\right) dz.$$
(C.3)

To this end, by using the binomial expansion theorem ([69] [eqn 1.111]), the integral I_{A_1} is simplified to

$$I_{A_1} = \sum_{k=0}^{n} {n \choose k} \int_{0}^{\infty} z^{k+m_{IR}N-1} \exp\left(-\left(\frac{m_{IR}}{\bar{\gamma}_{IR}} + \frac{m_1}{\bar{\gamma}_1}\gamma\right)z\right) dz.$$
 (C.4)

Finally, I_{A_2} can be readily solved with help of ([69] [eqn 3.351.3]). By substituting (C.4) into (C.3), an exact expression of the unconditional CDF can be attained as in (4.11).

In PDF derivation, the conventional method is applying the first derivative of the CDF with respect to γ ; However, our derived CDF expression in (4.11) is looking tedious to be derived in this way. Thus, the density function of the first hop SINR (γ_{SR}) can be determined using the standard analysis to find a PDF of ratio of two RVs, by using the following formula

$$f_{\gamma_{SR}}(\gamma) = \int_0^\infty (z+1) f_{\gamma_1}((z+1) \gamma) f_{\gamma_{IR}}(z) dz.$$
 (D.1)

Then, by substituting the PDFs of γ_1 and γ_{IR} from (4.7), and (4.9) respectively into (D.1) with some simplifications, the integral can be written as

$$f_{\gamma_{SR}}(\gamma) = \frac{\left(\frac{m_1}{\bar{\gamma}_1}\right)^{m_1 L_1} \left(\frac{m_{IR}}{\bar{\gamma}_{IR}}\right)^{m_{IR}N} \gamma^{m_1 L_1 - 1} \exp\left(-\frac{m_1}{\bar{\gamma}_1}\gamma\right)}{\Gamma(m_1 L_1) \Gamma(m_{IR} N)} \times \int_0^{\infty} (z+1) (z+1)^{m_1 L_1 - 1} z^{m_{IR} N - 1} \exp\left(-\left(\frac{m_{IR}}{\bar{\gamma}_{IR}} + \frac{m_1}{\bar{\gamma}_1}\gamma\right)z\right) dz.$$
(D.2)

Using the binomial expansion theorem ([69] [eqn 1.111]), the integral I_{B_1} in (D.2) is reduced to

$$I_{B_1} = \sum_{n=0}^{m_1 L_1} {m_1 L_1 \choose n} \int_0^\infty z^{n + m_{IR} N - 1} \exp\left(-\left(\frac{m_{IR}}{\bar{\gamma}_{IR}} + \frac{m_1}{\bar{\gamma}_1}\gamma\right)z\right) dz.$$
(D.3)

Finally, by change the variable $t=\left(\frac{m_{IR}}{\bar{\gamma}_{IR}}+\frac{m_1}{\bar{\gamma}_1}\gamma\right)z$, with some manipulations. The integral I_{B_2} can be solved as

$$I_{B_2} = \frac{(n + m_{IR}N - 1)!}{\left(\frac{m_{IR}}{\bar{\gamma}_{IR}} + \frac{m_1}{\bar{\gamma}_1}\gamma\right)^{n + m_{IR}N}}.$$
 (D.4)

The exact unconditional average error probability for the first hop, i.e., $P_{SR}(e)$ can be obtained by averaging the conditional AWGN error probability $P_e(e|\gamma_{SR})$ in (4.16) over the PDF of γ_{SR} which is derived in (4.13). According to [105], the conditional error probability can be written as

$$P_e(e|\gamma_{SR} = \gamma) = \frac{\Gamma(\beta, \alpha \gamma)}{2 \Gamma(\beta)}.$$
 (E.1)

By using the upper incomplete Gamma function utility in [134], the (E.1) formula can be expressed as

$$P_{e}(e|\gamma_{SR} = \gamma) = \frac{1}{2 \Gamma(\beta)} G_{1,2}^{2,0} \left(\alpha \gamma \middle| 1, \beta\right), \tag{E.2}$$

now by substituting the derived corresponding PDF of γ_{SR} , i.e., (4.13) and (E.2) into (4.16). We get the integral formula

$$P_{SR}(e) = \frac{\left(\frac{m_{1}}{\bar{\gamma}_{1}}\right)^{m_{1}L_{1}} \left(\frac{m_{IR}}{\bar{\gamma}_{IR}}\right)^{m_{IR}N}}{2 \Gamma(\beta) \Gamma(m_{1}L_{1})\Gamma(m_{IR}N)} \sum_{n=0}^{m_{1}L_{1}} {m_{1}L_{1} \choose n} (n + m_{IR}N - 1)!$$

$$\times \int_{0}^{\infty} \gamma^{m_{1}L_{1} - 1} G_{1,2}^{2,0} \left(\alpha \gamma \left| \frac{1}{0,\beta} \right.\right) \exp\left(-\frac{m_{1}}{\bar{\gamma}_{1}}\gamma\right) \left(\frac{m_{IR}}{\bar{\gamma}_{IR}} + \frac{m_{1}}{\bar{\gamma}_{1}}\gamma\right)^{-(n + m_{IR}N)} d\gamma . \tag{E.3}$$

To solving the resulting integral, i.e., I_{C_1} , ([133] [eqn 8.4.2.5 and 8.4.3.1]) are used to express its integrands in terms of Meijer's G-functions as

$$\exp\left(-\frac{m_1}{\bar{\gamma}_1}\gamma\right) = G_{0,1}^{1,0}\left(\frac{m_1}{\bar{\gamma}_1}\gamma \middle| \frac{1}{0}\right),\tag{E.4}$$

$$\left(\frac{m_{IR}}{\bar{\gamma}_{IR}} + \frac{m_1}{\bar{\gamma}_1}\gamma\right)^{-(n+m_{IR}N)} = \frac{\left(\frac{m_{IR}}{\bar{\gamma}_{IR}}\right)^{-(n+m_{IR}N)}}{(n+m_{IR}N-1)!} G_{1,1}^{1,1} \left(\frac{m_1 \,\bar{\gamma}_{IR}}{m_{IR} \,\bar{\gamma}_1}\gamma \,\middle| \, 1 - (n+m_{IR}N)\right), \quad (E.5)$$

by using the above utilities, the integral I_{C_1} in (E.3) can be written in the following form

$$I_{C_{1}} = \frac{\left(\frac{m_{IR}}{\bar{\gamma}_{IR}}\right)^{-(n+m_{IR}N)}}{(n+m_{IR}N-1)!} \times \int_{0}^{\infty} \gamma^{m_{1}L_{1}-1} G_{1,2}^{2,0} \left(\alpha \gamma \begin{vmatrix} 1\\0,\beta \end{pmatrix} G_{0,1}^{1,0} \left(\frac{m_{1}}{\bar{\gamma}_{1}}\gamma \begin{vmatrix} -\\0 \end{pmatrix} G_{1,1}^{1,1} \left(\frac{m_{1} \bar{\gamma}_{IR}}{m_{IR} \bar{\gamma}_{1}}\gamma \begin{vmatrix} 1-(n+m_{IR}N)\\0 \end{pmatrix} d\gamma \right). \tag{E.6}$$

Finally, take advantage of Mellin transform in above, the integral I_{C_2} can be calculated with the help of [135] as in (E.7).

$$I_{C_2} = \alpha^{-m_1L_1} G_{2,1:0,1;1,1}^{0,2:1,0;1,1} \begin{pmatrix} \frac{m_1}{\alpha \ \tilde{\gamma}_1} \\ \frac{m_1 \ \tilde{\gamma}_{IR}}{\alpha \ m_{IR} \ \tilde{\gamma}_1} \end{pmatrix} \begin{vmatrix} 1 - m_1L_1 \ , \ 1 - m_1L_1 - \beta \ : \ - \ ; \ 1 - n - m_{IR}N \\ 1 - m_1L_1 - 1 \ : \ 0 \ ; \ 0 \end{vmatrix}.$$
 (E.7)

F Derivation of (4.19)

In the dual-hop DF relaying networks, the per-hop average ergodic capacity can be expressed by using the PDF of SINR as

$$\bar{C}_{SR} = \int_0^\infty \log_2(1+\gamma) f_{\gamma_{SR}}(\gamma) \, d\gamma, \tag{F.1}$$

by perfectly substation the PDF of the first hop SINR RV in (F.1), the integral formula is attained as

$$\bar{C}_{SR} = \frac{\left(\frac{m_1}{\bar{\gamma}_1}\right)^{m_1 L_1} \left(\frac{m_{IR}}{\bar{\gamma}_{IR}}\right)^{m_{IR}N}}{\Gamma(m_1 L_1) \Gamma(m_{IR}N)} \sum_{n=0}^{m_1 L_1} {m_1 L_1 \choose n} (n + m_{IR}N - 1)! \\
\times \int_0^{\infty} \gamma^{m_1 L_1 - 1} \log_2(1 + \gamma) \exp\left(-\frac{m_1}{\bar{\gamma}_1}\gamma\right) \left(\frac{m_{IR}}{\bar{\gamma}_{IR}} + \frac{m_1}{\bar{\gamma}_1}\gamma\right)^{-(n + m_{IR}N)} d\gamma .$$
(F.2)

In order to evaluate the integral I_{D_1} in (F.2), we represents the exponential and power functions in terms of Meijer's G-function using (E.4) and (E.5), respectively. Besides, the logarithm function can also expressed as a Meijer's G-function by utilized ([136][eqn 7]), as

$$\log_2(1+\gamma) = \log_2(e) \ G_{2,2}^{1,2} \left(\gamma \begin{vmatrix} 1,1\\1,0 \end{vmatrix}, \right), \tag{F.3}$$

using the utilities in above, the integral $I_{\mathcal{D}_1}$ in (F.2) can be written as

$$I_{D_{1}} = \frac{\log_{2}(e) \left(\frac{m_{IR}}{\tilde{\gamma}_{IR}}\right)^{-(n+m_{IR}N)}}{(n+m_{IR}N-1)!} \times \int_{0}^{\infty} \gamma^{m_{1}L_{1}-1} G_{0,1}^{1,0} \left(\frac{m_{1}}{\tilde{\gamma}_{1}}\gamma \middle| 0\right) G_{1,1}^{1,1} \left(\frac{m_{1} \tilde{\gamma}_{IR}}{m_{IR} \tilde{\gamma}_{1}}\gamma \middle| 1-(n+m_{IR}N)\right) G_{2,2}^{1,2} \left(\gamma \middle| 1,1\right) d\gamma . \tag{F.4}$$

To this result in hand, the desired closed form solution for I_{D_2} is given by [137] as Mellin transform of the product of three Meijer's G-functions and it can be given as

$$I_{D_2} = \left(\frac{m_1}{\bar{\gamma}_1}\right)^{-m_1 L_1} G_{1,0:1,1;2,2}^{0,1:1,1;1,2} \begin{pmatrix} \frac{\bar{\gamma}_{IR}}{m_{IR}} & 1-m_1 L_1 & 1-n-m_{IR} N ; 1, 1 \\ \frac{\bar{\gamma}_1}{m_1} & - & : & 0 & ; 1, 0 \end{pmatrix}. \quad (E.5)$$

PUBLICATIONS FROM THE THESIS

Contact Information: tansal@yildiz.edu.tr

Papers

- 1. Awfa Aladwani, E. Erdogan, and T. Gucluoglu, "Impact of Co-Channel Interference on Two-Way Relaying Networks with Maximal Ratio Transmission," Electronics, vol. 8, no. 4, p. 392, Apr. 2019.
- 2. Awfa Aladwani and T. Gucluoglu, "Exact Analysis of Maximal Ratio Transmission Based Decode-and-Forward Relaying with Arbitrary Number of Co-channel Interferers," IEEE Access, vol. x, pp. xx-xx, 2020,(submitted).
- 3. Awfa Aladwani and T. Gucluoglu, "Exact Performance Analysis of Maximal Ratio Transmission with Multi-hop Decode-and-Forward Interference-Limited Relaying System under Weibull Fading Channel," IEEE Open Journal of Signal Processing, vol. x, pp. xx-xx, 2020, (prepared for submission).